in: CHEMISTRY AND BIOCHEMISTRY OF PLANT PIGMENTS
(T.W.Goodwin, Editor) Second Edition Volume 2
Academic Press London New York San Francisco
1976

Chapter 22

Flash Kinetic Spectrophotometry in the Study of Plant Pigments

WOLFGANG JUNGE

Max-Volmer Institut für Physikalische Chemie und Molekularbiologie, Technische Universität Berlin, Berlin, Germany

I Introduction

Pulse spectrophotometry is being used to study the kinetic behaviour of physicochemical systems containing pigments, the spectral changes of which are used as indicators of certain molecular events. Usually the system is perturbed by a pulse which is short compared with the typical response times of the system. Absorbancy changes of pigment molecules are monitored spectrophotometrically. The pattern of relaxation times is analysed for functional interrelationships between the different components.

This method was introduced by Norrish and Porter (1949), who studied rapid photochemical reactions stimulated by light flashes. It was extended to non-photochemical reactions by the application of temperature jumps (Czerlinsky and Eigen, 1959), electric field, and pressure jumps. The highest time resolution obtained so far which is

limited by the duration of the shortest pulse (a single pulse extracted from a pulse train emitted by a mode-locked laser) is of the order of picoseconds (Rentzepis, 1968). This method was successfully applied to a study of the primary processes of photosynthesis (Witt, 1955; Kok, 1957). It was refined for higher time resolution and higher sensitivity (Rüppel and Witt, 1969).

The special advantage of flash spectroscopic experiments with photosynthetic systems is based on three features: first, the stimulus, light, is the natural driving force of photosynthesis; second, spectrophotometry monitors the properties of natural pigments *in situ*, without major disturbances of the system; third, light pulses of sufficient energy can be generated at any duration down to the picosecond range. These properties of flash spectrophotometry have facilitated detailed insight into the primary processes of photosynthesis which in part was not to obtain by other methods. However, as with all kinetic approaches, flash spectroscopy is not self-consistent and many of the results it produced had to be based or at least to be corroborated by biochemical or structural studies.

This chapter is an introduction to flash spectroscopy as applied to photosynthesis. It is divided into three major sections: a digression on molecular spectroscopy recalling some necessary background, a section on instrumentation and on specific difficulties and pitfalls inherent in the method, and finally a section on the primary processes of photosynthesis exemplifying the application of flash spectroscopy rather than presenting a detailed picture of the biological subject.

II Digression on molecular spectroscopy

A MOLECULAR STATES AND ORBITALS

1 Electronic states

Electrons moving in the electric field of one or several atoms of a molecule find certain stationary states of motion, each of which is characterized by a sharply defined value of the total (kinetic + potential) energy of the electron. As is well known, quantum mechanics provides a formalism to calculate both the stationary orbitals of electrons and the corresponding eigenvalues of the total energy (for a concise introduction to quantum mechanics for the non-physicist, see Hanna, 1969).

In wave mechanics an orbital is described by a wave function $\phi(x, y, z)$, a function of the space coordinate but not of time, since the

orbitals are supposed to be stationary. The absolute square of this function is devised to describe the probability density for observing an electron in the position given by the space coordinates x, y, and z. The probability that an electron is found in a volume element dx, dy, dz around x, y, z is $|\phi(x, y, z)|^2\ dx \cdot dy \cdot dz$. In consequence the integral over the probability extended over the whole space has to be 1, which means: it is certain that the electron will be found somewhere.

Although quantum mechanics yields analytic functions for the electronic orbitals in a hydrogen atom, the solution of the formalism for the electronic orbitals in larger molecules is rather difficult, if not impractical. The complication arises from the necessity to incorporate the mutual interaction of many electrons and nuclei into the formalism. However, with the aid of large electronic computers several larger molecules have been tackled by approximation methods. For our purpose it is sufficient to simplify the picture by assuming that a molecule is made up of several nuclei with inner electrons plus outer electrons not interacting with each other, which move on stationary orbitals each belonging to a distinct energy level. The lowest possible energy level is called the ground state, the higher ones the excited states of the molecule. This of course is a gross oversimplification, since the positions of the remaining electrons will depend on the kind of orbitals just occupied by the distinguished ones.

Most electronic orbitals are restricted to rather small portions of the molecule, e.g. the orbital of an electron from one hydrogen of a methyl group extends across a few ångström units only.

However, there is a class of molecules, a common property of which is that part of the electrons occupy orbitals which are delocalized over ten or multiples of ten ångström units. This class of conjugated π-electron systems is of particular interest in the context of our topic, since it contains all plant pigments absorbing in the visible or the near ultraviolet. Two typical examples are illustrated in Fig. 1, a linear polyene and a cyclic one, 1,3,5-hexatriene and benzene, respectively. In chemical notation this class of molecules is characterized by alternating (conjugated) single and double bonds. Each carbon atom (or hetero atom) in the conjugated chain contributes one electron into delocalized π-orbitals. The dependence of the wave functions on the coordinate along which the conjugated π-electron chain extends is illustrated in Fig. 1 in a reasonable approximation. In the linear hexatriene the wave functions come close to standing waves in a box, all of them having a node on the

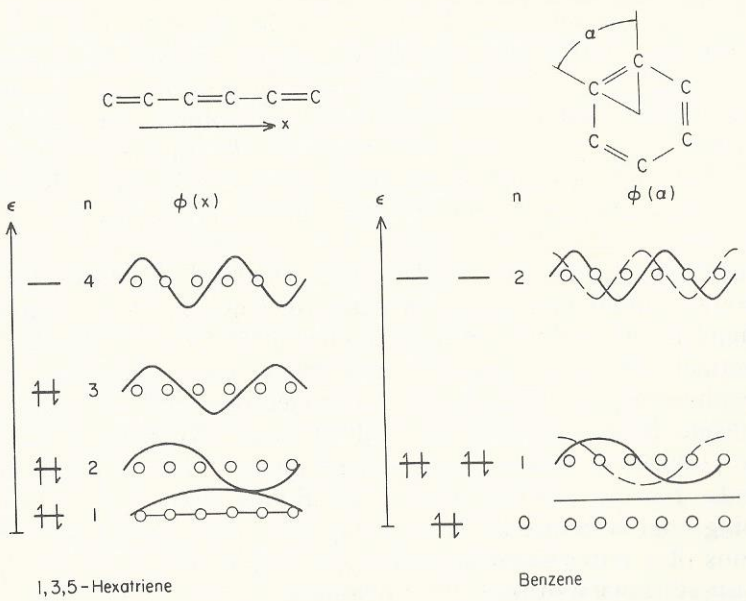

FIG. 1. Energy levels and wave functions of two π-electron systems.

boundary. The discrete energy levels belonging to these orbitals are illustrated at the right of the wave functions. In the linear polyene each orbital has a distinct energy characterized by a quantum number, n, while in the cyclic system two orbitals ($n > 0$) share the same energy. In the latter case one calls these energy levels degenerate. There is a total of six electrons in each system. Pauli's exclusion principle states that any orbital can be occupied by, at maximum, two electrons (with opposite spin). Thus, the distribution of electrons over energy levels, which is illustrated in Fig. 1, characterizes the ground state of the molecule. For hexatriene, the first excited state is obtained if one electron from the level with the quantum number $n = 3$ is lifted up to the level $n = 4$. In benzene it is obtained if one electron is lifted from $n = 2$ up to $n = 3$.

It comes out that the energy term system of conjugated π-electron systems is more and more compressed the larger the π-electron system is. In consequence, the energy necessary for the promotion of one electron from the highest occupied level in the ground state to the next unoccupied level is the smaller, the larger the conjugated π-electron system. This is why large π-electron systems have adsorption bands in the visible region, which means that they interact with

low energy light quanta, while smaller ones absorb in the u.v. (high energy light quanta). This is illustrated in Fig. 5.

Molecular energies are measured either in electron volts (eV), wave number (cm^{-1}), or frequency (Hz). These units are related by equation (1), wherein h is Planck's constant, c_0 is the vacuum light velocity, λ is the wavelength of light, ν is the frequency, e is the electric charge of an electron, and V is the electric potential difference through which an electron has passed.

$$\epsilon = h\nu = hc_0/\lambda = eV \tag{1}$$

The conversion factors between these units are given in Table I.

TABLE I

Conversion factors for molecular energies

	To be converted into			
Energy in	eV	cm^{-1}	Hz(s^{-1})	kcal $mole^{-1}$
eV	1	8067	$2{\cdot}418 \times 10^{14}$	23.05
cm^{-1}	$1{\cdot}240 \times 10^{-4}$	1	$2{\cdot}998 \times 10^{10}$	$2{\cdot}859 \times 10^{-3}$
Hz	4.136×10^{-15}	$3{\cdot}336 \times 10^{-11}$	1	$9{\cdot}541 \times 10^{-14}$
kcal $mole^{-1}$	4.337×10^{-2}	349·9	$1{\cdot}048 \times 10^{13}$	1

2 *Vibronic states*

A hydrogen atom is made up of two particles, a proton and an electron. It possesses six degrees of freedom. Its state is fully characterized by its electronic orbital plus the translational state of its centre of gravity. In molecules, however, there are more degrees of freedom. In addition to electronic motion around nuclei, the nuclei may oscillate against each other. Moreover, molecules undergo translational and rotational motion. Most important for our purposes are the vibrations. As electronic motion, vibration is characterized by certain stationary modes, each associated with a discrete energy level. Each of the electronic states is superimposed by a set of discrete vibrational modes. The energy difference between adjacent vibrational modes is smaller (typically by more than one order of magnitude) than the difference between adjacent electronic states. The gross structure of vibrational energy levels of a molecule is illustrated on the left of Fig. 2.

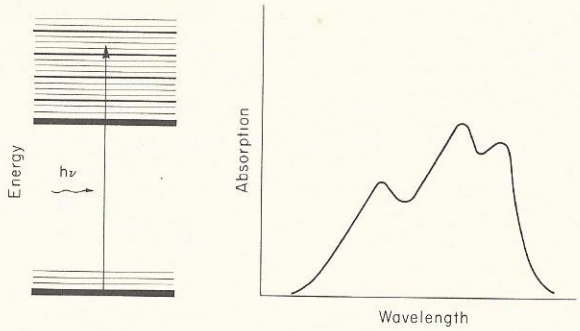

FIG. 2. Vibronic energy levels and absorption spectrum of an organic molecule.

3 *Boltzmann's distribution law*

In thermal equilibrium the distribution of molecules of a given species over their different vibronic states is described by Boltzmann's distribution law, which states: the relative occupation numbers (N_1, N_2) of two states having energies ϵ_1 and ϵ_2 and degeneracies g_1 and g_2, respectively, are

$$N_2/N_1 = g_2/g_1 \exp(-(\epsilon_2 - \epsilon_1)/kT) \qquad (2)$$

wherein k is Boltzmann's constant

$$k = 1{\cdot}3804 \times 10^{-16} \text{ erg deg}^{-1} = 8{\cdot}6165 \times 10^{-5} \text{ eV deg}^{-1}$$

and T is the absolute temperature. Thus, for two non-degenerate electronic states the energy distance of which is: $\Delta\epsilon = 2$ eV (corresponding to a frequency of $4{\cdot}8 \times 10^{14}$ Hz, or a wavelength of absorption of 620 nm, red light) the relative occupation numbers at 300°K are related:

$$N_2/N_1 = 2{\cdot}5 \times 10^{-34}$$

In thermal equilibrium at room temperature only the lowest electronic state of a molecule is occupied. The distance between adjacent vibrational sublevels is at least one order of magnitude narrower than the distance between electronic levels. The relative occupation numbers of two vibrational sublevels, the energy distance between which is 10^{13} Hz:

$$N_2/N_1 = 0{\cdot}2$$

At room temperature the lowest vibrational sublevel has a considerably higher occupancy than higher ones, however the occupancies of high levels are not negligible.

B ABSORPTION–EMISSION

1 *The dual character of light*

Light is part of the electromagnetic phenomenon, the spectrum of which extends from radio frequencies up to the frequencies of X-rays (10^{18} Hz). While in some experiments light behaves as a continuous wave phenomenon (e.g. in interference experiments), in others it acts

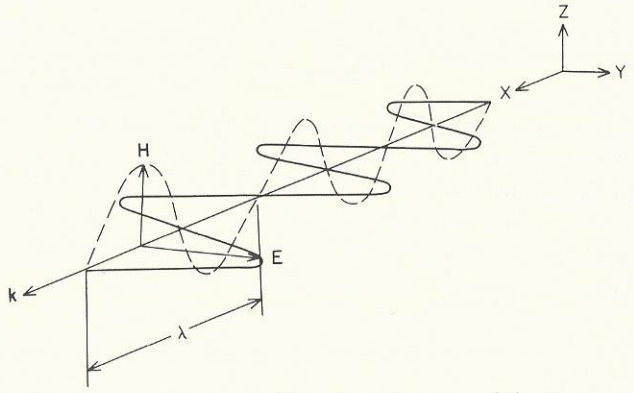

FIG. 3. An electromagnetic wave. The electric vector (**E**), the magnetic vector (**H**), and the propagation vector (**k**) are perpendicular to each other.

as if it were a stream of particles (e.g. in collision experiments). Since in spectroscopy both aspects are used, we will briefly sketch the dual behaviour of the same entity, light. Since Maxwell's classical electrodynamics, light is described as a continuous electromagnetic field oscillating in time and space. A plane wave of light is characterized by the following elements: the vector of propagation **k** (see Fig. 3), the direction of polarization (by convention it coincides with the direction of the magnetic field vector **H**), the intensity I, the wavelength λ (or frequency ν) and the phase angle θ. Figure 3 shows a snapshot of an electromagnetic wave travelling in the x-direction. For any point on the x-axis, the electric field vector and the magnetic field vector are enveloped by sine waves. Both fields are perpendicular to each other, they are in phase. The propagation

vector is perpendicular to both of them ($\mathbf{k}^\circ = \mathbf{E}^\circ \times \mathbf{H}^\circ$). The wavelength λ is related to the frequency ν by equation (3).

$$\lambda\nu = c \tag{3}$$

where c is the light velocity in the medium, which is related to c_0, the light velocity *in vacuo*, by the relationship: $nc = c_0$ ($c_0 = 2{\cdot}9979 \times 10^{10}$ cm s^{-1}) where n is the refractive index of the medium. The intensity of light defined as energy flux per square centimetre is proportional to the averaged absolute square of the electric field strength over one period.

The alternative aspect of light is a stream of particles carrying momentum:

$$p = h\nu/c \cdot k^\circ$$

and energy:

$$\epsilon = h\nu$$

both proportional to the frequency of the wave. The particle flux density is proportional to the intensity of the wave. The formalism of quantum mechanics does not incorporate the particle aspect of light explicitly. Instead, light is treated as a Maxwellian wave interacting with molecular antennae or coming from a molecular emitter. However, when qualitatively discussing absorption or emission of light one speaks of emission or absorption of one quantum.

2 *Rate laws*

There are three modes of interaction between a molecular two-state system with an electromagnetic wave. These modes are illustrated in Fig. 4.

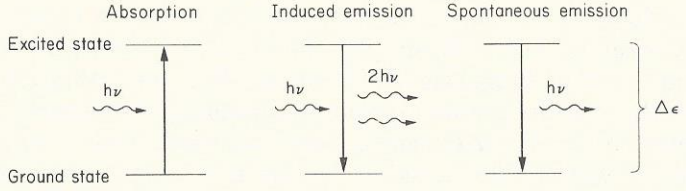

FIG. 4. Three modes for the interaction of a light quantum with a molecular two-state system.

a. Absorption. If the electromagnetic wave is in resonance with the two-state system, that is if $\Delta\epsilon = h\nu$, then a quantum might be absorbed and the system is transferred from the ground state to an excited state. In electronic transitions one electron is promoted to a higher energy level. The probability for excitation is proportional to the intensity of the lights (which is proportional to the particle flux density) and it is proportional to the number of molecular systems which are in their ground state N_0.

$$P_{\mathrm{ABS}} = BIN_0$$

b. Induced emission. If the two-state system is in its excited state a resonant wave may induce emission of a quantum and transition of the molecule into the ground state. As above, the probability is proportional to the intensity I and to the number of molecules in the excited state.

$$P_{\mathrm{IE}} = BIN_1$$

c. Spontaneous emission. In the absence of a radiation field deexcitation occurs via spontaneous emission of a quantum, the probability of which is proportional to the number of excited molecules.

$$P_{\mathrm{SE}} = AN_1$$

The net absorption or emission has the probability

$$P_{\mathrm{net}} = AN_1 + BI(N_1 - N_0) \tag{4}$$

For molecules in thermic equilibrium with their microenvironment, the lower electronic state is practically the only populated one. Thus, the major result of electromagnetic radiation is to transfer the molecules into an excited state. The Einstein coefficients A and B are intrinsic parameters of the given transition.

3 *Band spectra*

As illustrated in Fig. 2 the electronic energy levels of molecules are superimposed by vibrational energy levels. A complex molecule, say of N atoms, possesses $3N - 3$ (translation) $- 3$ (rotation) degrees of

freedom for vibrational motion. Each of these vibrational degrees of freedom has its own system of discrete energy levels. Since vibrational motion along different degrees of freedom is independent from each other, each vibrational energy level belonging to one degree combines with the levels from the remaining degrees of freedom. Thus the vibrational substates of a given electronic state form a rather complex system. The majority of the energetic sublevels are unresolved in common u.v. or visible spectrophotometers. This makes absorption spectra of organic dyes appear as broad bands. The width of these bands is determined by the probability of a transition from the occupied sublevels of the electronic ground state into different vibrational sublevels of the excited state. This probability is governed by the Frank-Condon principle (see Hanna, 1969). A mixture between resolved and unresolved subtransitions within a single electronic transition is observed in carotenoids as illustrated in Fig. 5 and schematically in Fig. 2. Here the vibrations of C—C conjugated double bonds have rather high frequencies (1600 cm^{-1}) which give rise to subbands about 30 nm apart from each other within a single electronic $\pi \rightarrow \pi^*$ transition.

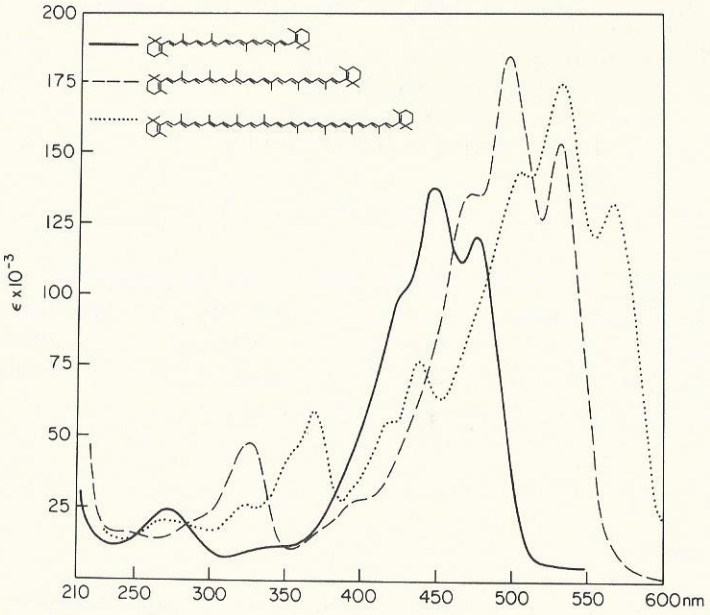

FIG. 5. Absorption spectrum of three symmetrical carotenoids with different lengths of their π-electron system (Vetter *et al.*, 1971).

4 *Deexcitation processes*

Possible fates of a light quantum which excites an organic dye into a higher vibronic state are illustrated in Fig. 6. It as assumed that the quantum is resonant with a subtransition of the second excited electronic state of the dye.

Since at room temperature molecules vibrate in their lowest mode, absorption most probably starts from the lowest vibrational substate of the electronic ground state, S_0. Deexcitation from the higher

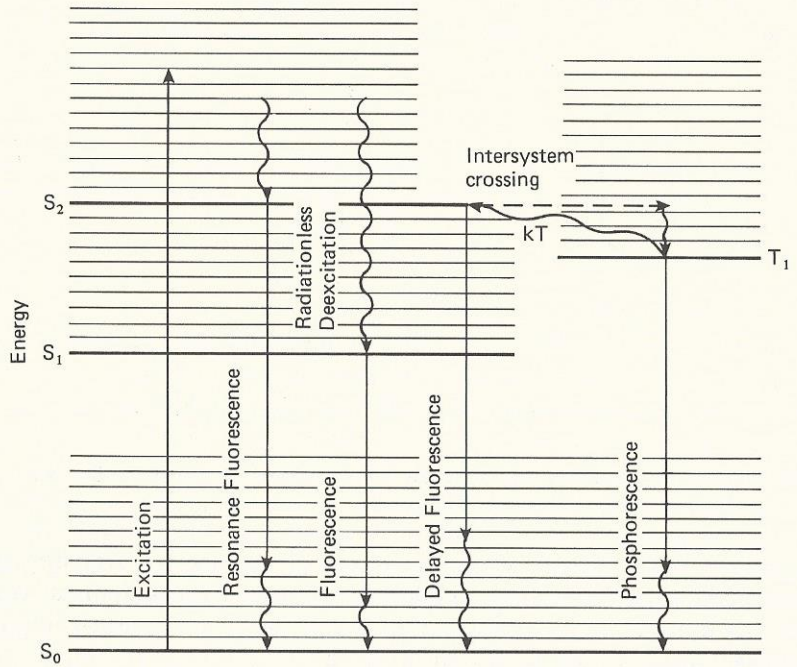

FIG. 6. Possible fates of a quantum of light in the vibronic energy system of a molecule. S, singlet states; T, metastable triplet state.

vibrational substate of S_2 may occur by two processes: first, *radiationless deexcitation* either to the vibrational ground state of S_2 or via substates to S_1; second, by resonant fluorescence. In *resonant fluorescence* a quantum of light is emitted, the energy of which is smaller than the energy of the exciting quantum. This is why fluorescence is always at longer wavelengths (smaller energy) than absorption. The relaxation time for fluorescence of organic dyes is in the order of 10^{-8} s. Radiationless deexcitation within the vibrational

substates of S_2 has relaxation times in the order of 10^{-12} s. Thus it precedes resonant fluorescence. In radiationless deexcitation, part of the photic energy is dissipated as heat. If higher vibrational substates of the lower electronic state (say S_1) overlap with the substates of the higher state (S_2) then radiationless deexcitation may go down even to the vibrational ground state of S_1. Under these conditions no resonant fluorescence resulting from S_2 will be observed. Instead, excitation into both electronic excited states, S_2 and S_1 results in fluorescence coming from S_1. This is illustrated in Fig. 7. This situation is encountered, for example in chlorophyll, where excitation into the Soret band and excitation into the Q-band both produce fluorescence from the Q-band.

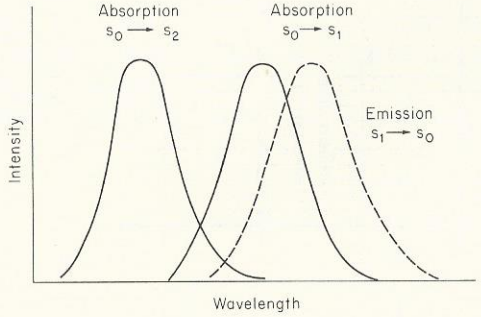

FIG. 7. The interrelationship between emission and absorption. For the transitions between singlet states, see Fig. 6.

Under special conditions, deexcitation occurs by transfer into metastable states (e.g. the triplet state or a photochemical intermediate state). These metastable states have comparatively long lifetimes (e.g. triplet states of π-electron systems, 10^{-1}–10^{-3} s). They decay via three pathways: *phosphorescence*, the emission of a quantum after a relatively long lifetime; *delayed fluorescence*, the emission of a quantum from the higher unstable state after thermal lifting up from the metastable state (the rate of delayed fluorescence is strongly temperature dependent); *radiationless deexcitation*, dissipation of energy into heat or conversion into useful work (in photochemistry).

Besides these processes, deexcitation of an individual molecule may occur via resonant energy transfer through neighbouring molecules, the excited states of which overlap with the states of the former. Resonant energy transfer is different from spontaneous

emission (as defined in Section IIB1) and reabsorption of a quantum. It may become more efficient than the other deexcitation processes if the molecules are close enough. Resonant energy transfer is a dominant process within the antennae system of photosynthesis (for more details, see Section IID4).

5 *Transition moments*

The probability that a molecular two-state system absorbs light depends on the absolute square of the scalar product of the electric vector of the light (**E**) and the transition moment (**M**) of the molecule.

$$p \approx |(\mathbf{E}\cdot\mathbf{M})|^2 \tag{5}$$

The transition moment is defined by the wave functions of the two orbitals between which a transition occurs (ϕ_1,ϕ_2) as follows:

$$\mathbf{M}_{12} = e \int \phi_1 \mathbf{r} \phi_2^* dv \tag{6}$$

Wherein e is the electronic charge, **r** is the space vector, and dv is the infinitesimal volume element, integration is extended over the whole space. ϕ/ϕ^* has the physical meaning of a probability density, $e\phi\phi^*$ is a probabilistic charge density, thus **M** has the dimension of a dipole moment. The transition moment is analogous to the dipole moment of a radio antenna. Equation (5) has two important consequences, selection rules and polarization effects in absorption and emission.

a. Selection rules. A transition between two states according to equation (1) occurs only if the transition moment is non-vanishing. This is not always the case. As an example, let us evaluate the transition from an orbital which is symmetric with respect to reflection at the xy-plane to another orbital sharing this property (see Fig. 8, upper). Since the x component of **r**, the space vector, is antisymmetric (changes sign) upon the same symmetry operation, integration over x yields 0. Thus the x component of the transition moment vanishes. As illustrated in the lower half of Fig. 8 the same symmetry properties of the wave function make the y component of the transition moment generally non-vanishing. (For a more general treatment, see Hanna, 1969.)

Strict all or none selection rules apply to atoms, while selection rules are less stringent with molecules. This is due to the modulation of symmetry by vibrational or collisional distortion of the molecular geometry.

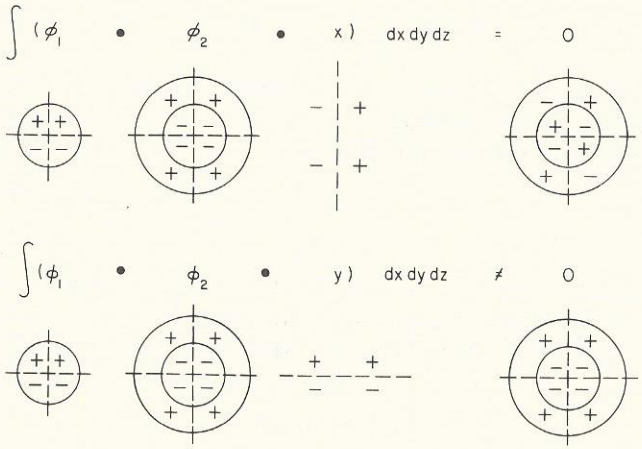

FIG. 8. Symmetry properties of two hypothetical molecular orbitals (ϕ_1,ϕ_2) and their influence on the magnitude and the direction of the transition moment between them.

b. Polarization effects. Another consequence of equation (5) is that the absorption probability depends on the angle between the electric vector of the exciting light and the direction of the transition moment of the molecule. The probability is maximum if the electric vector is parallel to the transition moment. The direction of the transition moment is defined by the molecular geometry which determines the wave functions ϕ_1,ϕ_2. In the example given in Fig. 8, the symmetry of the two orbitals is such that the x-component of the transition moment vanishes while the y-component is non-zero. Thus by studying the absorption of oriented molecules with respect to the direction of the electric vector of linearly polarized light, one gets information on the direction of the transition moment within the molecular coordinate system, or vice versa, if this is known from theoretical studies one obtains information on the orientation of the molecule with respect to the laboratory system.

A few examples: In a linear polyene, as illustrated in Fig. 1, the transition moment of the lowest energy transition ($n = 3 \rightarrow n = 4$) is directed along the long axis of the molecule. In contrast to this in benzene the transition moment of the lowest transition has no unique direction within the molecule. All directions within the ring plane are equally probable in absorption. In chlorophyll the Soret and the Q-band transitions are polarized within the plane of the porphyrin ring (Weiss *et al.*, 1965). However, these absorption bands are composites

of several subtransitions. This is reflected by mixed polarization within the band.

For a more detailed introduction into molecular spectroscopy, see Clayton (1970) and for a monograph see Murrell (1963).

C MEASURING ABSORPTION SPECTRA

1 *Lambert-Beer's law*

A beam of light passing through a homogeneous medium is attenuated by the amount dI in each section of thickness dx. The loss, dI, in intensity by absorption is proportional to the concentration of the absorbing species, c (only one species assumed), the thickness of the section, dx, and the incident intensity, I,

$$dI = -\alpha c I\, dx \tag{7}$$

wherein α is a wavelength dependent proportionality constant. Integration over the thickness l of an absorption cell yields the transmitted intensity after the passage through the cell.

$$I_{tr} = I_o \exp(-\alpha c l) \tag{8}$$

For convenience, one prefers the exponential at basis 10

$$I_{tr} = I_o\, 10^{(-\epsilon c l)} \tag{9}$$

wherein the proportionality constant α is substituted by the *decadic molar extinction coefficient* ($\epsilon = \alpha/2{\cdot}3$, ln $10 = 2{\cdot}3$). In some literature ϵ is called molar absorbancy index. ϵ has the dimension litre $\cdot$ mole^{-1} cm^{-1}. It is an intrinsic property of each molecular species. Usually it is tabulated for the peak wavelengths of an absorption band. The whole exponent is called the absorption of the sample, A (and sometimes optical density, OD). It is obvious that the absorption of a composite homogeneous sample is additive in the concentration of the different species.

$$A_{result} = \sum_i \epsilon_i c_i d \tag{10}$$

The relative transmission of the sample is

$$T = \frac{I_{tr}}{I_o}$$

The relative absorbed intensity

$$\Delta I/I = (I_{tr} - I_o)/I_o$$

While the exponential term A, absorption, is more appropriate for analytical purposes, since it is linearly related to the concentration of absorbing species, the absolute or relative absorbed intensity is important for photochemical considerations. It shows how much energy goes into a system.

2 *Practical difficulties*

Systematic errors in measurement of the absorption or the relative transmission of a sample arise from a couple of effects which are briefly sketched below.

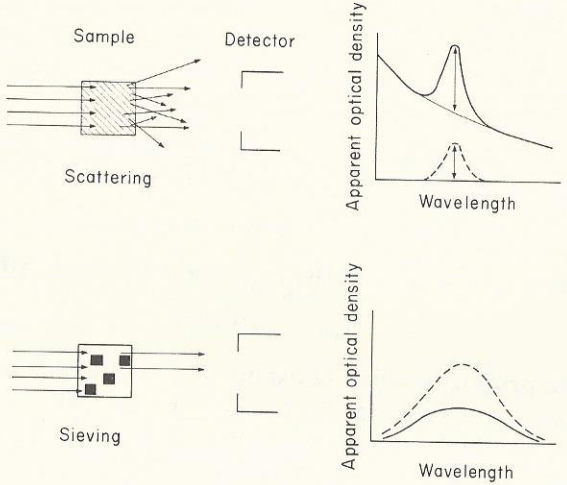

FIG. 9. The effect of scattering and of sieving on the apparent optical density of a sample. Solid lines indicate the apparent absorption, and broken lines the absorption in the absence of the disturbing effect.

(a) The wall of the absorption cell reflects back part of the impinging intensity. This is equivalent to an increase of absorption. The reflection of an air-glass interface for perpendicular incidence of visible light is about 5%.

(b) Absorption of the solvent or of the absorption cell material mimics absorption of the sample. The effects (a) and (b) can be overcome in a split beam spectrophotometer, where the transmitted intensity of the sample cell is related to the transmitted intensity of a reference cell containing the solvent only but no solute. Since the spectral dependency of these effects is rather flat in the visible, their effect on single beam spectra is only a rather homogeneous increase in the apparent absorption, but no finer spectral structure.

(c) Fluorescence of the sample tends to decrease the apparent absorption of the sample. Since fluorescence is emitted into the whole solid angle, while the interrogating light of the spectrophotometer is collimated, the relative effect of fluorescence can be lowered by setting the light detector at a larger distance from the sample so that it just catches the collimated interrogating beam, but only a minimal fraction of fluorescence. A check-up for the influence of fluorescence (and scattering) artefacts in measurements of absorption is made by comparative experiments at different solid angles between the sample and the light detector surface.

If these experiments yield the same results the influence of fluorescence and scattering is negligible.

(d) If the sample is turbid and scatters light (see Section IIIB2). The effect on the apparent absorption is threefold (see Fig. 9, above).

(i) Since part of the scattered light does not hit the detector, even though it is transmitted through the absorption cell, the absorption is over-estimated. The spectral dependence of scattering depends on the particle geometry and the refractive indices of the particles and the solvent (see Section IIIB2 for references). If this is rather flat in the visible spectral range, then it just produces an underground absorption with soft curvature as illustrated in Fig. 9 (above).

(ii) The effective optical path of a light quantum in the medium increases. Therewith, the probability to be absorbed increases. This leads to higher absorption than in clear solution. This is illustrated in Fig. 9 (above), where the area under the absorption band which is superimposed on the smooth, scattering spectrum is larger than the area measured for the same dye concentration in a clear solution. The effect of scattering on the optical path is most readily tested experimentally. A certain amount of a dye is added to a turbid suspension, the molar extinction coefficient of which is known from a clear solution. The ratio between the observed absorption and the expected

one equals the ratio between the effective optical path and the geometrical one.

(e) If the dyestuff is not homogeneously distributed in an absorption cell, the apparent absorption spectrum is flattened as illustrated in Fig. 9 (below), owing to the sieve effect (Duysens, 1956). This is relevant in studies with suspended algae or chloroplasts, where pigments are highly concentrated in thylakoid membranes. This effect is rather difficult to correct for quantitatively.

D DYES AS INDICATORS OF MOLECULAR EVENTS

If a dyestuff undergoes a chemical reaction or if it is transferred to another environment its electronic orbitals are deformed which alters the absorption spectrum. These spectral changes can be used as indicators of the respective event. (For a general reference concerning the use of dyes in analytical chemistry, see Bishop, 1972).

1 Redox reactions

Reduction is transfer of an electron to a compound, while oxidation is the removal of an electron from a compound. If the pH value is not too high, redox reactions are accompanied by protolytic reactions as illustrated for 2,6-dichlorophenolindophenol in Fig. 10. The conjugated π-electron system of this compound, which determines the absorption spectrum in the visible, extends over both rings in the

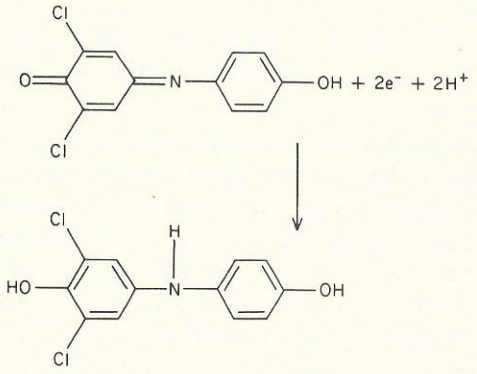

FIG. 10. The change in the electronic configuration of 2,6-dichloroindophenol on reduction at pH 7.

oxidized species, while on reduction it is split into two separate benzoic rings. As discussed in Section IIA1, the wavelengths of absorption increase with the length of the conjugated π-electron system. Thus one expects a shift in the absorption spectrum from longer towards shorter wavelengths on reduction. In fact, the blue colour (red absorption, blue transmission) of the oxidized dye is bleached on reduction. Since reduction shifts the absorption band of most dyes by several hundred nanometres, there is practically no overlap of the absorption bands of the reduced and the oxidized form. Thus the extent of absorption, say at the peak wavelength of the oxidized species, is proportional to the concentration of this species. Any change of absorption at this wavelength can be used as a linear indicator of the number of electrons transferred to the dye. Calibration is easy once the molar extinction coefficient of the dye is known from the literature or is determined by measuring the absorption of the known concentration of the oxidized species. The above dye was used by several authors to determine the number of electrons transferred through the electron transport chain of photosynthesis by pulse spectrophotometry (Kok *et al.*, 1966; Schliephake *et al.*, 1968; Ke *et al.*, 1971). For the spectral changes of plant pigments upon redox reactions *in vitro* see the following references: Seifert and Witt, 1968 (chlorophyll *a*), Chibisov *et al.*, 1965 (chlorophylls); Henninger *et al.*, 1966 (plastoquinone *b*); Singh and Wassermann, 1971 (cytochrome *f*); Katoh *et al.*, 1971 (plastocyanin); Mitsui and Arnon, 1971 (ferredoxin).

2 Protolytic reactions

While the colour change in redox reactions is due to a change in the number of π-electrons protonation of the cationic alkaline form of a dye acts indirectly on the π-electron system by changing the interference of non-bonding electrons with the π-electron system (hyperconjugation). Especially molecules which contain atoms with non-bonding electrons as oxygen and nitrogen react by a spectral shift in the visible to changes in their state of protonation. An example is illustrated in Fig. 11. *p*-Nitrophenol when protonized absorbs in the u.v. On dissociation at pH 9 the absorption is shifted towards longer wavelengths. A solution of the deprotonated dye appears yellow. A precise description of the changes in the π-electron system upon protonation is difficult. Several more or less equivalent descriptions exist, one of which is illustrated in Fig. 11. The transition from a benzoic (acid pH) to a quinonoid (basic pH)

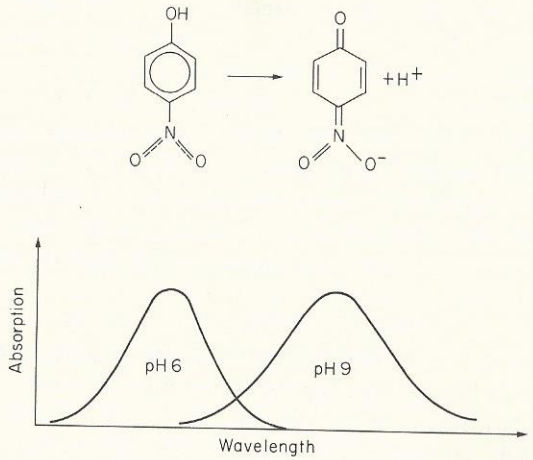

FIG. 11. The electronic structure and the absorption bands of paranitrophenol at different pH values.

π-electron system is a gross approximation. Several mesomeric states and hyperconjugations of the hetero atoms have to be taken into account. Usually, shifts of absorption bands on protonation and deprotonation are smaller than in redox reactions. However, as illustrated for the dye phenol red in Fig. 12, there is practically no overlap of the absorption band of the acid form with the peak wavelength of the alkaline form. Thus, the absorption at the peak wavelength of one form can be used as a linear indicator of the concentration of this form in solution. The response curve of a pH-indicating dye is illustrated in Fig. 13. The relative absorption on the indicator at the peak wavelength of the alkaline form (no overlap with the absorption spectrum of the acid form) is plotted against the pH value in a solution of the dye. At extremely alkaline pH the relative absorption is 1. At extremely acid pH it is 0. It was assumed that the dissociation constant K of the indicator equals 10^{-7}.

$$K = \frac{[I^-] \cdot [H^+]}{[IH]}$$

If the dissociated (I^-) and the associated (IH) form of the indicator are the only ones present then the sum of their respective concentrations is constant.

$$[I^-] + [IH] = [I_0]$$

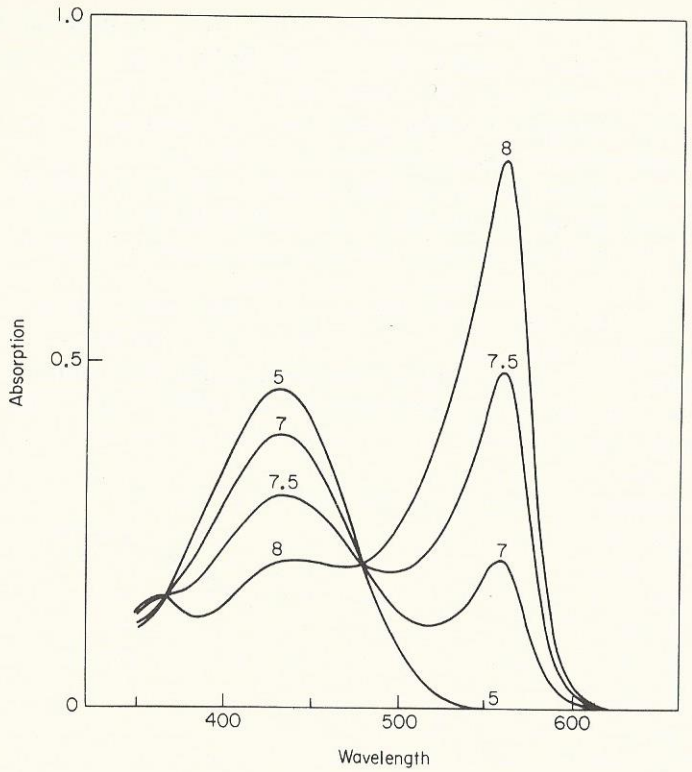

FIG. 12. The absorption spectrum of phenol red at different pH values.

And it follows

$$[I^-]/[I_0] = K/(10^{-pH} + 10^{-pK})$$

As is obvious from Fig. 13 the range over which the response of the indicator to pH is linear is rather small. It extends about ± 0·5 pH units around the mid-point pH which equals the pK value of the indicator (pK = −lg K). For tabulated pK values of pH-indicating dyes, see Bishop (1972). pH-indicating dyes have been frequently used to study protolytic reactions in cell organelles by spectrophotometric techniques. A necessary condition for the use of dyes is that they do not interfere with the biological activity. Several dyes have fulfilled these conditions in studies on the primary processes of photosynthesis (Schliephake *et al.*, 1968—bromthymol blue; Grünhagen and Witt, 1970—umbelliferone (used in fluorescence); Schröder *et al.*, 1971—phenol red; Junge and Ausländer, 1974—cresol red). From the

beginning of studies with pH indicating dyes in submicroscopic membrane systems (Chance and Mela, 1966) there has been discussion of whether or not absorbance changes from these dyes indicate pH changes, binding changes, or solvatochromic effects (Cost and Frenkel, 1967; Mitchell *et al.*, 1968). To make sure that absorbancy changes of a dye indicate pH changes and not something else, it is advisable to use dye concentrations in excess of those necessary to saturate specific binding sites at an organelle and in addition to apply the following tests (Junge and Ausländer, 1974): (i) the absorbancy change should be reciprocal to the buffer capacity of the system under study; (ii) the difference spectrum of absorbancy changes obtained with the organelle plus and minus buffer should correspond to the expectation for the response of the dye to pH changes *in vitro*.

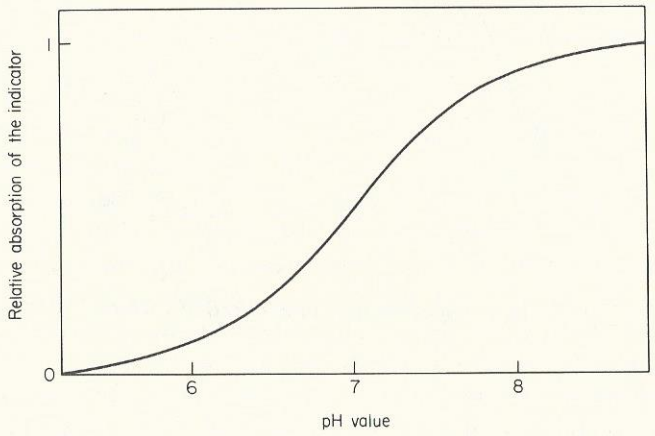

FIG. 13. The dependence on the relative absorption of the deprotonized form of a pH indicating dye with a pK value of 7 in dependence on the pH value.

3 *Electrochroism–solvatochroism*

If a molecular two-state system is exposed to a strong electric field exceeding say 10^5 V cm^{-1} two things may happen: (i) the molecule orientates owing to the interaction of its ground-state dipole moment with the electric field; (ii) the wave functions of the respective states are deformed. The latter leads to a shift of the respective energy levels and in consequence to shifts in the absorption bands of the dye. This effect is called *Stark effect* for atoms in the gas phase and

electrochroism for shifts of the unresolved band spectra of molecules in condensed phases (Labhart, 1967: Liptay, 1969). The first two terms in a power series expansion of the frequency shift of the absorption spectrum of a dye with fixed orientation towards the electric field vector are linear and quadratic in the electric field strength (E). They depend on the difference of the permanent dipole moments of the ground and the excited state $(\mu_1 - \mu_0)$ and on the difference in the polarizability $(\alpha_1 - \alpha_0)$ respectively.

$$\Delta\nu = \frac{1}{h}(\mu_1 - \mu_0)\cdot\mathrm{E} + \tfrac{1}{2}\mathrm{E}\cdot(\alpha_1 - \alpha_0):\mathrm{E} \qquad (11)$$

The direction of the shift in the absorption band towards higher or lower energies (shorter or longer wavelengths) of the first-order effect depends on the direction of the difference dipole-moment with respect to the electric field vector. The second-order effect is usually a shift towards lower energies owing to higher polarizability of the ground state in comparison with the polarizability of the excited state. Order of magnitude calculations (Labhart, 1967; Liptay, 1969) and experimental results on porphyrins (Malley *et al.*, 1968; Kleuser and Bücher, 1969; Schmidt *et al.*, 1971) indicate that the shifts of the rotational and vibrational transitions are smaller than those contributed by the electronic transition. Therefore, a nearly homogeneous shift of a whole absorption band can be expected. If the frequency shift is small as compared with the bandwidths the difference spectrum of a pigment between the two states, with and without electric fields, should be simply the first derivative of the absorption spectrum. Of course, one may think of other mechanisms that can give rise to spectral changes of a dye molecule exposed to transient electric fields, a field-induced change of chemical equilibrium as well as local conformational changes in its microenvironment that may influence the interaction of neighbouring pigments (Junge *et al.*, 1970a).

The effect of an electric field on the wavelength absorption is illustrated in Fig. 14. If the dipole moments of the excited state and the ground state $(\mu_1 - \mu_0)$ differ from each other (polarizability neglected), the energy levels of these states are shifted by different amounts in an electric field. This shifts the centre wavelength of an absorption band as illustrated in Fig. 15. For a molecule where the components of the dipole moment which are parallel to the direction of the electric field of the two states differ by 1 Debye* the

* 1 Debye is the dipole moment of two elementary charges of opposite sign which are 0·28 Å apart.

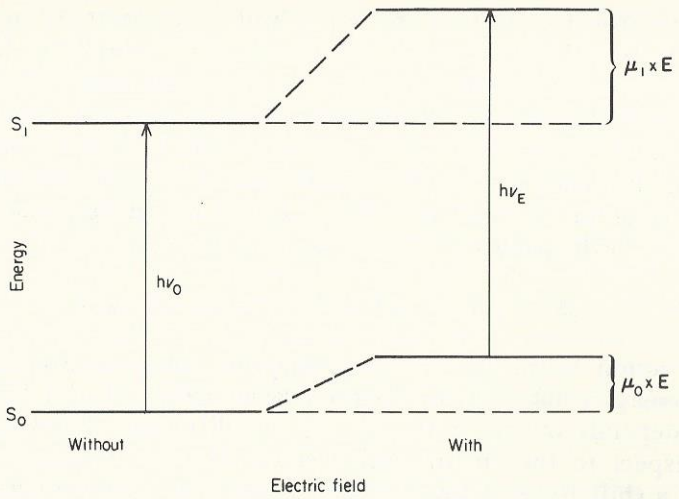

FIG. 14. Shifts in the energy levels of a molecular two-state system induced by high electric field strengths: μ_1 and μ_2 are the dipole moments of the excited and the ground states, respectively; E is the electric field strength.

wavelength shift of a band which is centred around 500 nm is rather small. At a field strength of 10^5 V cm^{-1} $\Delta\lambda$ = 0·042 Å, which is very small compared to the some 10 nm widths of absorption bands of most organic dyes. These shifts are hard to resolve spectrally. However, if the electric field is applied transiently to the dye, absorbancy changes will result, the spectrum of which is proportional to the first derivative of the absorption band. This holds in a good approximation when the shift is small as compared with the bandwidth. This, as illustrated in Fig. 15, transforms the task of resolving small spectral changes in the absorption spectrum into the resolution of small amplitude changes in difference spectra.

Electrochroic band shifts of chloroplast bulk pigments were used to elucidate the electric phenomena in the primary processes of photosynthesis (for detailed references, see Section IVC1). For the electrochroic responses of plant pigments (chlorophyll and carotenoids) *in vitro*, see the following references: Labhart (1961); Malley *et al.* (1968); Kleuser and Bucher (1969); Schmidt *et al.* (1971); Schmidt and Reich (1972).

Analogous to the influence of a directed external field on the spectra of organic dyes is the influence of local fields from dipolar solvent molecules in the neighborhood of a dye molecule in solution. A shift in the absorption spectra of organic molecules depending on

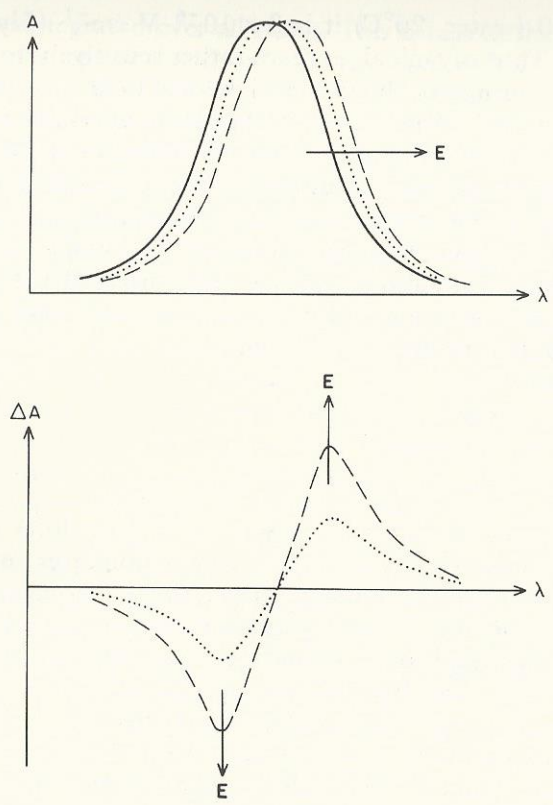

FIG. 15. The electrochroic shift of the absorption band of a dye which is exposed to a high electric field strength (E). The lower part shows the difference spectrum between the state in the presence of the electric field strength and in the absence of the electric field strength. This difference spectrum roughly corresponds to the first derivative of the absorption band.

the dielectric constant of the solvent is named *solvatochroism*. Solvatochroic effects are more pronounced for dyes with a large dipole moment in their respective ground states. A dipolar dye, when dissolved in a polar solvent, induces a more or less regular cage of solvent molecules. The addition of the dipolar electric fields of the solvent molecules of the cage creates a permanent electric field at the locus of the dye molecule. The magnitude of this "reaction field" is rather large, and so are the shifts of the respective absorption bands. For a molecule the diameter of which is 0.8 nm carrying a relatively small dipole moment of 1 Debye the reaction field in a medium with a dielectric constant $\eta = 2$ (a hydrocarbon phase) is 2×10^{-6} V cm^{-1},

while at $\eta = 80$ (water, 20°C) it is 3×10^{-6} V cm^{-1} (Liptay, 1969; equation 19). Thus organic dyes react rather sensitively to changes in their microenvironment. The rather high local field strength around a dye in a condensed phase biases it against a superimposed external electric field. In the condensed phase local fields exist even around molecules with no permanent dipole moment in their ground state. This is probably one reason for the observation of pseudolinear electrochroism of symmetrical carotenes (Schmidt *et al.*, 1971) which, if isolated, should reveal a second-order effect only, since neither their ground state nor their first excited state possesses a permanent dipole moment.

4 *Resonance interaction*

While the electrostatic interaction with a solvent shifts the absorption bands of molecules by at most a few nanometres, another type of a quantum-mechanical dynamic interaction of molecules in resonance may shift the absorption bands by 10 nm or more. A molecular two-state system is said to be resonant with another one if the energy difference between their two states is equal.

In the classical picture, an emitter or a receiver of electromagnetic radiation is represented as an oscillating dipole, an antenna. The dipole moment of an antenna finds its quantum mechanical analogue in the transition moment between two states (see Section IIB5). Classical dipoles interact, their energy of interaction is

$$\Delta\epsilon = \frac{\mu_A \cdot \mu_B}{|r_{AB}|^3}$$

wherein μ_A and μ_B are the respective point dipole moments and r_{AB} is the radius vector between them. Analogous to this is the interaction energy between two transient quantum mechanical dipoles in resonance:

$$\Delta\epsilon = \frac{M_A \cdot M_B}{|r|^3} \qquad (12)$$

wherein M_A and M_B are the respective transition moments of the two molecules A and B. Equation (12) holds for an idealized two-state system. (For real molecules with their unresolved substates,

it has to be integrated over all states. This brings in the overlap of the respective absorption bands of the two molecules.) The energy of interaction thus depends on the mutual distance and the relative orientation of the two molecules.

Resonance interaction of two molecules with identical energy levels leads to a splitting of these energy levels as illustrated in Fig. 16. The difference between the two new levels is $2\Delta\epsilon$. A detailed analysis of the influence of the geometry of an aggregate of pigments on the term system and on the selection rules governing its absorption behaviour was given by Kasha (1963). The result for a dimer of two identical molecules is illustrated in Fig. 16. The arrows in the upper part indicate the transition moments of the two components and the resulting transition moments of the dimer, respectively. The resulting transition moment of the dimer is calculated by addition or subtraction of the true transition moments of the components. In the parallel and in the head-to-tail arrangement one of the two superpositions cancels. According to equation (5) this implies that only one transition is observed in absorption. The non-zero resulting transition moment is attributed to one of the two energy levels of the dimer by analogy with electrostatics. The coulomb interaction energy of two dipoles in parallel arrangement is higher than the coulomb interaction energy of two dipoles with opposite direction. Thus, in the parallel arrangement, the non-

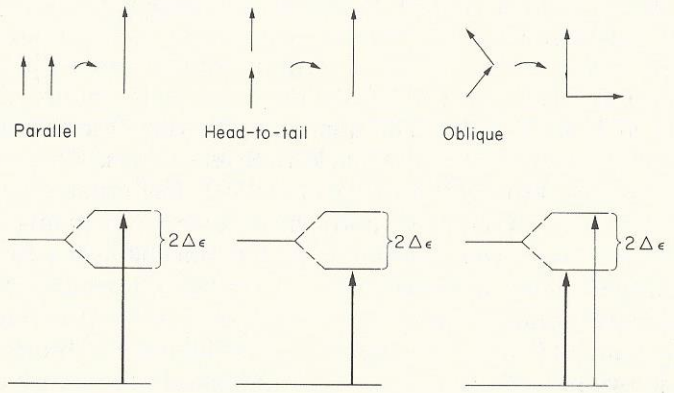

FIG. 16. Splitting of the energy levels in a dimer of two molecules under exciton interaction. Above: the superposition of the two monomeric transition moments to form the resulting transition moment of the dimer. The arrows in the lower part illustrate the selection rules for the dimer (McRae and Kasha, 1964).

vanishing transition moment belongs to the higher energy transition. For a parallel dimer one expects a shift of the absorption lines (absorption bands) to shorter wavelengths while for the head-to-tail one, one expects a shift to longer wavelengths. In an oblique dimer, however, both transition moments are non-zero, thus a band splitting occurs. This illustration refers to dimers. If N identical molecules interact in an oligomer there is a split into N energy levels. The selection rules are similar to those for dimers; however, the band shifts and the splittings are larger.

Resonance interaction of chlorophyll oligomers is one of the reasons for the rather large shifts of the *in vivo* bands of chlorophyll *a* in comparison to their position in dilute solutions (Hochstrasser and Kasha, 1964). Resonance interaction in an oblique dimer was considered as a possible reason for the double band of the photochemically active chlorophyll a_1 in the photosynthetic lamella (Döring *et al.*, 1968b).

Resonance interaction of two transition dipoles causes transfer of excitation energy between interacting molecules. This "resonance energy transfer" is distinct from spontaneous emission and reabsorption of a quantum, as described by the Einstein coefficients A and B (see equation 4). The rate of resonance energy transfer may exceed the rate of spontaneous emission by several orders of magnitude. At strong coupling the transfer time, according to Heisenberg's uncertainty principle, is conjugated to the interaction energy: $\Delta\tau \sim 1/\Delta\epsilon$. Two extreme cases of resonance energy transfer are to be distinguished. If the interaction energy is weak and, in consequence, the transfer time is long in comparison with the time for vibrational relaxation (10^{-12} s), the transfer is unidirectional as illustrated in Fig. 17 (left). The quantum, by vibrational relaxation, drops out of resonance before back transfer occurs. This case was first discussed by Förster (1946, 1947, 1959). The transfer of energy from the antennae system of photosynthesis in green plants into the photochemical traps was attributed to this mechanism of resonant energy transfer. The other extreme case is characterized by resonant energy transfer which is very rapid compared with the vibrational relaxation time (Fig. 17, right). This mechanism is bidirectional. Before vibrational relaxation occurs, the excitation energy is transferred manyfold between the interacting species. In the extreme case the excitation energy (the exciton) is delocalized over a whole aggregate of interacting molecules. At intermediate interaction energies there is some vibrational relaxation between subsequent transfer steps. However, the transfer is still bidirectional (weak exciton

coupling). For specific references as to exciton coupling, see Kasha, 1963; Hochstrasser and Kasha, 1964; McRae and Kasha, 1964. Which type of exciton interaction governs the function of the antenna system in photosynthesis of green plants is still under discussion (Borisov and Ilina, 1973).

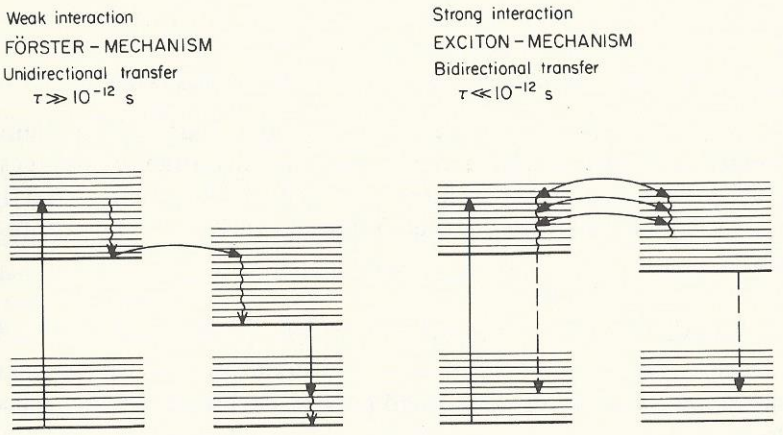

FIG. 17. Resonance energy transfer by the Förster mechanism and by the exciton mechanism, respectively (τ is the transfer time for a quantum of energy between two molecules).

III Flash kinetic spectrophotometry

A PRINCIPLE

Flash kinetic spectrophotometry is applied to study photochemically stimulated reactions. The system under study is excited by a flash, the duration of which is short compared with the response times of light-induced reactions. The kinetics of these reactions are interrogated by monochromatic measuring light tuned to pigments which participate in the reaction. The principle set up is illustrated in Fig. 18. A monochromatic interrogating beam impinges on an absorption cell containing the sample. To avoid excitation of the sample by the interrogating light, its intensity is kept low. The transmitted intensity is passed through a guard filter onto the cathode of a photomultiplier. The guard filter shields the cathode of the photomultiplier from the wavelength of the exciting light. The output of the photomultiplier, a voltage proportional to the incident light intensity, is amplified and displayed on an oscilloscope screen.

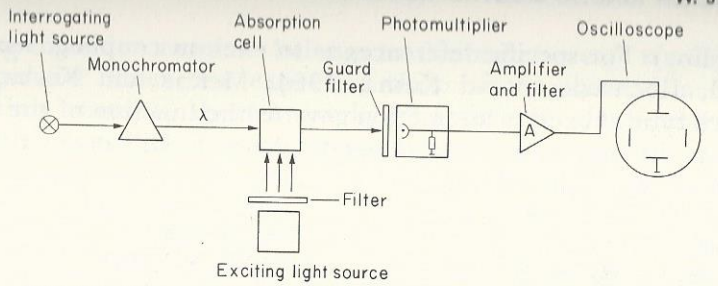

FIG. 18. The set-up of a kinetic flash spectrophotometer.

On excitation of the sample with a short flash photochemical processes are stimulated which lead to absorbancy changes of pigments involved. This induces changes in the transmitted light intensity which according to Beer's law are related to the absorption changes:

$$\Delta I_{tr} = \int_{A}^{A+\Delta A} \frac{dI}{dA} \cdot dA = -I_0 (10^{-(A+\Delta A)} - 10^{-A}) \qquad (13)$$

If the change in absorption is small ($\Delta A \ll 1$) this can be linearized as follows:

$$\frac{\Delta I_{tr}}{I} \approx -2{\cdot}3\ \Delta A \qquad (14)$$

The relative error of this linear approximation is in the order of ΔA. In studies on photosynthesis the linear approximation is rather precise since only a small fraction of the overall pigment contents of chloroplasts is chemically reactive, so that the relative change of absorption is rather small ($\Delta A/A < 10^{-2}$).

The time resolution of kinetic spectrophotometry is limited by two factors: the duration of the exciting flash and the response time of the detection system. These factors are discussed below in Section IIIC4–6. The sensitivity of the method to resolve small absorbancy changes is limited by three factors: random noise, due to the discrete nature of light, flash and fluorescence bursts which overload the detection system, and artefacts due to changes in light scattering of the sample. These factors are discussed in Section IIIB.

Besides a discussion of the limiting factors, Section III gives a description of major components of a kinetic spectrophotometer. The presentation will be restricted to a single beam spectrophotometer. However, the same components can be used to construct double-beam spectrophotometers of the cross-beam, the split-beam, or the double-beam type.

B LIMITING FACTORS FOR THE SENSITIVITY

1 *Shot noise*

a. The origin of shot noise. The major source of statistical noise in spectrophotometry is shot noise produced by the cathode of a photomultiplier. In order to understand the origin of statistical noise at the output of a photomultiplier, one has to consider that the apparently continuous light impinging on the photocathode represents a "machine-gun fire" of photons randomly distributed in time. The function of the cathode of the photomultiplier is to convert about one in ten of these photons into a photoelectron which then is multiplied by passing across the subsequent dynode stages of the photomultiplier. The amplified electronic current finally flows across a load resistor where it is converted into the output voltage of the photomultiplier.

The amplification of the photomultiplier is such that the short pattern of the primary photoelectrons is not fully smoothed out, but appears at the amplified level of the output. Usually subsequent stages of the signal processing which follow the anode of the photomultiplier limit the response time of the detection system. For the sake of simplicity* let us assume that we attach an ideal rectangular integrating filter to the output of the photomultiplier. This integrates over all (amplified) shots falling into the time range $\Delta\tau$, the integration interval of this device. After the time $\Delta\tau$ it puts out the integrated value and gets ready for another integrating step of the same length. Such a filter would convert a continuous transient signal into a sequence of discrete steps. It is an approximation of the input characteristics of a digital transient recorder (see Section IIIC6).

Let us assume that the average number of amplified shots falling into the time interval $\Delta\tau$ is N. Since the shots are stochastically distributed in time, their standard deviation is:

$$\sigma = \sqrt{N} \qquad (15)$$

In our case N is the number of photoelectrons released from the cathode of the photomultiplier during the interval $\Delta\tau$.

$$N = \phi \cdot Q \cdot \Delta\tau \qquad (16)$$

* For a rigorous treatment of noise, see Schwarz (1959).

Where ϕ is the quantum flux impinging upon the cathode (quanta/s), Q is the quantum efficiency of the cathode (electrons released per quantum absorbed), and $\Delta\tau$ is the integration interval. Thus the standard deviation in the output of the integrating filter is

$$\sigma = \sqrt{(\phi Q \Delta\tau)} \tag{17}$$

The signal itself is proportional to N, the average number of shots falling into the integration interval. In our context, we are interested rather in small differences in the transmitted light intensity than in the steady state value. However, ΔN is proportional to N as is obvious from analogy to equation (14):

$$\Delta N/N = -2{\cdot}3\Delta A \tag{18}$$

Thus the signal-to-noise ratio for measuring changes in transmitted intensity becomes:

$$\mathrm{S/N} = |\Delta N|/\sigma$$

$$\mathrm{S/N} = 2{\cdot}3\Delta A \sqrt{(\phi Q \Delta\tau)} \tag{19a}$$

Frequently one discusses noise problems in terms of frequencies (f) and of the bandwidths in frequency space (Δf). The frequency bandwidth is reciprocal to the integration time constant of the filter: $\Delta f = \beta/\Delta\tau$. The proportionality constant β is in the order of 1. Its value, as calculated by Fourier transformation, depends on a convention as to where to cut off the frequency spectrum for sufficient precision. Thus, in the frequency representation the signal-to-noise ratio becomes:

$$\mathrm{S/N} = 2{\cdot}3 \times \sqrt{\beta} \times \Delta A \sqrt{(\phi \cdot Q/\Delta f)} \tag{19b}$$

What do we learn from equations (19a) and (19b)? The signal-to-noise ratio can be improved by: (i) selecting a photomultiplier cathode with a high quantum yield (Q); (ii) increasing the intensity of the interrogating light (ϕ); (iii) increasing the integration time constant or by narrowing the frequency bandwidths of the detection system, respectively.

If one aims at resolving absorbancy changes at a given signal-to-noise ratio, say of 10/1, then according to equations (19a, b), the sensitivity, that is the minimum absorption change to be resolved at this precision, is conjugated to the integration time $\Delta\tau$. The latter, however, has to be matched to the relaxation time τ of the event under study (see below). To avoid major distortion of the signal (say

10% error in the rise time τ) a choice of $\tau/\Delta\tau = 20$ has to be considered as a lower limit. Thus, the sensitivity is reciprocal to the square root of the first-order time constant of the signal:

$$\Delta A_{\min} \sim 1/\sqrt{\tau_s} \tag{20}$$

Before making quantitative estimates, it has to be mentioned that the above defined signal-to-noise ratio is impractical. Instead of the standard deviation upon which it is based, rather the peak-to-peak value of the noise is relevant for the precision of the read-out of a signal from the oscilloscope screen. Thus, let us define a practical signal-to-noise ratio. This is about a factor of 10 smaller than the ratio given in equation (19) (for a detailed analysis of this factor, see Landon, 1941; Rüppel and Witt, 1969). A quantitative evaluation of the interrelationship between sensitivity and time resolution is given in Table II. It is based on the following parameter values: $\mathrm{S/N}_{\mathrm{pract}} = 10/1$, $Q = 0{\cdot}03$ (as realistic for a cathode with a S20 characteristic at a wavelength of 700 nm), a factor of 0·1 inserted into equations (19a, b) according to the above remark, $\Delta\tau = T/20$ (as justified below), quantum fluxes $\phi = 35{\cdot}10^{11}$ and $35{\cdot}10^{13}$, respectively (corresponding to 10 and 1000 erg/s at 700 nm, respectively).

TABLE II

Limiting sensitivity for absorbancy changes (ΔA) with a first-order rise time (T) at two different radiant fluxes across the cathode of a photomultiplier

T	$\Delta A^{\min}$ (10 erg/s)	$\Delta A^{\min}$ (1000 erg/s)
10 μs	2×10^{-1}	2×10^{-2}
100 μs	6×10^{-2}	6×10^{-3}
1 ms	2×10^{-2}	2×10^{-3}
10 ms	6×10^{-3}	6×10^{-4}
100 ms	2×10^{-3}	2×10^{-4}

These values for the light intensity and the integration time constant are justified below. At the above light fluxes and quantum yields there is no way of improving the sensitivity without lowering the signal-to-noise ratio in single flash experiments or admitting higher than 10% distortion of the rise time of the signal. An improvement of the signal-to-noise ratio is possible only by repetitive measurement of the signal and averaging.

b. Improving the signal-to-noise ratio. (i) The absorption of the sample. To minimize the signal-to-noise ratio with respect to the absorption of the sample its partial derivative with respect to the absorbancy A has to be set zero. We assume that the absorbancy change induced by a saturating flash is a constant fraction of the total absorption at a given wavelength: Then from $\Delta A(\lambda) = \alpha A(\lambda)$ it follows: $A_{opt} = 2/\ln 10 = 0{\cdot}87$. This corresponds to a transmission of 13·5% (Rüppel and Witt, 1969). This optimum is independent of whether or not there are more than one chemical species absorbing at the given wavelength while only one contributes to absorbancy changes in consequence of an exciting flash.

(ii) The intensity of the interrogating light. As obvious from equations (19) the signal-to-noise ratio increases with the square root of the intensity of the interrogating light. In photosynthesis applications the upper limit of the light intensity is usually not limited by the maximum ratings of the photomultiplier cathode but by the tolerance of the photosynthetic system to continuous light. This tolerance varies according to the partial event under study. Grossly speaking, the measuring light intensity is appropriate if much less than one quantum is offered to each photochemical reaction centre per relaxation time of the event under study. While the rate limiting step of the electron transport chain is characterized by a relaxation time of about 10 ms, the light-induced pH difference under low light intensity relaxes in the order of seconds. Thus the measuring light intensity can be higher in studies of the electron transport chain than in studies on flash-induced pH changes. This gross rule can be applied to estimate the tolerable light intensity. However, it is easier and safer to determine the limiting light intensity empirically by increasing the intensity until a further increase changes the signals which are studied.

Light intensities of 100 erg cm^{-2} s^{-1} are safe for most studies on the electron transport. At the absorption of the sample which is optimum for the signal-to-noise ratio (see above) this produces about 10 erg cm^{-2} s^{-1} transmitted intensity through the sample. With a 1 cm^2 absorption cell this produces 10 erg s^{-1} on the photocathode of the multiplier. This value entered into the quantitative estimate for the sensitivity given in Table II. For a better signal-to-noise ratio it is advisable to use as high a measuring light intensity as possible. To overcome these rather low limiting intensities in studies where very small, rapidly relaxing absorbancy changes are to be resolved, it might be advantageous to pulse the interrogating light, thus offering a higher intensity for the short time interval of interrogation. This

avoids a high continuous light load imposed on the system.

Pulsing is most easily done by placing a triggerable photoshutter between the interrogating light source and the sample as illustrated in Fig. 27.

(iii) The integration time constant (electrical bandwidth). According to equations (19) the signal-to-noise ratio improves if the integration time constant is increased (if the electrical bandwidth is decreased). There is an upper limit for increasing the integration time constant. This is determined by the relaxation time of the event under study. As an example for a reasonable matching let us consider a simple first-order kinetic which is processed via an RC low-pass filter (see Fig. 19), the time constant of which is $\tau_F = RC$. The first-order event is described by a rising time function:

$$F(t) = 1 - \exp(-t/\tau_s)$$

wherein τ_s is the time constant of the first-order event. When processed through the low-pass filter, the output becomes:

$$F(t) = 1 - \frac{\tau_s}{\tau_s - \tau_F} \exp(-t/\tau_s) + \frac{\tau_F}{\tau_s - \tau_F} \exp(-t/\tau_F).$$

This expression is obtained by means of Laplace transforms (for an introduction, see Holbrook, 1966). Figure 20 shows how the signal is distorted after procession via the low-pass filter for different ratios of the filter time constant (τ_F) versus the time constant of the signal (τ_s). As obvious from Fig. 20, filter time constants which are twenty times smaller than the time constant of the signal are to be recommended, if one aims at at least 10% precision in the read-out of the rise time of the event. The error in the half rise time of the signal in dependence on the ratio of the two time constants is given in Table III.

TABLE III

The error in the apparent half rise time of a first-order signal (rise time T) after procession via an RC low-pass filter ($RC = \tau$)

T/τ	Percentage error in $T_{1/2}^{app}$
50	2
20	7
10	14
5	30

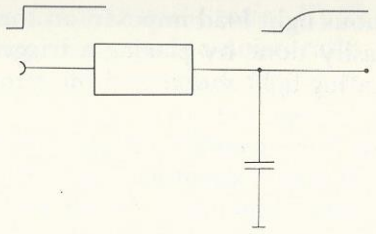

FIG. 19. An *RC* low-pass filter.

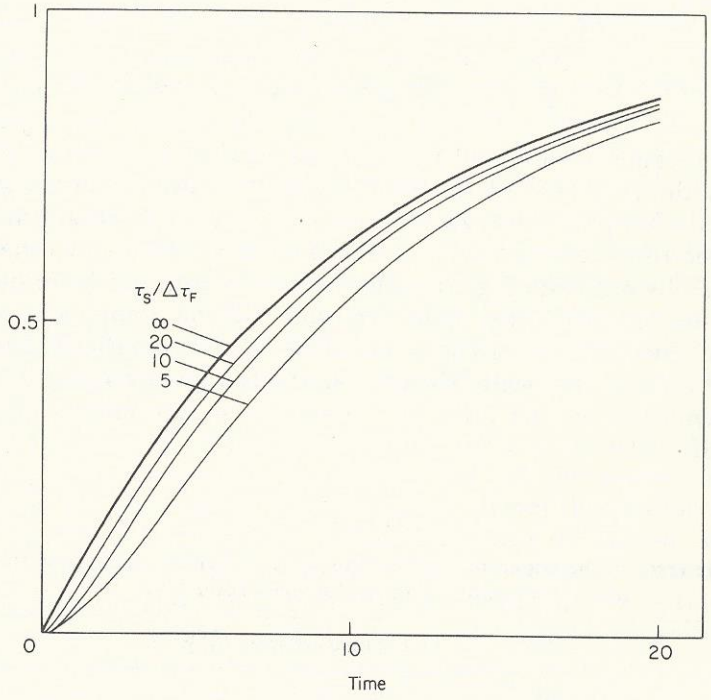

FIG. 20. Distortion of a signal with an exponential rise (heavy line) by a low-pass filter as illustrated in Fig. 19 (τ_S is the exponential rise time of the undistorted signal, τ_F is the integration time constant of the low-pass filter, $\tau = R \cdot C$).

(iv) Averaging: As discussed in Section IIIB1*a*, the signal-to-noise ratio is proportional to the square root of the number of photoelectrons falling into the time interval across which integration is made. It has been shown above that the variables entering into equations (19), the light intensity and the integration time constant, have upper limits in a given application. So the sensitivity of the measurement can be increased only if the signals are induced repetitively and averaged. This is equivalent to a multiplication of the number of photoelectrons which enter into the integration. The signal-to-noise ratio after averaging over M signals in a reasonable approximation is $\sqrt{M}$ times the signal-to-noise ratio from a single excitation experiment

$$(S/N)_M \cong \sqrt{M} \cdot (S/N)_1 \qquad (21)$$

So, averaging over 10^4 signals allows the detection of 100 times smaller absorbancy changes at a given time revolution, e.g. detection of $\Delta A = 2 \times 10^{-4}$ instead of 2×10^{-2} at 100 ms time revolution (see Table II). For averaging of transient signals, digital multichannel analysers are commercially available, which are described below. Since these devices, in principle, now cover a time domain ranging from 10 ns per channel up to seconds, other averaging techniques become less and less important. The improvement of the signal-to-noise ratio by averaging is limited too. Owing to noise generation in the averaging device the gain in signal-to-noise ratio after the number of repetitions exceeded a maximum value is no longer proportional to the square root of M. Usually, the signal-to-noise ratio can be improved more than a hundredfold corresponding to averaging of 10^4 cycles before the intrinsic noise production of the averager comes into play (for details see Buchwald and Rüppel, 1971).

2 *Changes in the light-scattering properties of the sample*

In spectrophotometry light scattering in turbid suspension may mimic absorption and introduce errors into the quantitative determination of extinction coefficients, as pointed out in section IIC2. Even worse, in kinetic flash spectrophotometry transient scattering changes due to conformational changes of the samples may mimic absorbancy changes. Since the extent of changes in the transmitted intensity as detected by the photomultiplier which are due to scattering may be of the same order as the absorbancy changes, a closer look at this phenomenon seems worthwhile.

Rayleigh scattering of a particle for light with wavelength beyond the absorption band of the particle is due to the electric polarizability of a molecular system. The oscillation of the electric dipole induced by the electric component of the light acts as a high frequency emitter radiating with dipole characteristics around the axis of the electric vector of the light. Since the loci and the orientation of different particles in an aqueous suspension are random, the scattering pattern, that is the angular distribution of the scattered light intensity, of say a chloroplast suspension, shows no interferences resulting from the partial waves of different particles. In X-ray scattering experiments these patterns are evaluated to elucidate the fine structure of biological objects (e.g. chloroplasts; Kreutz, 1970). For light in the visible spectral range these patterns are much less pronounced.

The scattering amplitude at a given angle of observation depends on the geometry and the refractive index of the particles (Van Holde, 1971, Section 9). The effect of scattering in flash kinetic spectrophotometry is threefold:

(a) Scattering increases the effective path of light through the absorption cell (as illustrated in Fig. 9). Thus it induces overestimation of extinction coefficients. This effect can be determined by adding a known amount of the dye to a turbid suspension and comparing the apparent absorption with the expectation for a clear solution.

(b) Scattering mimics absorption: for maximum signal-to-noise ratios one tends to image the interrogating light source to the cathode of the photomultiplier (see Section IIIC1). If the suspension in the absorption cell is turbid, part of the intensity will be scattered out of the original beam which leads to underestimation of the transmitted intensity, or overestimation of the absorption. The wavelength dependence of Rayleigh scattering is characterized by a factor $1/\lambda^4$. This means that scattering increases continuously towards shorter wavelengths. A fine structure is superimposed on this gross structure of the scattering spectrum. Scattering depends on the refractive index of the scattering particles which according to Kramer-Kronig's relation is related to the absorption. Scattering is stronger in spectral regions of absorbancy bands of molecules in the sample (for the scattering spectrum of a chloroplast suspension, see Yamashita *et al.*, 1968).

The effect of scattering can be partly compensated by placing the cathode of the photomultiplier directly onto the absorption cell, in order to catch as much of the scattered light as possible. More efficient, although not easy to handle, is an Ulbricht sphere collecting the light of almost the full solid angle.

(c) Scattering changes mimic absorbancy changes: Excitation of a chloroplast suspension with light stimulates the generation of electrochemical potential of the proton across the functional inner membranes (see Section IV). This causes the inner vesicles of chloroplasts to respond osmotically which, depending on the salt conditions, results in swelling or shrinkage.

Size changes induce changes in the light-scattering properties. Studies on this phenomenon reveal apparent transient absorbancy changes which are due to changes in the shape plus others due to changes in the refractive index of the functional membranes of photosynthesis (Deamer *et al.*, 1967). The relaxation time of these effects was mostly in the order of seconds, however, even more rapid changes in the ms range have been observed (Junge and Heathcote, unpublished observation).

The scattering changes were used to study volume changes in photosynthetic systems (Packer, 1963; Izawa *et al.*, 1963; Deamer *et al.*, 1967; Yamashita *et al.*, 1968). In the context of this article they are an undesired effect which limits the resolution of a kinetic spectrophotometer. Since a theoretical correction for the effect of scattering (Amesz *et al.*, 1961; Latimer *et al.*, 1968; Bryant *et al.*, 1969) is almost impractical it is advisable to check for the relative contribution of scattering changes to the apparent absorbancy changes by an experimental test: the absorbancy changes are recorded at different distance of the photomultiplier cathode from the absorption cell, corresponding to a variation of the solid angle for capturing scattered light between $\cong 0$ to 2π. Any difference in the extent or in the kinetics of the apparent absorbancy changes indicates the presence of transient scattering changes.

3 *Flash bursts and fluorescence artefacts*

In flash spectrophotometric studies one operates at the rather low interrogating light intensity with a high photomultiplier amplification. The energy of the actinic flash is high. During the firing of the flash scattered flash light impinges on the cathode of the photomultiplier, the intensity of which usually is higher than the intensity of the interrogating light. The same may hold for fluorescence

originating from the sample. This may cause temporary blank-out of the detection system at least for the flash duration. Since the duration of the exciting flash is chosen to be short compared with the relaxation time of the event under study, a short artefact would not be that harmful. However, overload of the detection system by a short pulse causes slow recovery of the detection system which may mimic absorbancy changes at a time range much larger than the flash duration. This is illustrated in Fig. 21. The upper part of Fig. 21

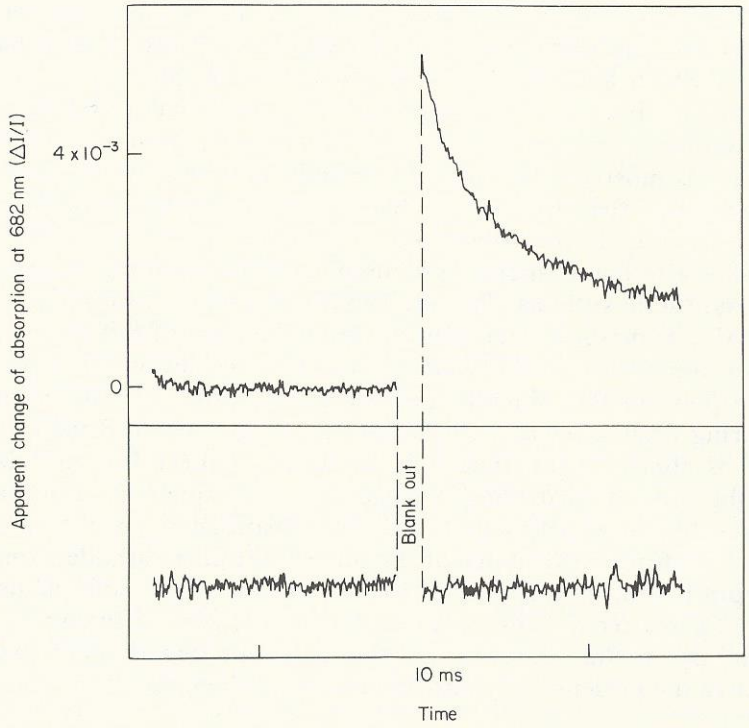

FIG. 21. Example of a flash burst artefact and its elimination with the aid of a digital averaging computer. The signal in the upper part was obtained by excitation of a cuvette filled with diluted milk which was excited by flashes with a half time of 15 μs at the beginning of the blank-out. The slow signal following the blank-out is an artefact caused by the relaxation of the detection system. The trace in the lower part was obtained by subtracting the same number of repetitions from the upper signal, but with the interrogating light switched off in the presence of an auxillary light source supplying the same intensity to the cathode of the photomultiplier as before. Note that the noise level in the lower part is increased.

shows an apparent absorbancy change obtained on excitation of the diluted milk suspension (apparent absorption about 1). The apparent transient absorbancy change is entirely due to a relaxation of the detection system after receiving the intensive scattered flash light, the duration of which was 15 μs.

To minimize the effect of flash bursts and fluorescence artefacts the following operations might be useful:

(a) *Guard filters* placed on the cathode of the photomultiplier with a low transmission at the wavelength of the exciting light are useful for the elimination of the flash burst. However, they will not eliminate fluorescence which occurs at the wavelength of the interrogating beam.

(b) *Restriction of the solid angle* defined by the centre of the absorption cell and the cathode of the photomultiplier reduces both the effect of scattered flash light and fluorescence. Since scattered light and fluorescence are emitted into the full solid angle while the interrogating beam can be focused into a narrow angular domain, the ratio of interrogating intensity over flash burst or fluorescent intensity can be increased by narrowing the solid angle. However, this method becomes inefficient with strongly scattering samples. There restriction of the solid angle decreases both the flash-burst artefact and the transmitted measuring light intensity which in heavily scattering samples is emitted almost into the full solid angle. Moreover, narrowing of the solid angle might become harmful since it increases the relative contribution of transient scattering changes to the apparent absorbancy changes of the sample.

(c) *Subtraction of the artefacts* is a safe method if all other methods fail. In cases where averaging computers are used one might proceed as follows:

(i) Measure the absorbancy changes superimposed by the artefact by averaging over, say, M repetitions.

(ii) Subtract the same number of artefacts after switching off the interrogating light (Döring *et al.*, 1968b). When subtracting the flash-burst artefact in the absence of measuring light it is safer to keep the photomultiplier at the same operational point. That is, to present the same continuous light intensity as before to the cathode of the photomultiplier, however, now without having passed through the absorption cell. Under these conditions sub-

traction allows for almost complete elimination of even severe flash-burst artefacts, as is obvious from a comparison of the upper trace with the lower trace in Fig. 21. If subtraction is made in the absence of any continuous light which keeps up the same operational point of the photomultiplier, subtraction does not necessarily lead to the elimination of the artefact.

(d) A rapid kinetic spectrophotometer with high frequency *modulated interrogating light* was constructed by Buchwald (1972) for measuring absorbancy changes even at wavelengths which coincide with the peak wavelengths of fluorescence emission from chloroplasts. Since fluorescence and flash burst artefacts are not modulated by the same frequency as the interrogating light, their contribution to the output of a photomultiplier can be eliminated by selective electronic filters set to the specific frequency of the modulation of the interrogating light. However, this technique, which requires extreme linearity of the applied photomultiplier and opto-electronic modulation techniques, is not easy to handle.

C INSTRUMENTATION

1 *Mechanical and optical set-up*

The small absorbancy changes which are to be resolved in photosynthesis require special attention to mechanical, optical, and electronic stability of the set-up. For maximum mechanical stability it is advisable to isolate the interrogating beam, including the components from the light source to the photomultiplier mechanically from all other components which generate mechanical noise, such as ventilators, flash lamps, thermostats, photoshutters, and the ground, of course. A simple set-up which is used in the Max-Volmer Institut consists of a heavy double-T steel bar which carries the interrogating beam, mounted elastically on car inner tubes. The rather low eigenfrequency of the heavy bar prevents interference with mechanical noise in the subsecond time domain of interest. Flash lamps and auxilliary equipment may be mounted on separate table or racks. The optical set-up of the interrogating beam is determined by the following five factors:

(a) Usually the photosynthetic system tolerates only relatively low intensities of the interrogating light. Thus imaging the light source on to the absorption cell is not critical.

(b) For a good signal-to-noise ratio it is essential that all quanta which pass the absorption cell are captured by the cathode of the photomultiplier. This is fulfilled if the light source is imaged through the absorption cell on the cathode of the photomultiplier as illustrated in Fig. 22. Since the light should pass through the absorption cell rather parallel, it is advisable not to use a condenser lens with too short a focal length. The adequate magnification and the relative positions of the interrogating light source, the condenser lens, the absorption cell are determined by the size of the absorption cell which is the limiting diaphragm in the beam. A condenser lens with a focal length of 10 cm is appropriate with absorption cells up to 2 cm optical pathlengths.

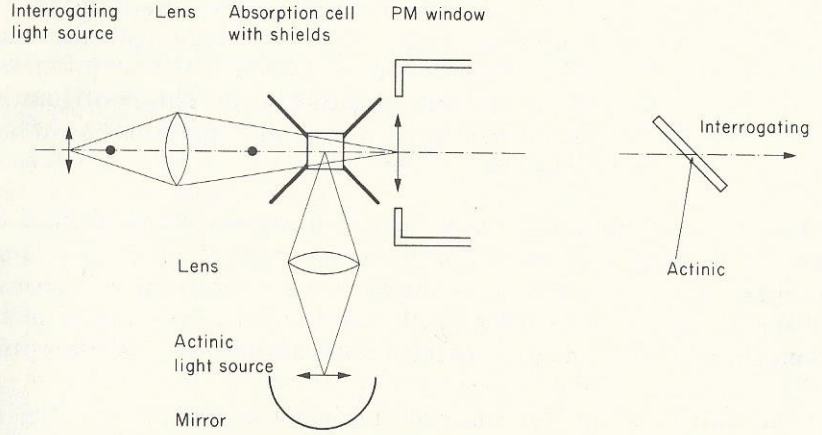

FIG. 22. Simple optical set-up for a flash kinetic spectrophotometer. On the right, the geometry if a narrow cuvette is used.

(c) For good optical stability it is important not to use too critical imagings, e.g. to image the periphery of the light source straight on to the periphery of the photomultiplier window or any diaphragm in the beam. In this case mechanical instability causes intensity fluctuations which are seen by the photomultiplier. For maximum stability it is advantageous to align the optical components first, according to the above criteria and then, for fine adjustments, vary the relative positions of the optical components (lamp, lenses, diaphragm, absorption cell, and photomultiplier) with respect to each other while watching the d.c. output of the photomultiplier for maximum intensity. At maximum intensity the influence of mechanical instability on the photomultiplier output is at its minimum.

(d) Stray light not passing through the absorption cell decreases the extent of the apparent absorption changes. Appropriate shields and diaphragms have to be used to avoid the possibility that light not passing through the sample hits the cathode of the photomultiplier. An appropriate diaphragm is illustrated by heavy black bars in Fig. 22. This, besides acting as a diaphragm for the interrogating beam, provides an additional shield of the photomultiplier cathode against the actinic flash light.

(e) In those cases where flash bursts or fluorescence artefacts are to be avoided, the photomultiplier has to be placed at a larger distance from the absorption cell. The solid angle formed by the cuvette and the aperture of the photomultiplier can be further restricted by a diaphragm placed on the cathode. The interrogating beam is imaged onto this diaphragm, the shape of which should correspond to the shape of the lamp filament or the arc used for the interrogating beam. This configuration may be obtained by a single lens too, although this has to have a larger focal lens (say, 40 cm).

If a monochromator is used instead of an interference filter for tuning the interrogating light, then the optical imaging is more complicated. First, one images the light source onto the entrance slit of the monochromator then, with another lens, the exit slit of the monochromator is imaged to the photocathode via the absorption cell.

The optical set-up for the exciting beam is illustrated in Fig. 22 too. The light source is imaged on the absorption cell by a high aperture condenser lens. In addition, there is a spherical mirror placed behind the light source reflecting radiation from the lower half solid angle back into the light source for higher output. For minimizing the influence of scattered flash light to the cathode of the photomultiplier it is advantageous if the exciting light impinges perpendicular to the interrogating one in the sample (for the angular distribution of scattered light, see Van Holde (1971)). The geometry of the absorption cell depends on the geometry of the flash lamp. If the flash lamp is a point source or some approximation of a point source then one would use a square cuvette, but if the flash lamp is a long linear one it is advantageous to use long cylindrical or long rectangular cells. When studying a suspension of chloroplasts in a solution containing a high dye concentration, which produces a high non-chloroplast absorption it is advantageous to use flat cuvettes, as

illustrated in the right of Fig. 22. With such a narrow cuvette the proportion of chloroplast volume to water volume, that is the proportion of chlorophyll to the dye dissolved in water can be lowered, which decreases the underground absorption produced by the dye. To avoid reflection of the actinic light into the photomultiplier cathode the narrow cuvette should be placed at a 45° inclination with respect to the interrogating beam as illustrated in the right of Fig. 22. With this geometry it has to be taken into account that the optical path of the interrogating light is given by the thickness of the cell multiplied by the square root of 2, correcting for the inclination of the cell.

2 *The interrogating light source*

In photosynthesis applications the intensity of the interrogating light has to be kept rather low. Thus one chooses lamps with respect to stability rather than to power. Tungsten filament lamps are most adequate, especially those designed for maximum mechanical ruggedness, e.g. car lamps. Because of their smaller spot size, which is favourable for a good optical imaging, their higher temperature, which implies a higher output in the near u.v. and the visible, respectively, and their longer lifetime *tungsten iodine* lamps are very useful. A power of 50 W is quite sufficient (Varta 96372, Germany (12 V, 55 W), Osram 64625, Germany (100 W)). Tungsten iodine lamps with quartz bulbs are available for higher power (Sylvania BXM, U.S.A. (250 W)).

Although the radiative power of a tungsten filament lamp depends on the temperature of the filament which tends to smooth out instabilities in the electric current, still about 10% of relative current changes are transformed into intensity changes. Therefore, a highly stabilized d.c. power supply for the interrogating light source is obligatory for a sensitive kinetic spectrophotometer. The relative stability of the output current should be better than 10^{-4}. Suppliers of appropriate power supplies are Harrison, Hewlett-Packard, and Sörensen in the U.S.A., Heinzinger and Knott in Germany.

The u.v. output of tungsten filament lamps being poor, *deuterium lamps* are used for this special region. These lamps emit a rather flat spectrum between 170 and 360 nm with sufficient stability. Because of their higher luminance deuterium lamps at an electrical power above 30 W are already satisfactory in photosynthesis research. Suppliers of these lamps are Sylvania in the U.S.A., Kern, Quarz-

lampen in Germany. For deuterium lamps stabilized d.c. power supplies are required with higher voltages (500 V, e.g. Kepco).

Xenon and mercury arcs might be useful for special purposes. While the emission spectrum of the first is practically flat from the u.v. into the visible (a broad peak extends between 800 and 1000 nm) the latter emits a broadened line spectrum. Their high luminance makes them especially useful if a rapid time revolution of the event under study requires high interrogating light intensity. Moreover, their small spot size allows for a precise imaging of the light source on the entrance slit of a monochromator. However, these advantages are compensated for by the intrinsic instability of these lamps. It is not so much the integral emission which fluctuates, but the location of the arc with respect to the electrodes oscillates with frequencies in the millisecond range. By the optical imaging this is converted to intensity fluctuations on the cathode of the photomultiplier. Thus we regard arc lamps as useful only for study in the time range of microseconds and below, while overrated tungsten lamps, with a reduction of their lifetimes, are to be preferred in all other cases where high intensities are required. Suppliers of arc lamps are Hanovia, U.S.A. and Osram in Germany.

3 *Monochromator and filters*

(a) If spectra are to be scanned it is useful to have a monochromator between the interrogating light source and the absorption cell. The major advantage to dial a wavelength is contrasted by the disadvantage of the small optical aperture which leads to considerable losses in light intensity. Moreover, the imaging required to fiddle the beam through the two slits of a monochromator increases the sensitivity of the system for mechanical noise. Thus interference filters are to be preferred to a monochromator whenever high light intensity or special stability are aimed at. Relatively low cost monochromators are supplied by Bausch and Lomb (U.S.A.) with exchangeable gratings covering the range between 200* and 800 nm. They allow for a spectral resolution of 1 nm.

(b) *Interference filters* might be used for three different purposes: (i) for selection of the wavelengths of the interrogating beam placed between the interrogating light source and the absorption cell, (ii) as a guard filter protecting the cathode of the photomultiplier against the wavelength of the exciting light (the centre wavelengths of the guard filter are matched to the centre wavelengths of the first filter in the interrogating beam, while it is distinct from the wavelength domain of the actinic light.), (iii) for selecting the wavelength of the actinic light. Interference filters are sandwiched from an interferometer of the Fabry-Perot type (reflection filter) plus absorption filters which eliminate the unwanted periodic transmission peaks of the interferometer. Whenever used with high light intensity, it is safer to protect them with a heat-reflecting filter or simply a cuvette with water. Moreover, it is safer to direct the silvery, non-coloured side towards the light source. Interference filters with characteristic peak transmissions of about 50% and bandwidths of about 10 nm are supplied by several companies: e.g. Baird Atomic (U.S.A.), Schott and Gen. (Germany), Balzers (Lichtenstein). Special filters with, say, 90% peak transmission and either very small or very large bandwidths might be obtained from smaller companies on request, e.g. Spectra Labs (U.S.A.), Dr Anders (Germany). When interference filters are used as guard filters it has to be considered that they may have residual transmission peaks of, say, 0.1% in spectral ranges which are far beyond the wavelengths of their peak transmission. Therefore, the application of broad-band reflection filters or absorption filters in addition to an interference filter is recommended.

(c) *Broad-band reflection filters* are in principle similar to interference filters, though sometimes of simpler constructions (dielectric thin films instead of etalon plus mirrors). They are available with peak transmissions of 80% and transmission bandwidth up to some 100 nm or, alternatively, as high frequency or low frequency cut-off filters.

(d) *Absorption filters* as well as broad-band filters are useful for two purposes: (i) for selection of the spectrum of the actinic light, (ii) in addition to interference filters as a guard for the cathode of the photomultiplier. Usually they contain organic dyes which by absorption filter out certain spectral ranges. They are available in the form of glass slides or gelatin sheets (low cost, for low light intensity only). Suppliers of absorption filters are Wratten (U.S.A.), Corning (U.S.A.), Schott and Gen. (Germany). When used with high intensity light, it might be useful to combine them with a heat reflection filter.

* For studies in the u.v. ($\lambda < 400$ nm) quartz optics are required.

4 *The photomultiplier*

a. The principle. A photomultiplier consists of three major elements: the cathode made up of a light absorbing material with a low work function, several dynodes, and the anode (see Fig. 23). A photon impinging on the cathode (K) with a probability of a few per cent releases an electron which is accelerated towards the first dynode (D1) being about 150 V more positive than the cathode. When falling upon the first dynode the energy of the electron is partly lost in collisions with other electrons, which then become fast enough to leave the rather flat potential sink of the dynode material. This leads to a multiplication of the original electron (by a typical factor of 5 per dynode). This multiplication is repeated at each dynode stage until the final electron avalanche impinges on the anode (A). Thus at constant light intensity and constant interdynode voltages the photomultiplier acts as a source of constant electric current which is converted into a constant voltage by letting the anode current flow to ground via a load resistor (R_{load}). The photomultiplier is considered to be a linear transducer of intensity into voltage. The limits of this approximation were discussed by Land (1971). Manufacturers of photomultipliers (e.g. RCA, EMI) have edited concise brochures on the principle and operating conditions of photomultipliers.

b. Wiring. The electric potential difference which accelerates electrons between subsequent dynode stages is provided by setting the cathode on a negative high voltage and the anode on the ground. The dynodes are set on discrete voltages in between by connecting them with the dynode resistor chain, as illustrated in Fig. 23. For better linearity of the photomultiplier manufacturers recommend to set the cathode-first dynode and last dynode-anode potential at a fixed value, e.g. by Zener diodes as illustrated in Fig. 23.

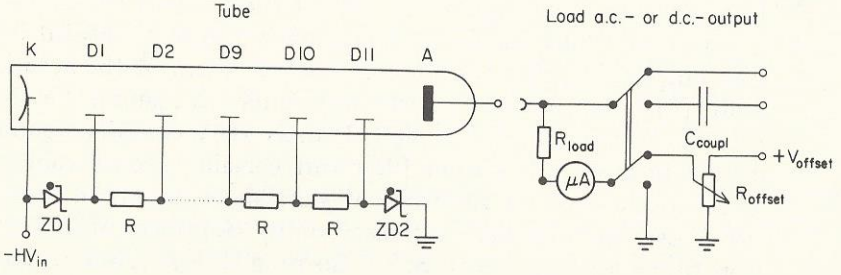

FIG. 23. Wiring, d.c. offset and output of a photomultiplier (for details, see text).

For pulse application it is useful to decouple the last dynodes to ground by capacitors (say of 0.05 μF). This, for the duration of the short pulse, backs the dynode potential against the additional electron current drain through the photomultiplier. However, in photosynthesis applications, where very small changes of light intensity, the signals, are superimposed to a high d.c. level, these capacitors are even harmful. Usually a short, but rather intense flash burst precedes the slower signal under study. By feeding electrons into the avalanche, produced by the flash burst, these capacitors are partly discharged. After the flash pulse is over, these capacitors have to be recharged again via the resistors in the dynode chain. A capacitor of, say, 0.05 μF recharges over a resistor of, say, 500 kΩ in 25 ms. While the capacitor recharges, the amplification of the respective dynode chains changes. This might give rise to slow artefacts following the rapid flash bursts interfering with the slow signal of interest. Therefore, it is recommended either not to add any capacitors into the dynode circuits, or to use large capacitors in experiments at a high time resolution where slower relaxation times after a flash burst do not interfere with the signal.

c. Operating conditions and ratings. Three major effects determine the operating range of the photomultiplier.

(i) The high voltage between cathode and anode: This should be between the maximum value as given by the manufacturer and a lower limit which differs from tube to tube. When running a, say, eleven-stage photomultiplier, which is wired according to Fig. 23 at a voltage of, say, 400 V, then the voltage between subsequent dynodes may be too low to counteract the formation of space charges which make the input-output characteristics of the photomultiplier non-linear. Thus it is safer to operate the photomultiplier at less stages (see subdivision *e* of this section) rather than at too low a voltage.

(ii) The maximum cathode current: This limits the maximum light intensity tolerated without damage of the cathode. Taking the spectral quantum efficiency of the specific cathode material into account (for a S20 characteristic at 600 nm the quantum efficiency is 7%) the maximum light intensity at this wavelength follows from the maximum cathode current as specified by the manufacturer (say 5 μA for an EMI D214B). For the above example the maximum energy flux tolerated by the photomultiplier is 1500 erg/s.

Exceeding these limits may cause irreversible decrease in the quantum efficiency of the cathode.

(iii) The maximum anode current: Typical ratings given by the manufacturers are about 1 mA. However, it is rarely necessary to draw such high currents from the anode. Instead, another condition for safe operation is to be met, the maximum electron current which is drawn through the dynode chain should be at least one order of magnitude lower than the current which flows through the dynode resistor chain. This is to provide a constant potential difference between subsequent dynodes independent of changes in the light intensity. For an eleven stage photomultiplier with twelve resistors in the chain, each of which is 50 kΩ, the resistor current at 1200 V is 2 mA. Thus the anode d.c. current should be kept below 100 μA.

d. Shielding. The electron beam in the photomultiplier is sensitive to electric and magnetic stray fields from outside the photomultiplier. The interference is lower the higher the supply voltage. However, it is worth shielding the photomultiplier tube electrically and magnetically. Tubes of a magnetically shielding material can be obtained from the suppliers of photomultipliers. Materials such as permalloy or mu-metal are highly absorbent for magnetic radiation; however, they saturate at relatively low field strength. In case of magnetic trouble even after application of a shielding tube it might be helpful to mantle this tube with an iron tube which attenuates the magnetic field and brings it into the response range of the inner shield. To avoid interference of the magnetic shielding tube with the electron optic imaging in the first dynode stages, the shielding tube has to be connected with the high negative potential of the cathode. In addition to the magnetic shielding tubes, an electrically tight envelope is recommended especially in applications where photosynthesis is excited with a laser flash.

e. Tube selection. The following considerations enter into the decision about the choice of a photomultiplier tube.

(i) Spectral sensitivity: As discussed in Section IIIB1, the signal-to-noise ratio increases with the square root of the quantum efficiency of the photocathode (equations 19). Thus one chooses a tube having maximum quantum efficiency in the spectral range of interest. The best compromise in the wavelengths from 200 nm up to 750 nm is a cathode with a S20 characteristic (quartz window required for the u.v.).

(ii) Geometrical features: For studies on turbid samples a tube with a large cathode area is preferred in order to catch as much scattered light as possible. In this respect end-on photomultipliers with 2 inch windows are adequate.

(iii) Number of stages: The number of dynode stages to be chosen depends on the light level and the maximum ratings for the anode current. For studies where the intensity of the interrogating beam does not exceed 100 erg/cm^{2}s an eleven-stage photomultiplier is appropriate (EMI 9558 BQ, RCA 7265). However, for higher light intensities the maximum ratings for the anode current can be met only if this tube is operated at too low a voltage. This, as discussed above, may cause non-linearities in the input-output characteristics. In these cases it is recommended to use photomultiplier tubes with fewer stages (e.g. EMI D 214 B) or to short circuit the last dynodes of an eleven-stage tube with the anode.

f. Output. Absorbancy changes, according to equation (14) are proportional to relative intensity changes. The photomultiplier is considered as a linear device converting relative intensity changes into relative changes of the output voltage. This requires:

(1) transformation of the photomultiplier current into a voltage by letting the current flow across a load resistor to earth (see Fig. 23);
(2) record of the d.c. output voltage of the photomultiplier;
(3) record of the transient voltage changes.

At first sight the largest *load resistor* seems to be the most adequate since it provides the highest output voltage at a given current. An upper limit for the load resistor is set by the time resolution aimed at. The photomultiplier itself plus its load resistor acts as in integrating device. The integration time constant is given by the product of the load resistor with the wiring capacitance (stray capacitance) of the photomultiplier which is in the order of 50 pF. The interrelationship between the load resistor and the maximum obtainable time resolution is illustrated in Table IV. Estimate is based on a ratio of 20 between the half rise time of the signal over the integration time of the photomultiplier for minor distortions of the rise time as discussed in Section IIIB1.

There is another factor limiting the load resistor. This is *anode saturation*. If the load resistor is so big that the current produced by the photomultiplier which flows across its load resistor produces an

TABLE IV

Time resolution of a photomultiplier with a stray capacitance of 50 pF depending on the input resistance of the subsequent amplifier stage

$R(\Omega)$	RC	T_{resol}
100k	5×10^{-6}	10^{-4}s
10k	5×10^{-7}	10^{-5}s
1k	5×10^{-8}	10^{-6}s
100	5×10^{-9}	10^{-7}s

output voltage which is, say, 10% of the voltage between the anode and the last dynode (about 100 V) then any increase of the light intensity would increase this voltage and thus decrease the voltage difference between the last dynode and the anode. This reduces the amplification of the last stage. To avoid such negative feedback the load resistor chosen should be such that the maximum possible current produces an output voltage which is less than 1% of the voltage between the anode and the last dynode on the photomultiplier.

The *d.c. output* can be monitored by introducing an ammeter (say 100 μA full scale) in series with the load to ground.

Transient variations of absorbancy produce transient variations of the input intensity of the photomultiplier and these are processed as transient variations of the output voltage by either of two ways which both eliminate the high d.c. level to which they are superimposed:

(a) the photomultiplier output can be connected via a capacitor (as illustrated in Fig. 23) to the subsequent amplifier stages. This *a.c. coupling* suppresses signal components with relaxation times lower than the time constant of the high-pass filter which is given by the coupling capacitance (see Fig. 23) times the input resistance of the next stage to which it is coupled. By analogy with the situation with the low-pass RC filter (see Fig. 19) it is safe to use a.c. coupling only if the signal under study is at least one order of magnitude faster than the time constant of the high-pass filter.

(b) Another way of eliminating the d.c. level of the photomultiplier output and to record transient changes of the output voltage only is to compensate the negative d.c. level by a positive voltage forced upon one leg of the load resistor. This, together with a galvanic coupling of the photomultiplier output to the next amplifier stages, is illustrated in Fig. 23. (Since light intensity is transformed into an electron beam which flows via the load resistor from the anode to earth, the anode goes negative on illumination of the cathode.) In order to avoid changes in the effective load resistor on variation of the offset resistor of the compensation, the latter has to be small in comparison with the first.

g. Power supply. Since the amplification of the photomultiplier depends exponentially on the high voltage applied between cathode and anode, relatively small fluctuations of the high voltage give rise to even larger fluctuations in the output of the photomultiplier. Highly stabilized power supplies are to be used. As a rough guide, one chooses a power supply the relative stability of which is one order of magnitude higher than the smallest absorbancy changes to be resolved ($\Delta U/U = 10^{-6}$ for absorbancy changes $\Delta A/A = 10^{-5}$). Suppliers of stabilized high voltage power supplies for photomultipliers are Kepco, Ortec (U.S.A.), Knott, Nucletron (Germany). The supply for the offset voltage has also to be highly stabilized.

5 *The actinic flash light*

a. Flash lamps. (i) The principle: Xenon-filled arc lamps which are pulsed by a capacitor discharge are the usual way of obtaining actinic flashes in the visible spectral range covering the time domain between 1 μs and 100 ms. The emission spectrum of a xenon arc is rather flat in the visible and in the near u.v. The principle for the transformation of electric into radiant energy by such a flash lamp is as follows: a high voltage is applied between two electrodes of the xenon-filled lamp bulb. As long as the steady state concentration of ions in the gas is low, which it usually is, the lamp behaves like an insulator. However, this concentration is raised above the critical level by applying a high voltage (several ten kV), high frequency pulse via a trigger electrode. Once the ion concentration exceeded the critical value an ion avalanche rapidly builds up, due to collision between ions which are accelerated between the two electrodes with gas atoms. Light emission is due to collisional excitation of ions and atoms. The processes terminate when the capacitor supplying the high voltage is discharged.

The electric energy consumed by the flash lamp is given by

$$\epsilon = \frac{C}{2} U^2$$

where C is the capacitance and U is the voltage of the condenser before the discharge. The conversion factor of electric energy into light energy output is in the order of 1%. However, this refers to broad-band emission. In biological applications only part of the total output energy can be used for exciting a specific dye. Thus the practical conversion factor may be even below 0.001. The duration of the flash depends on several factors: the time constant of the electric discharge ($\tau = RC$, where R is the arc resistance and C as above), the discharge energy (see Boag, 1968), the composition of the gas and the geometry of the flash bulb (the latter determine the quenching velocity for excited molecules, the afterglow). While the latter two factors are determined by the manufacturer of the flash bulb, the first two are in the hands of the experimenter. For short-pulse duration it is advisable to minimize the resistance and the inductance in the discharge circuit (close packing of the capacitor and the lamp, use of low inductance capacitors, eventually waveguide technique) and to use higher voltage together with small capacitors. For extremely short flashes (of the order of 0.1 μs) one uses voltages which would cause spontaneous breakdown of the gas discharge. To avoid this, the high voltage is applied to the lamp via a triggerable spark gap. These spark gaps are not easy to handle since they are efficient emitters of electromagnetic high frequency radiation interfering with the detection system and especially with the program structure of a digital averaging computer.

(ii) Selection of flash lamps: The parameters determining the selection of flash lamps are now described. The *arc dimensions* determine the efficiency of optical imaging of the arc on the absorption cell. Three major geometries are available: linear arcs (to be used as long cylindrical cuvettes—suppliers are Xenon Corp., EGG, PEK (U.S.A.)), helical arcs and coiled ones (suppliers are GE (U.S.A.), Osram (Germany)). The latter are most appropriate for use with rectangular absorption cells.

The maximum *energy and power ratings* as given by the manufacturers determine whether the flash lamp is saturating (energy) and which is the highest possible repetition (power) in periodical applications. The minimum electric energy necessary to produce a light output sufficient to saturate photosynthesis in a suspension of spinach chloroplasts cannot be given in absolute terms since it depends strongly on the geometry of the arc and on the imaging on the sample. We find that a 12J (electric energy) lamp with coil geometry (Osram XIE 200, Germany) has a light output of 1mJ between 600 and 690 nm which saturates photosynthesis under the following conditions: the absorbancy of a chloroplast suspension is 1 for the region of excitation, the arc is perfectly imaged on to the absorption cell (by a lens plus a mirror as illustrated in Fig. 22), the output is optically filtered to excite either of the two major absorption regions of chloroplast bulk pigments. For fractionated chloroplasts as well as for bacterial chromatophores where the antenna system per reaction centre is smaller and thus less efficient, higher energies are necessary for saturation.

The *maximum repetition rate* for the lamp ignition is limited by two factors: the relaxation time of the gas discharge (the lamp will fire spontaneously if the high voltage is applied say, 100 μs after the first ignition since there is still an overcritical ion concentration left) and the maximum power rating. If an electric energy of, say, 10 J per flash is necessary for saturation and if the maximum power ratings of the lamps are 200 W then the repetition rate of 20 Hz is the upper limit. If higher repetition rates are aimed at, the energy per flash has to be reduced, e.g. for 100 Hz down to 2 J per flash. If energy reduction is not adequate then alternating firing of several flash lamps placed around the cuvette is the only way out.

The *flash duration* limits the maximum time resolution of the kinetic spectrophotometer. Flash lamps of the above-mentioned suppliers have half durations of emission ranging from 2 μs to 20 μs. Special flash lamps having shorter half times (0.4 μs) even at reasonable energies per flash (20 J) are also available (PEK, U.S.A.). However, the handling of such a lamp, which is supplied with 30 kV, i.e. more than the spontaneous breakdown voltage, requires a more sophisticated set-up (Wolff and Witt, 1969). In applications with repetitive pulses the lifetime of the flash lamp is important. Improved technology has led to average lifetimes exceeding 10^5 pulses. Then, shading the lamp bulb by material evaporated from the electrodes lowers the light output.

(iii) Wiring: Wiring of a flash lamp is illustrated in Fig. 24. The capacity of the condenser C is determined by the available voltage and the maximum energy of the lamp ($C = 2(\epsilon/U^2)$). The condenser is charged via a load resistor, R_{load}, which has to be chosen such that the refill of the capacitor after discharge via the flash lamp is slower than the relaxation time of residual ionization in the lamp bulb ($R_{load} > \tau_{relax}/C$, $\tau_{relax} \cong 1$ ms). Moreover, an unloading resistor has to be provided for discharging the capacitor in case of malfunction of the lamp. The lamp is triggered by a high voltage pulse transformed from a, say, 300 V, 50 ns pulse up to a level of say 50 kV by a tesla coil.

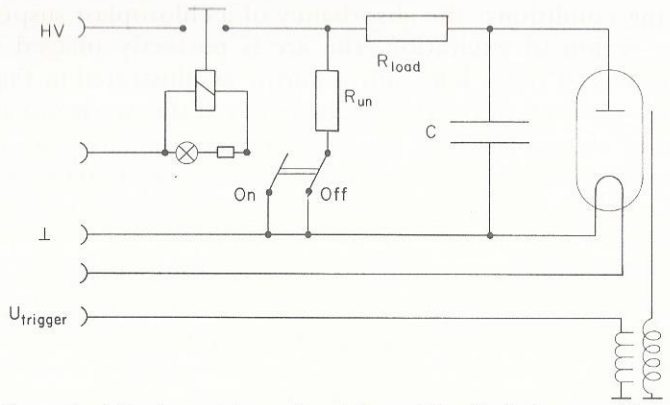

FIG. 24. The principle for wiring of a triggerable flash lamp with a heated cathode.

b. Lasers. Lasers have two major advantages over flash lamps: they emit extremely short pulses, and their whole light output energy goes into a single, sharply defined wavelength.

(i) Principle: Laser action is based on the fact that a molecular two-state system when exposed to light, the frequency of which is resonant with the energy gap between the two states ($\Delta\epsilon = h\nu$), may either absorb or emit a quantum of light depending on whether the system is in the lower or in the upper state. The net probability for stimulated emission according to equation (4) is proportional to the light intensity times the difference in the occupation numbers of the two states

$$P = BI(N_2 - N_1)$$

In thermal equilibrium the upper level according to Boltzmann's law is less populated than the lower one, so no net stimulated emission occurs. In lasers one induces an inversion of the occupation numbers by optical pumping with a flash lamp. The flash lamp, emitting light of higher frequency than that corresponding to the energy gap between the two distinguished levels, excites the system into higher levels which by radiationless decay rapidly discharge into the upper level until an inversion of the occupation numbers is obtained. For laser action it is favourable if the excited state is a metastable one. A resonant light wave travelling through an inverted medium stimulates emission of light. The angular characteristics of emission from each molecule are those of an oscillating dipole which is circularly symmetric around the axis of the E-vector of the stimulating light. Before special precautions for a selection are made the spectral

characteristics of the emitted light must correspond to those for fluorescence of the molecular system (in cases of organic dyes it is a broad-band emission). In lasers one selects emission into a narrow, angular as well as spectral range (coherent radiation) by placing the inverted medium into a resonant cavity, in the simplest case a pair of plane parallel mirrors. This, by reflecting the light back and forth through the medium, which by stimulated emission leads to a continuous amplification, finally forms a photon avalanche selected spatially (oblique wavefronts leave the cavity after a few reflections and are no longer amplified) and spectrally (only those waves resonant in the cavity are reflected with low losses). In order to outcouple photic energy, one of the two mirrors of the cavity is set at, say, 50% transmission, while the other one is made almost totally reflecting. This is illustrated in Fig. 25. The conversion factor between electrical input and coherent radiation output is usually of the order of 1%. Lasers are available as continuous wave or as pulse sources. Since in photosynthesis studies the interrogating light beam is easy to realize with conventional light sources, lasers were used exclusively in the pulsed version for excitation. Their application to photosynthesis started with solid-state lasers (Chance and De Vault, 1964; Wolff and Witt, 1969). However, more recently, liquid-dye lasers became available, which are more advantageous owing to their tunable output wavelength. In the following paragraphs these different lasers are briefly described with emphasis on methods for tuning their output wavelengths and for pulse shaping.

(ii) Solid-state lasers: Among solid-state lasers (for a review, see Gürs, 1969) the most prominent ones in the market are the ruby laser and the YAG (garnet) laser. Both the ruby and the Nd doped

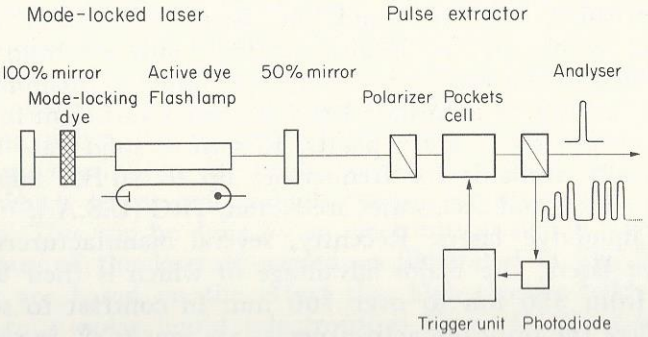

FIG. 25. The elements of a mode-locked laser plus a pulse extracting device (for details, see text).

YAG emit pulse trains roughly filling the time profile of emission of the exciting flash lamp. Their respective wavelengths of emission are 694.3 nm (ruby) and 1065 nm (Nd) at room temperature. While the ruby laser is appropriate for excitation of the long wavelength tail of the antennae system of photosynthesis in green plants, the Nd output has to be frequency doubled before fitting into the chloroplast absorption spectrum (see below). There are several methods for modifying the emission spectrum of a solid-state laser with a reasonable efficiency (about 10%) concerning the output energy and conservation of the short pulse duration and the low beam divergence.

Frequency doubling of laser emission can be performed with about 10% efficiency by using non-linear crystals (e.g. ADP) which generate the second harmonic of the incident light (one supplier is Korad, U.S.A.) A frequency doubled Nd laser emits at 530 nm, just adequate for excitation into the tail of carotenoid absorption bands and residual chlorophyll absorption bands in chloroplasts. Another method for tuning the emission of a solid-state laser is the generation of coherent Raman scattered light. If monochromatic light passes through a medium the absorption bands of which are out of resonance with the light, part of the light is scattered. This is due to the interaction of the electric field with the electric polarizability of the molecules in the medium as has been discussed above (Rayleigh scattering). Now the electric polarizability of molecules is modulated by their internal motion. This is why scattered light becomes modulated with the vibrational or rotational frequencies of the molecules. In terms of light quanta, the scattered quanta have different energies. This was used to extract a tightly packed quasi-continuum of spectral lines from a ruby laser pumped Raman cell. The conversion efficiency and the beam collimation could be enhanced by placing the Raman scatterer into a second resonant cavity tuned to the Raman wavelength of interest (Bhaumik, 1967). The pulse energy of solid-state lasers is always sufficient for saturating photosynthesis of green plants. Repetitive solid-state lasers are commercially available for frequencies up to 10 Hz. Suppliers of solid-state lasers and accessories are Korad, TRG (U.S.A.).

(iii) Liquid-dye lasers: Recently, several manufacturers offered liquid-dye lasers, the major advantage of which is their tunability ranging from 350 nm to over 700 nm. In contrast to solid-state lasers where the optically active species are ions (Cr^{3+} in ruby, Nd^{3+} in garnet) embedded into a crystal, it is an organic dyestuff dissolved in organic solvents in a liquid-dye laser. Tuning of a liquid-dye laser is

achieved by two means: coarse tuning by exchanging one dyestuff for another one, fine tuning by inserting an additional interferometer (either a grating or a Fabry-Perot interferometer) into the resonant cavity, the transmission (or reflection) of which selects for a discrete section of the dye's broad emission spectrum. Thus for covering the range between 350 and 700 nm one needs a set of more than ten different dyes, while a variation of about 10 nm of the wavelength can be dialled by the interferometer. The output energy of liquid-dye lasers ranges up to some joules per pulse of about 1 μs duration. Shorter pulses are obtainable by either of two ways: by pumping the dye with a short pulse from another laser (Avco, U.S.A.) or by extracting part of the total pulse duration via a Pockels switch (Electro-Photonics, Northern Ireland) as described below. The pulse energy per ns then is in the order of 0.2 mJ. Dye lasers for repetitive operation are available with pulse rates up to 10 Hz.

(iv) Pulse-shaping techniques: Shorter pulses may be obtained by one of the following methods. Inhibiting the formation of a photon avalanche in the laser cavity by spoiling its optical quality results in a higher inversion of the two laser states during optical pumping by the flash lamp. If then the optical quality is switched on (*Q switch*) the energy, which without this modification would have been emitted as a pulse train (in a ruby laser), is released into a single high-energy pulse the duration of which is considerably shorter and the energy is considerably higher than in the undisturbed system. This Q-switching technique produces pulses of some 10 ns durations with energies of the order of several joules. Q switching is obtained by rotation of one of the cavity mirrors at an appropriate speed (this installs the proper reflection conditions for a short time interval only) or by electroptical switches based on the Kerr effect or the Pockels effect (see below). Suppliers of Q-switching units are the above-mentioned suppliers of solid-state or liquid-dye lasers.

A flash-lamp pumped liquid-dye laser emits pulses of about 1 μs duration. Usually the energy is rather high (1 J), say two orders of magnitude higher than necessary for photosynthesis application. For higher time resolutions one might cut out, say, only 1% of the pulse length, which leaves still enough energy for saturation of photosynthesis. This can be done by an electroptical switch across which the output of the laser is passed, as illustrated in Fig. 25. These switches are based on the effect that high electric field strengths applied to a polar liquid (electroptical Kerr effect) or to a solid (Pockels effect) break the symmetry of the system and induce optical birefringence. Since the laser output is linearly polarized,

either by crystal anisotropy (in the ruby) or by Brewster windows (liquid dye laser) in the laser cavity, the electroptical switch can be set so that it blocks the laser beam until, by a high electric field pulse applied to the switch, birefringence opens the shutter.

In combination with a device for mode-locking the laser, such a pulse extractor can produce pulses down to a duration of 1 ps. The principle for mode-locking is as follows: the passive cavity of a laser is tuned for a series of discrete resonant modes. Each mode is characterized by special spatial distributions of the electric field strength (a standing wave) and by a distinct eigenfrequency. The longitudinal component of these modes is defined by the condition that a whole number of half waves must fit in between the cavity mirrors, which are at a distance L. Thus the wavelengths of the longitudinal modes are determined by equation (22), wherein n is a whole number.

$$\lambda_n = \frac{2L}{n} \tag{22}$$

Since wavelengths and frequencies are reciprocal to each other according to equation (3), the frequency gap between adjacent longitudinal modes are equidistant. The transverse geometry of the mirrors determines the other two dimensions of these modes in a more complicated way. Since the emission spectrum of the laser chromophore, especially with liquid-dye lasers, is rather broad in comparison with the wavelength distance of the adjacent modes, several modes are amplified by stimulated emission in the cavity. The laser output, if no special precautions are taken, is a mixture of different discrete frequencies although it covers altogether a wavelength range of less than 1 nm. Usually the phases of these modes are independent of each other. However, by introducing certain dyes into the cavity which act as a non-linear mixing device they may become locked up. Mode-locking leads to beats between these modes which produces a modulation of the output intensity with the beat frequency. This is the difference frequency between adjacent modes. In consequence the 1 μs pulse of a liquid dye laser is chopped up into a pulse train with a period of about 2 ns and a pulse duration of about 10 ps. In the mode-locked laser as combined with the pulse extractor, as illustrated in Fig. 25, excitation pulses, with a duration in the order of 10 ps, can be obtained. This technique was applied to study the kinetics of reaction centres from bacteria (Netzel *et al.*, 1973) in this time span.

c. Flash lamps versus lasers. Flash lamps operated at relatively low voltages (say 2 kV) are superior if relatively low energy (say 10 mJ light output), high repetition frequencies (up to 1 kHz), long lifetime and low costs are aimed at.

For high-energy or shorter-pulse durations, flash lamps operating at higher voltages may be used. However, since their discharge voltage lies above the spontaneous breakthrough voltage, ignition is induced by triggering an extra spark gap in series with a flash bulb. This has disadvantages insofar as a spark gap is an efficient emitter of high frequency electromagnetic disturbances, which may cause trouble with the detection system. Careful electromagnetic sealing of the flash lamp chassis is obligatory. The application of electromagnetically disturbing flash lamps together with hardware digital averaging computers needs special care. Since the internal program structure of these computers is executed via low-voltage, high-frequency pulses, trapped pulses from a spark-triggered flash lamp often interfere with the computer program, causing misfunction. The latter disadvantage is shared by lasers which are pumped by a spark-triggered flash lamp. Because of their higher complexity lasers are less reliable than simple flash lamps. The field of their application should be restricted to cases where extremely short pulse duration and higher monochromatic output energy are required.

6 *Averaging computers*

As pointed out in Section IIIB1, the signal-to-noise ratio can be enhanced by averaging over many repetitive transient signals. Since nowadays digital multichannel analysers are commercially available for averaging transient signals down to the nanosecond range, we will neglect analogue averaging techniques (sampling).

The major advantage of digital averagers is that their memory (magnetic core) does not forget the stored information unless requested to do so. Thus even experimental results obtained on different days can be averaged. The principle of the digital averaging computer is as follows. It is made up of a gated digital voltmeter which converts an input voltage into a number of counts into a digital memory. There are, say, $2^{10} = 1024$ such memories. If triggered, the digital voltmeter measures the average input voltage during a certain time interval (dwell time per address) which is stored into memory No. 1. Then, by internal programming the computer gets ready for measuring the voltage during the subsequent time intervals. The information is stored into memory No. 2 and so on until after 1024 intervals all memories have their information. After

one accumulation period one ends up with the digital representation of the input voltage transient, digital both in voltage and in time. This cycle starts again when another trigger pulse is applied to the averaging computer. This trigger pulse has, of course, to be at a fixed phase correlation to the signal. The second signal is added to the memory in digital form to the content, which is already stored, and which resulted from prior runs. As discussed in Section IIIB1, the gain in signal-to-noise ratio is approximately proportional to the square root of the number of signal repetitions. The proportionally constant depends on the signal-to-noise ratio of the input signal; moreover, there is a gain saturation after more than 10^4 repetitions. The gain factor and the saturation value differ between different averaging computers (see Buchwald and Rüppel, 1971). Suppliers of averaging computers are Durrum, Nicolet Instruments, Northern Scientific (U.S.A.), Intertechnique (France), Sanai (Japan). The averaged signals are read out either on an oscilloscope screen, via an x–y recorder, or in digital form on tape. An example for the performance of an averaging computer in photosynthesis research is illustrated in Fig. 26. The original signal is buried in noise (S/N $\approx$ 1/5). It emerges after 128 repetititions (S/N $\approx$ 3) and it is extracted with a reasonable precision (S/N $\approx$ 12) after 2048 repetitions.

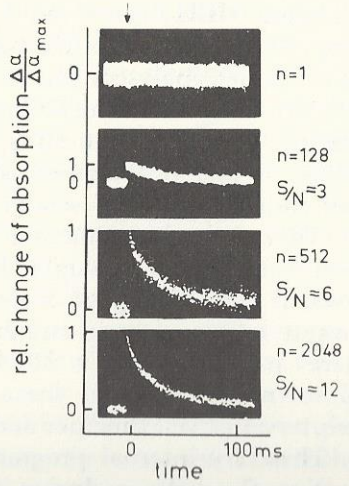

FIG. 26. The extraction of a signal which is buried in noise by averaging over repetitive transients by means of a digital averaging computer (Witt, 1967).

The dwell time per address of an averaging computer is variable. The minimum values are in the order of 10 μs per address. Thus a signal rising within 100 μs to its 90% value can be represented by a sequence of 10 spots in the digital display of the memory contents on an oscilloscope screen. If more rapid signals are to be recorded, the operational range of a conventional averaging computer can be extended by a transient recorder (by Biomation, U.S.A.) connecting the signal output of the photomultiplier (or the preamplifier) with the input of an averaging computer. A transient recorder consists of a very rapid analogue–digital converter (down to 10 ns dwell time per address) plus a buffer memory. Its memory capacity is much lower than that of the averaging computer, therefore it has to be used in conjunction with the storage capacity of the averaging computer. Taking advantage of the fact that transient signals in biological applications are repeated rather slowly, the signal, although rapidly digitized and stored in the buffer memory of the rapid transient recorder, is transferred much more slowly to the conventional averaging computer where it is added to the previous signals. Provided that the conventional averaging computer is equipped with an appropriate option the data transfer between buffer and averager proceeds in digital form. Otherwise, digital/analogue conversion and reconversion is necessary. When selecting a rapid transient recorder it is important to know that the full-time resolution is obtained sometimes only at a rather high input voltage level. Since the signals in photosynthesis are rather small, this might require use of a large bandwidth preamplifier between the photomultiplier and the rapid transient recorder. Both averaging computers and rapid transient recorders are easy to handle. Although they are fairly reliable components, there are two possible sources of trouble. First, as with all computers, air conditioning might be necessary: and second, their internal programming, which is transmitted by low voltage pulses, makes the device extremely sensitive to any high frequency electromagnetic scattered field (e.g. from flash lamps or laser components).

Most averagers are offered with options for secondary hardware data processing like smoothing, integration, differentiation, data transfer and arithmetic. In applications to photosynthesis it is advantageous to have two inputs and two separate memory registers in order to be able to compare or to subtract two different signals (e.g. for recording and subtracting flash burst artefacts or for comparison of absorbancy changes at different wavelengths). Recently, multipurpose computers have been offered with software for their application as averagers (Nicolet, Tektronix, U.S.A.).

When the kinetic spectrophotometer is equipped with an averager, the following data read-out units are advantageous. One oscilloscope (Hewlett-Packard, Tektronix, U.S.A.) is required to monitor the output of the photomultiplier. This is necessary to check the d.c. offset of the photomultiplier and the fitting of the signal plus noise band into the input limits of the averaging computer. Another oscilloscope is required to monitor continuously the memory contents of the averaging computer. This is advantageous as it allows continuous observation of the signal-to-noise level during the averaging process. After stopping the averaging cycles, the data are either photographed from the oscilloscope screen, written out by x–y recorder, or recorded on tape for further data processing in another computer.

7 *Synchronizing elements*

In order to synchronize the trigger of the flash lamp with the trigger of the averaging computer, a series of pulse generators is necessary, the operation of which is illustrated in Figs 27 and 28. Let us assume that we wish to excite the system with a series of five equidistant flashes (distance, say, 5 ms) at a relatively slow repetition rate (repetition period, say, 5 s). The response of the system is to be recorded at an interval between $t = -20$ ms and $t = 105$ ms in relation to $t = 0$, the time where the first of the five flashes is fired. The record starts 20 ms before firing the first flash in order to compare the signal with the previous dark level (see Fig. 26). In order to increase the signal-to-noise ratio without overloading the system with measuring light, the measuring light is pulsed by a solenoid-driven photoshutter opening at $t = -50$ ms and closing at $t = 150$ ms. Synchronization of the opening of the photoshutter with the triggering of the averaging computer and the oscilloscope and the firing of the five equidistant flashes is achieved by a series of pulse generators (Tektronix, Data Pulse, U.S.A.) the input-output characteristics of which are evident from inspection of Figs 27 and 28. If not already attached to the averaging computer, a counter has to be provided for counting the number of repetitions of the signals which are averaged by the computer. The synchronization which is illustrated in Figs 27 and 28 is sufficient for triggering flash lamps the jitter of which with respect to the triggering pulse usually is in the order of microseconds. In spectrophotometers for a higher time resolution, especially with laser excitation, it is safer to trigger

directly on the light pulse. This can be done by channelling out part of the excitation energy to a photocell which triggers the averager. Records of the dark level of absorption before the flash is easy if a

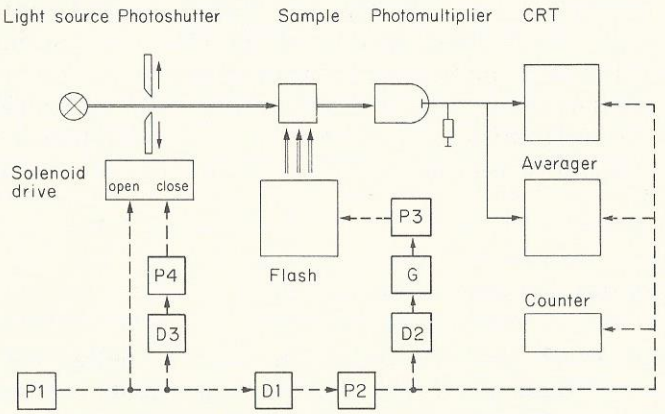

FIG. 27. The synchronizing system (dotted lines) for a flash kinetic spectrophotometer with an averaging computer (for the pulse sequence emitted by this synchronizing system, see Fig. 28).

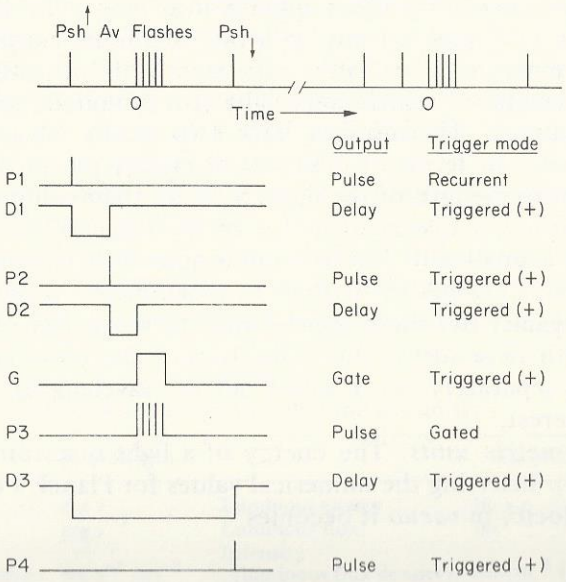

FIG. 28. The pulse sequence (above) and the input-output characteristics of triggering units.

rapid transient recorder (Biomation, U.S.A.) is applied. This possesses an operational mode named pretrigger recording. It continuously records the absorption level which is shifted through the buffer memory. When receiving the trigger pulse it continues the measurement for a preset section of the chosen measuring interval after which it stops measuring. If this section is set at, say, two-thirds of the measuring interval, then the record from this measurement consists of one-third resulting from the time period before the firing of the flash and two-thirds resulting from the time interval after.

8 *Calibration of light intensity and flash energy*

a. Thermopiles and photocells. In order to define the physical conditions of flash spectrophotometric experiments the intensity of the measuring light or auxiliary light has to be measured as well as the light output of the flash lamp. The photomultiplier, although a somewhat linear recorder of relative light intensity, is not easily calibrated absolutely. This is mainly due to irreversible ageing of the photocathode. The most reliable way is to use a calibrated thermopile, which converts incident quanta into heat. The heat is transformed into a voltage output via a pile of thermocouples. Thermopiles are commercially available calibrated both for pulse energy and for the intensity of continuous light (for suppliers, see the above laser companies). Thermopiles have two major advantages. First, their sensitivity in terms of intensity or energy per pulse is independent of the wavelength of the light. Second, their calibration is quite stable. Their major disadvantage lies in their size. Whenever the light intensity in a small spot has to be determined, it is advantageous to use a photocell together with a microammeter which has to be calibrated against the thermopile. Since the sensitivity of a photocell is wavelength dependent, the calibration of the photocell has to be carried out separately for a whole set of wavelengths covering the range of interest.

b. Photometric units. The energy of a light quantum is given by equation (1). Inserting the numerical values for Planck's constant and the light velocity *in vacuo* it becomes

$$e = \frac{2 \cdot 10^{-9}}{\lambda} \text{ erg}$$

(where λ is in nanometres). The energy of one mole of quanta, one einstein, is:

$$E = \frac{12 \cdot 10^{14}}{\lambda} \text{ erg} \cdot \text{mole}^{-1} = \frac{2 \cdot 85 \cdot 10^{4}}{\lambda} \text{ kcal} \cdot \text{mole}^{-1}$$

The energy of visible light quanta ranges from 31 kcal $mole^{-1}$ (700 nm) to 71 kcal $mole^{-1}$ (400 nm). The energy of a light pulse is either given in ergs or in joules, where 1 J is equivalent to 10^7 ergs. When intensity has a dimension of an energy flux per unit area, this is measured either in erg cm^{-2} s^{-1}, or in W cm^{-2} where 1 Ws is equivalent to 1 J. In photochemical applications light intensity is given in einstein $cm^{-2}s^{-1}$; however, it is evident from the above that this unit characterizes a particle flux density rather than an intensity.

A few examples of light intensities: the intensity of bright sunlight at the equator amounts to 10^6 erg $cm^{-2}s^{-1}$, of diffuse daylight 10^5 erg $cm^{-2}s^{-1}$, while saturation of photosynthesis in isolated chloroplasts requires about 10^5 erg $cm^{-2}s^{-1}$ into the major absorption bands of chlorophyll.

Complications arise from the use of *subjective photometric quantities* even in the literature on photosynthesis. Subjective photometric units are defined by experiments involving the average human eye as a detector. Thus they involve a particular spectral dependence of its quantum efficiency which is maximum at a wavelength of 555 nm (light-adapted eye, cone vision). When comparing the brightness of light at wavelengths 450 and 555 nm at equal physical intensity, the subjective brightness of light at 450 nm is lower than that at 555 nm. Table V gives a survey of physical units for light and their subjective correspondents.

Conversion of subjective into physical units and vice versa is carried out as follows: the radiant flux density (intensity) of 10^{-7} erg cm^{-2} s^{-1} at the maximum sensitivity of the eye (λ = 555 nm)

TABLE V

Physical and subjective photometric units

Physical unit		Subjective unit	
Radiant energy	erg	Luminous energy	lm x s
Radiant flux	erg s^{-1}	Luminous flux	lm
Intensity (radiant flux density)	erg s^{-1} cm^{-2}	Intensity (luminous flux density)	lm cm^{-2} (lx = lm m^{-2})
Radiant intensity	erg sr^{-1}	Luminous intensity	cd (lm sr^{-1})

sr, steradian; lm, lumen; lx, lux; cd, candela.

corresponds to a subjective luminous flux density of 619 lm cm^{-2} = 6.19×10^6 lx. At any other wavelength the radiant units must be corrected by the function $S(\lambda)$, the relative visibility of light with S (555 nm) = 1. Thus at a given wavelength 1 erg cm^{-2} s^{-1} = $6.19 \times 10^6 \times S(\lambda)$ lx. (For the spectral visibility curve of the human eye, see RCA-Electroptics Handbook, RCA, Harrison, New Jersey, 1968.)

IV Analysis of photosynthesis by flash kinetic spectrophotometry

In this section the application of the principles of kinetic flash spectrophotometry to the study of various aspects of the primary processes of photosynthesis in green plants is considered. Emphasis will be on examples which illustrate the special advantages of this method rather than on a full account of our present view on these processes. For recent reviews on the primary processes of photosynthesis, see Witt (1971) and Trebst (1974); for a recent multiauthor textbook, see Govindjee (1975).

The efforts of workers from different backgrounds has led to partial resolution of the primary processes of photosynthesis.

Biochemists have characterized most of the components of the electron transfer chain and the enzymes involved. Several functional and structural features of the thylakoid membrane have been elucidated (Trebst, 1974). Moreover, progress has been made in the resolution and reconstitution of the system of photophospholation (Racker *et al.*, 1971).

Structural research mainly by electron microscopy (Mühlethaler, 1972) and X-ray small angle scattering (Kreutz, 1970) has revealed a gross concept of the structure of the functional membrane, although at the present time the results of different authors are conflicting.

Flash polarography has yielded insight into the kinetics and the mechanism of the oxidation of water by light reaction II of photosynthesis (Joliot *et al.*, 1971). Fluorescence studies have produced an insight into the functions of the antenna system and of the primary photochemistry (Joliot *et al.*, 1968; Borisov and Ilina, 1973).

Flash spectrophotometry contributed to all these aspects and provided some information which was hardly accessible by other techniques. Some examples: the role of the photochemical reactive pigment chlorophyll a_1, which is only one out of several hundred chemically identical chlorophyll *a* molecules in the thylakoid membrane, could not have been elucidated by other techniques (except perhaps e.p.r.). The protective role of carotenoids which accept and dissipate excitation energy from chlorophyll molecules could not be detected by slow analytical methods. Because of the miniscule dimensions of the chloroplast inner membrane system the electric phenomena across the thylakoid membrane require a molecular voltmeter which was based on the electrochroic response of chloroplast bulk pigments.

In general, flash spectrophotometry is specially useful for studying events which are more rapid than a millisecond. One major disadvantage of this method in application to photosynthesis is that several different molecular events contribute absorbancy changes at a given wavelength. Resolution of the complex pattern of absorbancy changes into the separate events causing this pattern was obtained by kinetic analysis under modification of the chemical and physical conditions of chloroplasts in a suspension. Once the response of certain reactants to chemical or physical alterations of the system is known, measurements of the spectrum of absorbancy changes before and after the alteration yield information on the difference spectrum of this special reactant. From these spectra a kinetically well characterized component could be identified chemically. These techniques of analysis are illustrated in the following example.

A PRIMARY PHOTOCHEMICAL REACTIONS

1 Light reaction I

Kok (1956) discovered flash light-induced absorbancy changes at a wavelength of 700 nm, which he attributed to an unidentified pigment, P700. Later, negatively directed absorbancy changes at this wavelength were attributed the photo-oxidation of a special chlorophyll *a* molecule. Attribution of these absorbancy changes to a redox reaction was based on titration experiments. Chloroplasts were exposed to certain redox potentials poised by a given ratio of ferro- to ferricyanide. Kok (1961) and later Rumberg and Witt (1964) found out that the extent of the negative directed changes of absorption at 700 nm decreased if the redox potential became more positive (more oxidizing). The curve of the extent of the flash-induced absorbancy changes against the redox potential imposed on the system fitted perfectly with the expectation of a one-electron transfer reaction between P700 and the ferri/ferro couple. Since chemically oxidation decreased the extent, it was concluded that the negative-

directed absorption changes indicate a light-induced oxidation of this pigment. This interpretation of a single-electron redox reaction was corroborated by e.p.r. studies (Beinert and Kok, 1964).

The kinetics of the flash-induced absorbancy changes revealed a rapid decay and a slower recovery in about 20 ms as illustrated in Fig. 29. According to the above redox titration experiments, the rapid decrease of absorption indicates light-induced oxidation, the relaxation reduction in the dark. The decay of absorption upon excitation with a Q-switched ruby laser flash was extremely rapid. The half decay time as illustrated in the right of Fig. 29 was less than 20 ns (K. Witt and Wolff, 1970). This experiment at a very high time resolution was complicated by the high noise level associated with the necessary large bandwidths of the detection system. The signal-

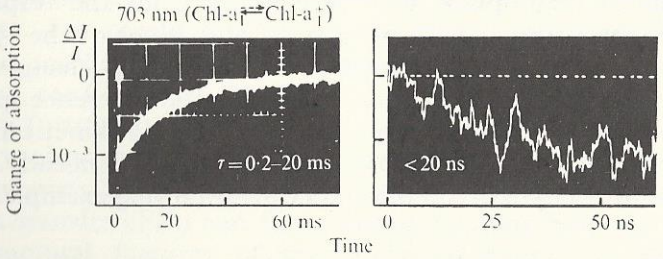

FIG. 29. Time course of the redox reaction of chlorophyll a_1 in chloroplasts. Left: at low time resolution (Witt *et al.*, 1961). Right: high time resolution (K. Witt and Wolff, 1970). (Reproduced, with permission, from Witt, 1971.)

to-noise ratio was improved by averaging over repetitive transients. Since rapid multichannel analysers (see Section IIIC6) were not available at the time of this experiment, a sampling oscilloscope was used (see Rüppel and Witt, 1969).

The slow relaxation of the signal was found to be accelerated by reducing agents such as PMS (Rumberg and Witt, 1964). This confirmed the attribution of the slow relaxation to the reduction of this pigment. Recent studies on the interaction of this pigment with its intrinsic reductants in the photosynthetic membrane revealed more complex relaxation kinetics which escaped prior observation for two reasons. First, because the integration time constant of the detection system was set to match the 20 ms rise time and second, because of insufficient elimination of fluorescence-burst artefacts. In addition to the relaxation time of 20 ms, as illustrated on the left of

Fig. 29, two phases relaxing at 20 and 200 μs were detected (Haehnel and Witt, 1971).

Two experimental observations led to the suggestion that the photoxidation of chlorophyll a_1 might be the primary photochemical act in photosystem I: first, the negative directed absorbancy changes at 700 nm could be stimulated by light, even at temperatures as low as −150°C (Witt *et al.*, 1961); second, oxidation proceeds at extremely high velocity (K. Witt and Wolff, 1970).

The absorbancy changes at 700 nm are not solely attributed to redox reactions. There is a minor component (about 20%) superimposed which is due to an electrochroic response of bulk chlorophylls to the light-induced electric potential difference (Emrich *et al.*, 1969; see Fig. 36). This component can be strongly accelerated and thus virtually eliminated by agents which increase the ionic permeability of the functional membrane of photosynthesis by orders of magnitude (see Section IVC).

The spectrum of the absorbancy changes of P700 was separated from the superimposed absorbancy changes by fractionation of chloroplasts. It came out that these absorbancy changes are the most stable ones which "survived" gross treatment. The absorbancy changes observed on photosystems I particles at different wavelengths of the interrogating beam could be attributed to the reaction of one and the same pigment by the agreement of their kinetic properties. The spectrum resulted in three major peaks, Besides the known one at 700 nm (Kok, 1956), there is another one at 430 nm (Witt *et al.*, 1961) plus a minor satellite at 682 nm (Döring *et al.*, 1968a). This spectrum is illustrated in the upper part of Fig. 30. It closely resembles the difference spectrum for the oxidation of chlorophyll *a* in butanol (Seifert and Witt, 1968). This corroborated the identification of P700 with a special chlorophyll *a* chlorophyll a_1 (Rumberg and Witt, 1964).

The double band in the red spectral region (682, 700 nm) was tentatively attributed to exciton splitting of the energy levels of two chlorophyll *a* molecules in a dimer (Döring *et al.*, 1968a; see Section IID4). This interpretation found support from studies on the changes in the circular dichroism of this double band (Phillipson *et al.*, 1972). In addition, e.p.r. studies revealed that the unpaired spin in oxidized chlorophyll a_1 is delocalized over two porphyrin rings, which proves the existence of a strongly interacting chlorophyll *a* dimer (Norris *et al.*, 1971).

Since the absorption of chlorophyll a_1 is only a small fraction (less than 1%) of the total absorption in the spectral region of the major

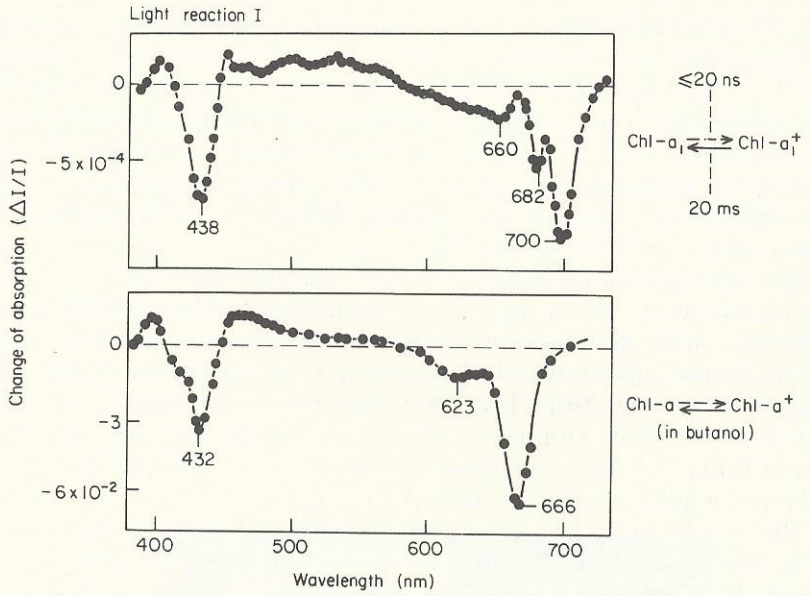

FIG. 30. Above: transient difference spectrum of the redox reaction of chlorophyll a_1 in chloroplasts (Döring *et al.*, 1968). Below: transient difference spectrum of the redox reaction of chlorophyll *a* in butanol (Seifert and Witt, 1968). (Reproduced, with permission, from Witt, 1971.)

chlorophyll *a* bands, it is rather hard to detect by conventional spectrophotometry (for a review on advanced absorption spectroscopy, see Butler, 1972). However, with kinetic flash spectrophotometry, which is "blind" for the high steady level of absorption, the absorbancy changes of chlorophyll a_1 were much more easily detected.

2 *Light reaction*

From the enhancement of photosynthetic O_2 evolution under continuous illumination at wavelengths between 700 and 730 nm by light of shorter wavelengths (absorption at 700 nm) Emerson (1958) postulated the existence of two light reactions in photosynthesis. Hill and Bendall (1960) postulated that these light reactions drive an electron transport by operation in series. This concept was confirmed by independent flash spectrophotometric studies of Kok *et al.* (1961), and Witt *et al.* (1961). However, absorbancy changes attributable to a redox reaction of the photochemically active pigment of light reaction II were not detected until 1967 (Döring *et al.*, 1967), more than ten years after the discovery of P700 (Kok, 1956). The absorbancy changes attributed to a chlorophyll which is linked to light reaction II activity peaked at 435 and 682 nm.

The reasons for the delayed discovery are threefold. First, the absorbancy changes of chlorophyll a_2 are superimposed to the side bands of those of chlorophyll a_1. Second, in the red spectral region the peak of chlorophyll a_2 coincides with the fluorescence peak of the antenna system. This causes severe fluorescence-burst artefacts, which were eliminated by the technique described in Section IIIB3, restriction of the solid angle between the sample and the photomultiplier cathode, and subtraction of the artefact in the absence of the interrogating beam. Third, the relaxation time of the absorbancy changes of chlorophyll a_2 is two orders of magnitude faster than the slow relaxation time of chlorophyll a_1. This causes a tenfold higher noise level according to equation (19).

Attribution of the absorbancy changes of chlorophyll a_2 to light reaction II was based mainly on their DCMU sensitivity which contrasts with the behaviour of chlorophyll a_1 (Döring *et al.*, 1968b). The kinetic properties of the absorbancy changes of chlorophyll a_2 came out as follows: there is a rapid decrease of absorption after a flash of light, the rise time of which is as yet not resolved, relaxing with a half time of 200 μs (Döring *et al.*, 1969). Recently another more rapidly relaxing component was discovered, with a relaxation time of only 35 μs (Gläser *et al.*, 1974). The resolution of this rapidly relaxing component of chlorophyll a_2 from the underlying fluorescence artefacts at 680 nm was obtained by means of a flash spectrophotometer with a modulated light beam as described in Section IIIB3. The resolution of the difference spectrum of chlorophyll a_2 from all other absorbancy changes was complicated (Döring *et al.*, 1969). Although this spectrum closely resembles the spectrum for the photoxidation of a chlorophyll *a* molecule, there are still open questions as to the nature of these absorbancy changes. It was open whether they indicated a redox reaction. This was confirmed only recently by e.p.r. (Van Gorkom *et al.*, 1974). Slight differences in the spectral characteristics of the two kinetically distinct components (Gläser *et al.*, 1974) shed doubt on the interpretation that both components characterize the reaction of one and the same pigment which reacts via two kinetically distinct channels.

The early observation of Emerson (1958) that there are two photochemical reactions in photosynthesis which obviously draw their

energy from different antennae systems, one of which can absorb light at 720 nm while the other cannot, was corroborated by flash spectrophotometry. The action spectrum for the oxidation of chlorophyll a_1 is shifted towards longer wavelengths in comparison to the action spectrum for the reduction of chlorophyll a_1 via light reaction II (Junge and Witt, in Witt, 1967). The same result confirmed Hill and Bendall's (1960) postulate that the two light reactions operate in series.

Since the fastest relaxation times detected so far for the two light reactions are 20 μs (light reaction I) and 35 μs (light reaction II), respectively, a flash which is intended to turn over each light reaction only once has to be considerably shorter than these relaxation times. Such a flash, in the following sections, is called a single-turnover flash.

3 *Protective reactions*

It is known that excited chlorophyll is destroyed in the presence of oxygen. Under non-saturating excitation of photosynthesis light quanta are efficiently channelled into photochemically active reaction centres. A photon absorbed by the antennae chlorophylls of photosystem I is trapped within 0.03 ns (Borisov and Ilina, 1973), which is very rapid compared with the fluorescence decay time of the monomeric chlorophyll *a* in solution (30 ns). However, if photosynthetic systems are excited at oversaturating intensities, the traps, which under continuous illumination regenerate only with the overall rate-limiting step of photosynthesis (about 10 ms), are not ready to accept a quantum of light. Thus, the excitation energy stays longer with the antenna system. This favours the possibility of irreversible chlorophyll oxidation. It had been postulated some time ago that carotenes play a protective role by absorbing superfluous excitation energy from the chlorophyll antenna system. However, final evidence for this was elaborated by flash spectrophotometry. Absorbancy changes were observed, the extent of which in contrast to all other absorbancy changes did not saturate at the low flash energies necessary to excite each photochemical reaction centre once (Zieger *et al.*, 1961; Mathis, 1969; Wolff and Witt, 1969). This implies that the reaction indicated by these changes occurs within the antennae system but not after the trap. The kinetics of these absorbancy changes, which peak at 514 nm, are characterized by a rapid rise (40 ns—Breton and Mathis, 1970; Wolff and Witt, 1969; K. Witt and Wolff, 1970) and slower decay (3 μs), the velocity of which is increased with increasing pressure of oxygen,

which is known to quench triplet states (Mathis and Vermeglio, 1972). The spectrum of these absorbancy changes closely resembles the spectrum of metastable states of carotenes *in vitro* (Chessin *et al.*, 1966). The most probable interpretation of these absorbancy changes is that superfluous energy within the antenna system which is not emitted as fluorescence is transferred to a carotenoid triplet state wherefrom it is dissipated as heat within 3 μs. This protects the antenna chlorophylls from oxidation.

B THE ELECTRON TRANSPORT CHAIN

Flash spectrophotometry resulted in a scheme for the electron transport system in photosynthesis of green plants which is illustrated in Fig. 31. In the middle, the different components and their relationships are illustrated; above, their typical relaxation times for

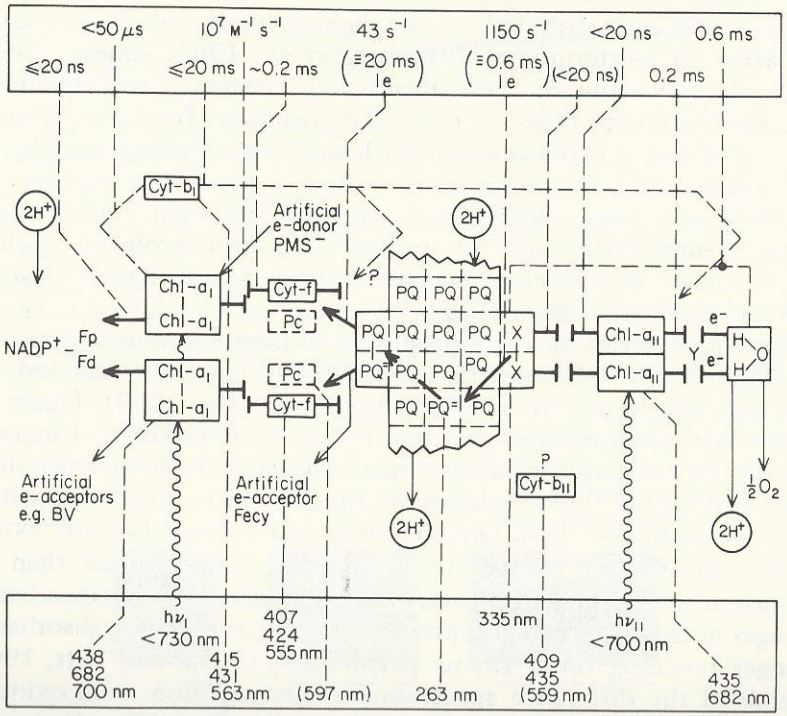

FIG. 31. Scheme for the electron transport from water to NADP based on flash spectrophotometric results. Above: Characteristic relaxation times of the partial reactions. Below: The characteristic wavelengths for the observation of the various components. (Reproduced, with permission, from Witt, 1971.)

one electron transfer are characterized; and below, the wavelengths for the interrogation of these components are given. Besides the pigments which are responsible for the activity of light reaction I and light reaction II, the scheme contains plastoquinone, which links up both light reactions for in series operation and, moreover, crosslinks several electron transport chains: cytochrome *f* and plastocyanin, the primary electron donors of light reaction I and ferrodoxin and flavoproteins as electron acceptors of light reaction I. These components are described in the following sections.

1 *The plastoquinone pool*

Bishop (1959) discovered that extraction of plastoquinone from chloroplasts inhibits oxygen evolution while recondensation restores this ability. Later, absorbancy changes were detected in the near u.v. which could be attributed to the light-induced reduction and re-oxidation of plastoquinone (Rumberg *et al.*, 1963; Amesz, 1964). From the behaviour of these absorbancy changes it was concluded that plastoquinone links up both light reactions for in series operations and that it exists as a pool with an electron storage capacity of about eight electrons per electron transport chain. The existence of an electron storage capacity between the two light reactions was independently elaborated by studies on oxygen evolution (Joliot, 1965) and of fluorescence changes associated with light reaction II activity (Malkin and Kok, 1966).

The direct access to these properties of plastoquinone as provided by flash spectrophotometry is illustrated in Figs 32 and 33 (Schmidt-Mende and Witt, 1968; Stiehl and Witt, 1969). Figure 32 (upper left) demonstrates the time course of absorbancy changes at 265 nm on excitation of a chloroplast suspension with a single short flash, and Fig. 32 (below) shows the time course on excitation with a long, photoshutter flash. On excitation of the long flash the extent of the absorbancy changes is up to eight times greater than on excitation with a single turnover flash. The decay of the absorbancy changes in the latter case is biphasic. The spectrum of the absorbancy changes revealing these kinetic peculiarities (Stiehl and Witt, 1968) resembled the difference spectrum for the transition from oxidized plastoquinone to reduced plastoquinone *in vitro* (Henninger and Crane, 1964). Negative-directed absorbancy changes at 265 nm correspond to a reduction of plastoquinone. Thus the transients illustrated in Fig. 32 can be interpreted as follows. Plastoquinone is

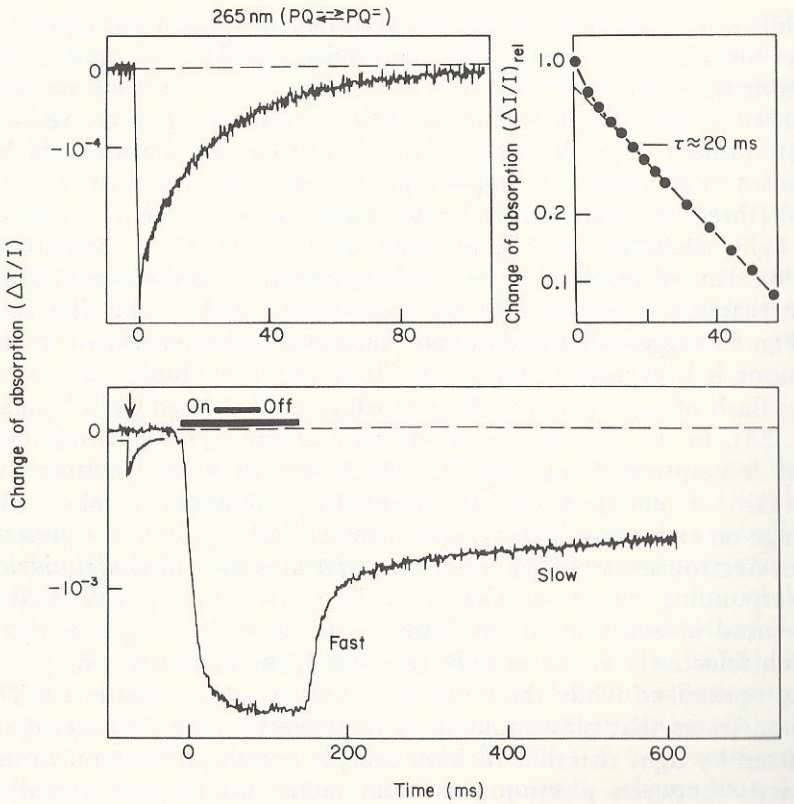

FIG. 32. Time course of the absorbancy changes of plastoquinone. Upper left: After excitation with a single-turnover flash. Below: On excitation with a long flash of light (Stiehl and Witt, 1969). (Reproduced, with permission, from Witt, 1971.)

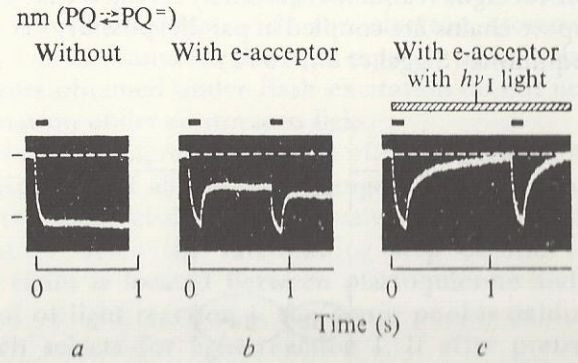

FIG. 33. Absorbancy changes of plastoquinone depending on the electron acceptor and on the light condition (Schmidt-Mende and Witt, 1968).

rapidly reduced in a single short flash. The half time of reduction was determined as 0·6 ms (Stiehl and Witt, 1968). Plastoquinone is reoxidized in about 20 ms; which corresponds to the slow phase of the reduction of chlorophyll a_1. Now in longer flashes, reduced plastoquinone is pooled up to about eight times the amount which is reduced in a saturating single-turnover flash. About half the reduced pool (three electronic equivalents) relaxes rapidly after switching off the light, while the rest relaxes much more slowly. The reductant and the oxidant of plastoquinone were attributed to light reaction II and light reaction I, respectively, but experiments such as that illustrated in Fig. 33 suggest that without any terminal electron acceptor plastoquinone is irreversibly reduced on illumination of chloroplasts with a long flash of light (the duration of which is illustrated by full bars in Fig. 33). In the presence of an electron acceptor, the plastoquinone pool is emptied in part to the equivalent of three electrons (the standard of one electron is determined by the extent of absorption change on excitation with a single-turnover flash). Thus in the presence of an electron acceptor light obviously activates an oxidizing equivalent corresponding to three electrons. If continuous far-red light is presented in addition to the flash (as illustrated in Fig. 33, right), which selectively activates light reaction I, the plastoquinone pool is fully reoxidized while the reduction kinetics remain unaltered. This demonstrates that plastoquinone is oxidized by light reaction I, and reduced by light reaction II. Moreover, it reveals an electron storage capacity between plastoquinone and chlorophyll a_1 (included) as illustrated in Fig. 34. This capacity was determined as $3e^-$ (Stiehl and Witt, 1969; Marsho and Kok, 1970). More detailed experiments on the sensitivity of the plastoquinone reduction and oxidation on a specific poison for light reaction II (DCMU) revealed that at least ten electron transport chains are coupled in parallel possibly via a common pool of plastoquinone (Siggel *et al.*, 1972).

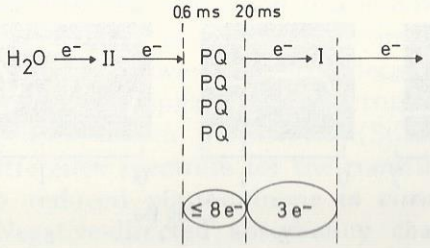

FIG. 34. The interrelationship between plastoquinone (PQ) with the two light reactions.

Spectrophotometric measurements on plastoquinone are technically somewhat difficult mainly because the effect of scattering is larger in the u.v. than in the visible (see the wavelength dependence of Rayleigh scattering, Section IIIB2). Moreover, the near u.v. region requires quartz optics instead of glass optics. Another technical aspect of Figs 32 and 33 is noteworthy. While the relatively larger absorbancy changes of plastoquinone under long flash excitation which relaxes slowly can be resolved in single-flash experiments without averaging, the smaller absorbancy changes on excitation with short single-turnover flashes at a time resolution of a tenth of a millisecond were resolved only by averaging techniques.

2 *The donor pool of light reaction I*

As is obvious from the absorbancy changes of plastoquinone there exists a storage capacity of about $3e^-$ per reaction centre I (and II) after plastoquinone. One electron is accounted for by chlorophyll a_1, which, although a dimer, undergoes a one-electron redox reaction as evident from the redox titration experiments and e.p.r. studies. Candidates for the remaining two equivalents are cytochrome *f* (Witt *et al.*, 1961) and plastocyanin (Katoh and Takamiya, 1963). Biochemical studies led to conflicting schemes for the functioning of cytochrome *f* and plastocyanin in the electron transport chain. Recent flash photometric studies revealed that cytochrome *f* does not participate in the linear electron transport scheme at a 1 : 1 stoicheiometry. Less than 15% of the electrons on their way from water to the terminal electron acceptor pass via cytochrome *f* (Haehnel, 1973). On the other hand, absorbancy changes of plastocyanin were detected, revealing an electron storage capacity of about 2, which together with the electron storage capacity of chlorophyll a_1 accounts for the total capacity of $3e^-$ (Haehnel, 1974). These results obtained under flash excitation do not necessarily bear on the situation under continuous light.

The technically interesting aspects of the experiments which led to the identification of absorbancy changes of plastocyanin is that the electron transport chain was successively titrated with groups of short flashes. Since the rate-limiting step of the total electron transport chain is located between plastoquinone and the primary donor pool of light reaction I, the donor pool is oxidized by far-red light which selects for light reaction I. If after pretreatment with far-red light photosynthesis is excited by a double flash of blue light which excites both light reactions, two electrons are pumped by light

reaction II via plastoquinone into the primary donor pool of light reaction I. Thus the redox state of the donor pool can be adjusted to a content of two electrons. If the system is now excited by another short flash, for the sake of simplicity selecting for light reaction I, then absorbancy changes of chlorophyll a_1 will result which very rapidly relax with the typical relaxation time between the donor pool and chlorophyll a_1 (200 μs) while an irreversible absorbancy change of plastocyanin will result. By this technique it was feasible to resolve the relatively small absorbancy changes of plastocyanin from the larger underground signals resulting from other events in photosynthesis.

3 *The acceptor system of light reaction I*

The first absorbancy changes detected which originate from a compound acting as an oxidant of light reaction I were those of the artifical electron acceptor 2,6-dichlorophenol-indophenol (Kok *et al.*, 1967). Only recently, Ke and coworkers (for a review, see Ke, 1973) reported on absorbancy changes which were attributed to the redox reaction of one of the intrinsic components on the reducing side of

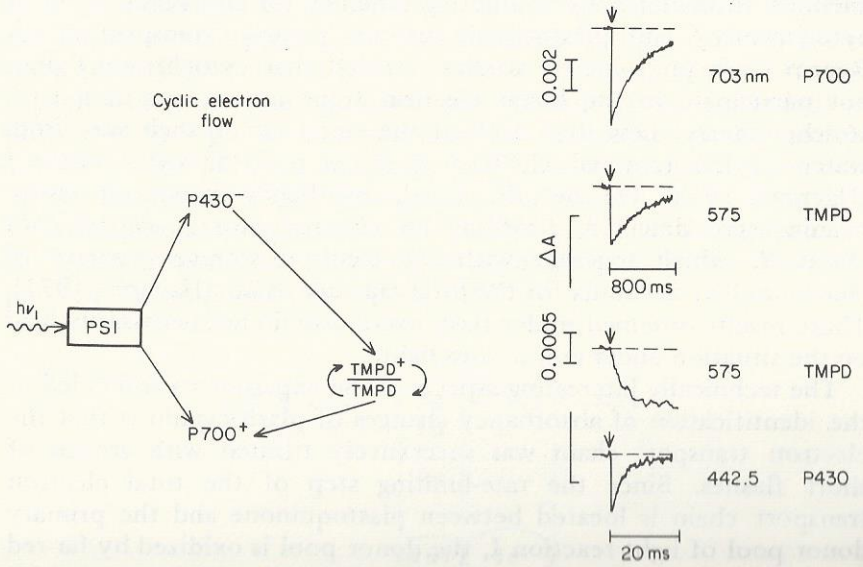

FIG. 35. Scheme for cyclic electron flow mediated by TMPD around photosystem I and the kinetics of the flash-induced absorption changes of P700, TMPD, and P430. (Reproduced, with permission, from Ke, 1973.)

light reaction I. The as yet not fully identified pigment responsible for these absorbancy changes was named P430. The kinetic properties of these absorbancy changes under conditions where cyclic electron transport around light reaction I was mediated by TMPD is illustrated in Fig. 35. The absorbancy changes at 705 and 442·5 nm are practically purely indicators of redox reactions of chlorophyll a_1 (P700), TMPD and P430, respectively. While the oxidation of P700 and the reduction of P430 are very fast, the reoxidation of P430 occurs in a few milliseconds. The reoxidation kinetically matches the kinetics of the TMPD reduction. On the other hand, the kinetics of the reoxidation of TMPD match the kinetics of the reduction of P700. This fits into the scheme for cyclic electron transport around light reaction I which is illustrated in the left of Fig. 35. The role of P430 (which is most purely indicated by absorbancy changes at 442·5 nm) was further corroborated by redox titration and correlation with e.p.r. studies. The spectral properties of these absorbancy changes plus the e.p.r. evidence favours the identification of P430 with "bound ferredoxin" (Ke, 1973).

C THE ELECTROCHEMICAL POTENTIAL GENERATION

1 *Electrochroic absorption changes of chloroplast bulk pigments*

The generation of an electric potential difference across the inner membranes of chloroplasts on illumination was detected via special absorption changes peaking around 515 nm which were sensitive to the alteration of the electric conductance of the inner membranes of chloroplasts (Junge and Witt, 1968). Two lines of evidence led to the conclusion that these absorption changes reflect the electrochroic response of chloroplast bulk pigments to a high electric field strength across the membrane.

Kinetic evidence came from the fact that the decay of these absorption changes after excitation with flashlight was accelerated by operations on the electric conductivity of the membrane (osmotic shock, detergents, ionophores). This acceleration was dependent on the concentration of permeating ions in a chloroplast suspension; it was specific for certain ions in the presence of specific ionophores, but unspecific in the case of osmotic shock or detergent treatment. Therefrom it was concluded that the above absorption changes are sensitive to the electric charge but not to the chemical nature of ions.

Spectroscopic evidence for the electrochroic nature of these absorption changes was provided by a comparison of the flash light-

induced difference spectrum of those absorption changes with the above kinetic properties resulting from isolated chloroplasts (Emrich *et al.*, 1969) with the spectrum of the electrochroic response of extracted chloroplast bulk pigments *in vitro* (Schmidt *et al.*, 1972). Reasonable agreement was obtained.

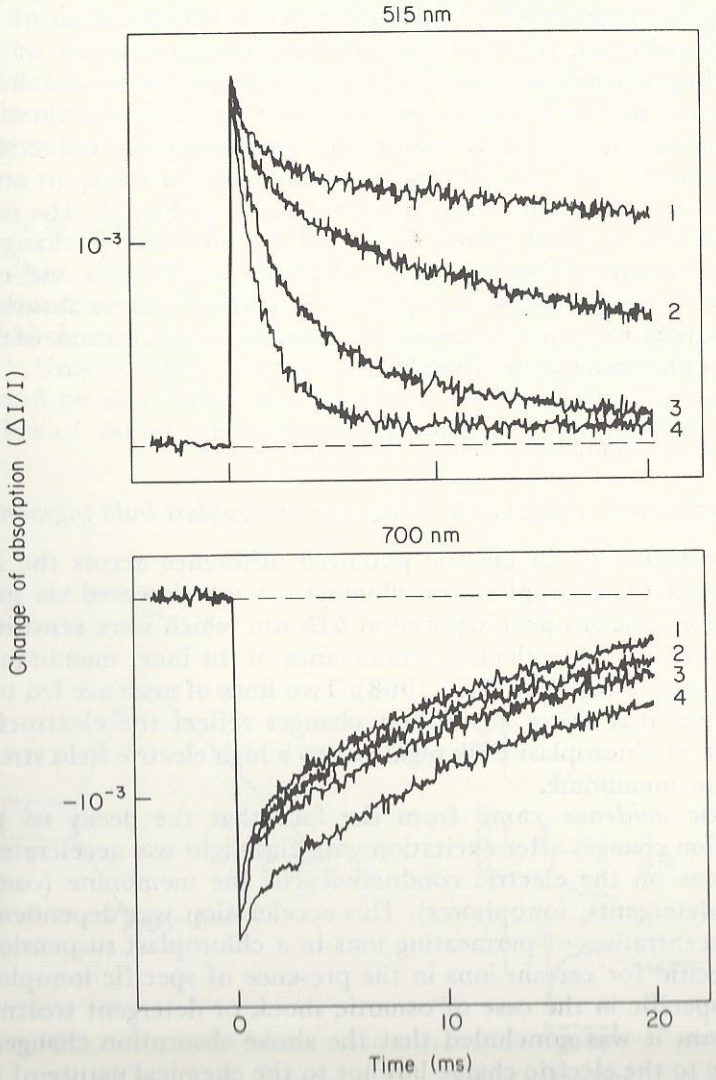

FIG. 36. The dependence of the flash-induced absorbancy changes at 515 and 700 nm on the concentration of the ion-transporting antibiotic gramicidin (Emrich *et al.*, 1969). Curve 1, no gramicidin; curve 4, 10^{-9} M gramicidin.

The dependence of the relaxation kinetics of the absorbancy changes at 515 nm on the ionophore concentration is illustrated in Fig. 36 (upper part). It is obvious that at this wavelength almost the full extent of flash-induced transient absorbancy changes is sensitive to ionophore treatment. The lower part of Fig. 36 illustrates the dependence of the absorbency changes at the peak wavelength of chlorophyll a_1 (700 nm) on the ionophore concentration. It is obvious that, at this wavelength, only a small fraction of the total absorbancy change is sensitive to ionophores. This illustrates how these components of the absorbancy changes at a given wavelength which are of electrochroic origin, can be extracted from the total absorbancy change. The separated electrochroic difference spectrum obtained on flash excitation of chloroplast suspension is shown in the upper part of Fig. 37 (Emrich *et al.*, 1969). The lower part of

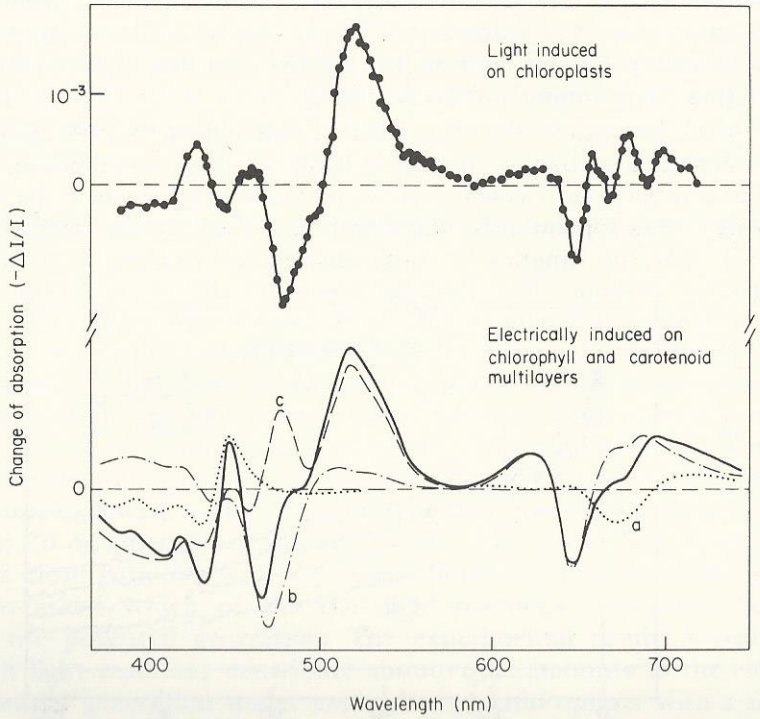

FIG. 37. Above: Light-induced difference spectrum of electrochroic absorbancy changes in chloroplasts isolated according to Fig. 36 (Emrich *et al.*, 1969). Below: Electrochroic absorbancy changes of chlorophylls and a carotenoid (c) induced by the application of high electric field strengths on these pigments imbedded in multilayers (Schmidt *et al.*, 1972).

Fig. 37 shows the *in vitro* response of chloroplast bulk pigments to high electric field strengths from experiments with microcapacitors *in vitro* (Schmidt *et al.*, 1971). Superposition of the electrochroic response of these pigments *in vitro* yielded a reasonable agreement with the electrochroic spectrum obtained from chloroplasts *in vivo*.

Similar absorption changes observed on excitation of bacterial chromatophores with a flash were attributed to electrochroic effects, too, because of the similarity between their difference spectrum with the difference spectrum obtained when chromatophores were submitted to a salt jump causing a diffusion potential (Jackson and Crofts, 1969). Recent studies at a higher spectral resolution gave evidence for a rather involved mechanism underlying the apparent first-order response of carotenoids to the transmembrane field (Crofts *et al.*, 1974). Direct evidence for the generation of an electric field across the photosynthetic membrane was provided by measurements of electric induction phenomena in chloroplast suspensions by means of macroscopic electrodes (Kok, 1972; Witt and Zickler, 1973; Fowler and Kok, 1974b) and by microelectrode techniques (Vredenberg and Tonk, 1975).

It might be argued that the electric field which is indicated by electrochroic absorbancy changes is localized in the membrane, but does not reflect an electric potential difference between the two aqueous phases separated by the membrane. This is to be rejected by the fact that the kinetics of these absorbancy changes is sensitive

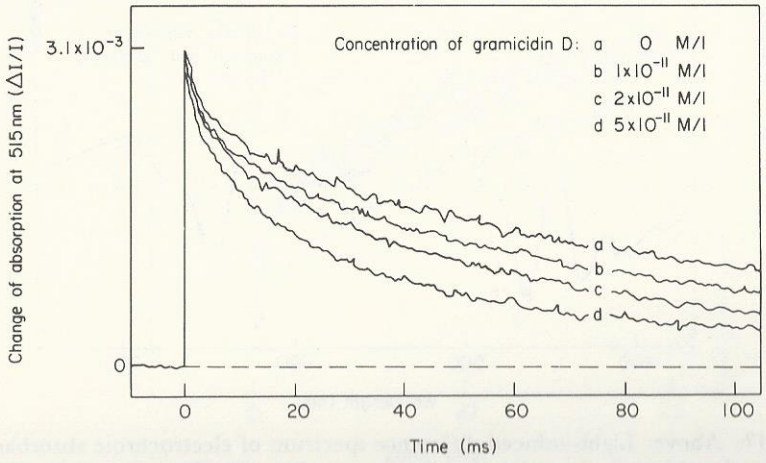

FIG. 38. The dependence on very small concentrations of the ion-transporting antibiotic gramicidin, of the flash-induced absorption changes at 515 nm in chloroplasts. The chlorophyll concentration in the cuvette was 10^{-5} M/l (Junge, 1968).

already to one molecule of gramicidin given on 10^5 chlorophyll molecules (Junge and Witt, 1968). 10^5 Chlorophyll molecules roughly correspond to the contents of one thylakoid. This experiment is documented in Fig. 38. It clearly demonstrates that the functional unit of the electric phenomena of photosynthesis is at least as big as one thylakoid. Because of the delocalization of the electric field across the membrane which according to Fig. 38 is confirmed at least on a millisecond time scale, the thylakoid membrane may be treated as an electric capacitor with a low leak conductivity incorporating light-driven electric generators (Junge and Witt, 1968). Correlation of the electrochroic absorbancy changes around 515 nm with the proton translocation across the thylakoid membrane (Reinwald *et al.*, 1968; Schliephake *et al.*, 1968) led to the conclusion that these absorbancy changes are linearly correlated with the electric potential difference across the thylakoid membranes. The linearity was corroborated by electric induction techniques (Witt and Zickler, 1974). This linearity was used to carry out current voltage studies on the mechanism of the electric conductance by means of spectrophotometry (Junge and Schmid, 1971; Schmid and Junge, 1975).

2 *Vectorial and protolytic properties of the electron transport chain*

As illustrated in the previous section, light induces an electric potential difference across the thylakoid membrane which is indicated by electrochroic absorbancy changes of chloroplast bulk pigments. It has been asked how close the electric potential generation which implies charge translocation across a membrane is coupled to the primary photochemistry of photosynthesis. The rise of the electrochroic absorbancy changes at 515 nm on excitation of chloroplasts with a short laser flash came out as extremely rapid (less than 20 ns, instrument limited—Wolff *et al.*, 1969). This is indicative of a close coupling with a primary photochemical reaction. It has been asked which of the two light reactions contributes to the electric potential generation. The experimental results reveal that both light reactions contribute about equal amounts to the electric potential generation under excitation of chloroplasts with a single-turnover flash (Schliephake *et al.*, 1968). The appropriate experiment is illustrated in Fig. 3. This shows the electrochroic absorbancy changes at 515 nm after excitation of chloroplasts with a short flash given at $t = 0$. On the left, both light reactions were active with TIP as terminal electron acceptor. In the middle, light reaction

II was blocked by addition of the specific inhibitor DCMU, while light reaction I remained still active by cyclic electron transport which was mediated by TIP. On the right, light reaction I was deactivated by ferricyanide plus DPIP acting as an efficient electron acceptor between the two light reactions. The attribution of the signals to light reaction I and light reaction II, respectively (in the middle and on the right of Fig. 39) was checked by measuring the respective action spectra. The electrochroic part of the resulting absorbancy changes under these conditions was labelled by acceleration with the ionophore gramicidin. The experiments show that both light reactions contribute about equally to the generation of an electric potential difference (Schliephake *et al.*, 1968).

The generation of the electric potential difference with contributions from both light reactions was understood by an alternating

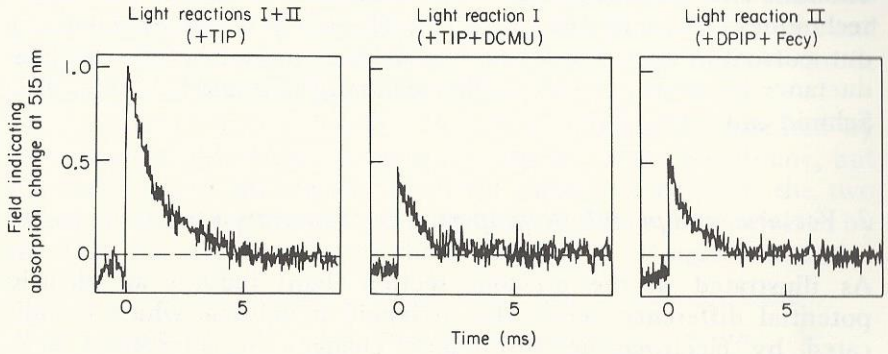

FIG. 39. The flash-induced absorbancy changes at 515 nm in the presence of the ion-transporting antibiotic gramicidin, depending on the activity of light reaction I and light reaction II. For details, see text (Schliephake *et al.*, 1968).

electron hydrogen-transport systems as illustrated in Fig. 40 (Schliephake *et al.*, 1968; Junge and Ausländer, 1974): water oxidation leads to the release of one photon per electron at the inner side of the membrane. Light reaction II activity promotes the translocation of one electron across a functional membrane from the inner to the outer side. The reduction of plastoquinone by light reaction II at the outer side of the membrane leads to the binding of one proton to an electron from the outer phase. Oxidation of plastoquinone occurs at the inner side of the membrane by plastocyanin, it leads to the release of one proton per electron into the inner phase. Finally, light reaction I translocates

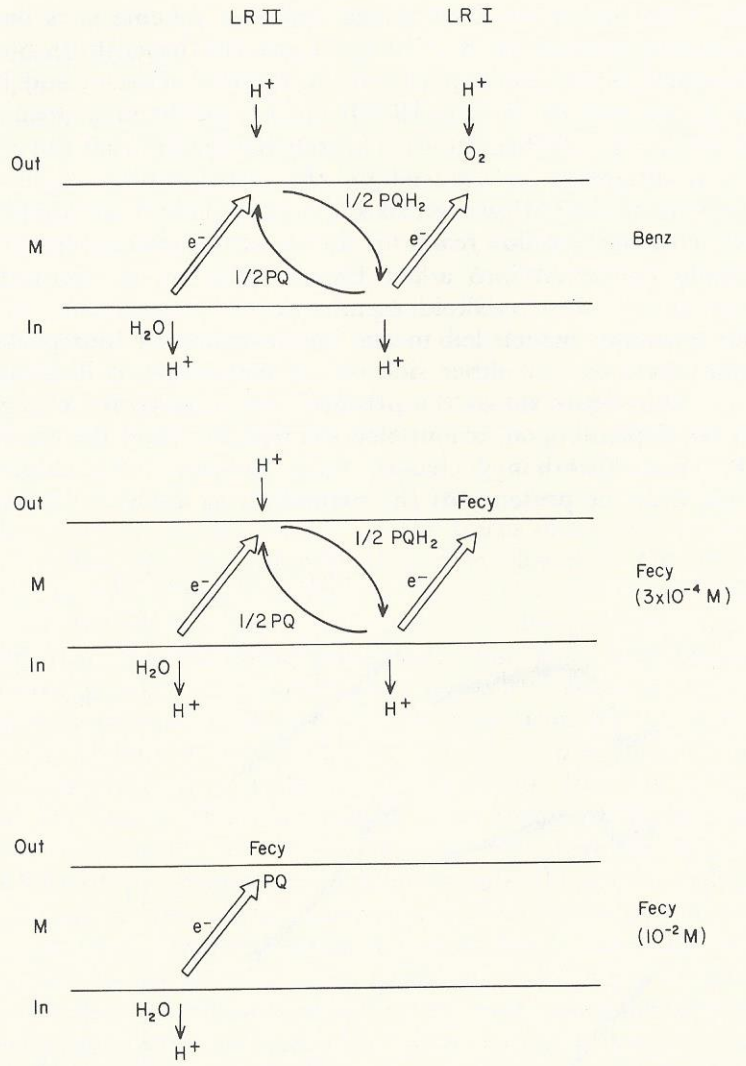

FIG. 40. Model for the vectorial and protolytic properties of the electron transport chain in the presence of different electron acceptors (Junge and Ausländer, 1974).

one electron from the inner to the outer side of the membrane and reduces the terminal acceptor at the outer side. Reduction of the terminal acceptor leads to the binding of $\nu H^+/e^-$ (for NADP: $\nu = \frac{1}{2}$, for BENZ and DPIP: $\nu = 1$, for Fecy: $\nu = 0$).

This vectorial electron hydrogen-transport scheme goes back to Mitchell's hypothesis (1961, 1966). It was confirmed both by flash spectrophotometry (Schliephake *et al.*, 1968; Ausländer and Junge, 1974; Junge and Ausländer, 1974) and by biochemical techniques (for a review, see Trebst, 1974). This scheme implies that the electric potential difference is induced by the translocation of electrons across a membrane. However, owing to the protolytic reactions in consequence of the redox reactions the electronic charge separation is ultimately converted into a net translocation of two protons per electron across the thylakoid membrane.

The technique which led to the identification of four protolytic reaction sites, two at either side of the membrane, is illustrated in Fig. 41. This figure shows the pH-indicating absorbancy changes of cresol red depending on various electron acceptors and the uncoupler FCCP. These absorbancy changes were obtained for a chloroplast suspension in the presence of the pH-indicating dye cresol red under

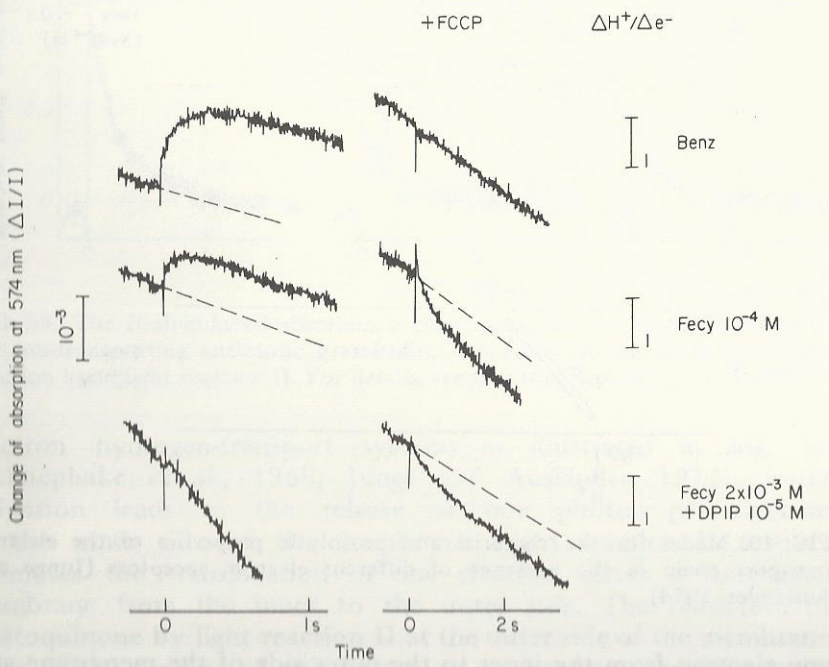

FIG. 41. The pH-indicating absorbancy changes of cresol red at 574 nm depending on different electron acceptors (right) and in the absence (left traces) and in the presence (right traces) of the uncoupling agent, FCCP (Junge and Ausländer, 1974).

excitation with single-turnover flashes. To separate the pH-indicating absorbancy changes of cresol red at 574 nm from the underlying absorbancy changes of other origins, the difference between signals obtained in the absence and in the presence of buffer was recorded. Subtraction of these signals was performed by the built-in arithmetic of an averaging computer. The signals depicted in Fig. 41 represent this difference. Cresol red in the absence of agents which increase the proton permeability of the thylakoid membrane indicates pH changes in the outer phase of thylakoids only. An increase of absorption indicates alkalization of the outer phase. Once the buffer capacity of a chloroplast suspension has been determined the absorbancy changes are easily calibrated into the number of protons taken up from the outer phase. This can be related to the number of electrons transferred through the chain as determined from oxygen production (Renger, 1971), dye reduction (Kok *et al.*, 1966), or by the absorbancy changes of chlorophyll a_1, the extinction coefficient of which is known (Ke *et al.*, 1971). The traces in the left column of Fig. 41 then read as follows: If benzyviologen is the terminal electron acceptor, two protons per electron are taken up from the outer aqueous phase while there is only one proton per electron if ferricyanide (low concentration) accepts electrons from light reaction I. No proton is taken up from the outer phase if ferricyanide (in higher concentrations) via DCIP accepts electrons from light reaction II; while benzylviologen, which channels electrons to oxygen, binds one proton per electron on reduction, ferricyanide does not at physiological pH values. Thus ferricyanide from lower to higher concentrations successively deactivates two protolytic reaction sites at the outer side of the membrane as schematically illustrated in Fig. 40. pH changes in the inner phase were indirectly measured by the dye cresol red too. In the presence of proton carriers like FCCP or other uncoupling agents the thylakoid membrane is highly permeable to protons so that information on protolytic reactions in the inner phase leaks into the outer one within say some 10 ms. In the presence of proton permeability increasing agents cresol red indicates the net proton production from both aqueous phases. The net proton production under the acceptor conditions of Fig. 41 can be read out from the right column in Fig. 41. It is nil for benzylviologen, +1 for ferricyanide in low concentrations and +1 for ferricyanide in high concentrations. This is compatible with the vectorial electron hydrogen-transport scheme which is illustrated in Fig. 40 (Junge and Ausländer, 1974). The attribution of the above characterized four protolytic reaction sites to the redox components, water, plasto-

quinone, and the terminal electron acceptor was further corroborated by kinetic correlations of these protolytic reactions with the corresponding redox reactions (Ausländer and Junge, 1974; Fowler and Kok, 1974a). Biochemical evidence led to similar conclusions. Studies with antibodies on the location of redox components in the membrane revealed that the reducing side of light reaction I lies at the outer side of the membrane (Berzborn *et al.*, 1966) and plastocyanin at the inner one (Hauska *et al.*, 1971). Studies with artificial mediators of electron transport which were distinguished by different hydrophobicity could be interpreted only by assuming vectorial electron transport at light reaction II (for a review, see Trebst, 1974).

These experimental results on the electrochemical generator are summarized in Fig. 42 (upper part).

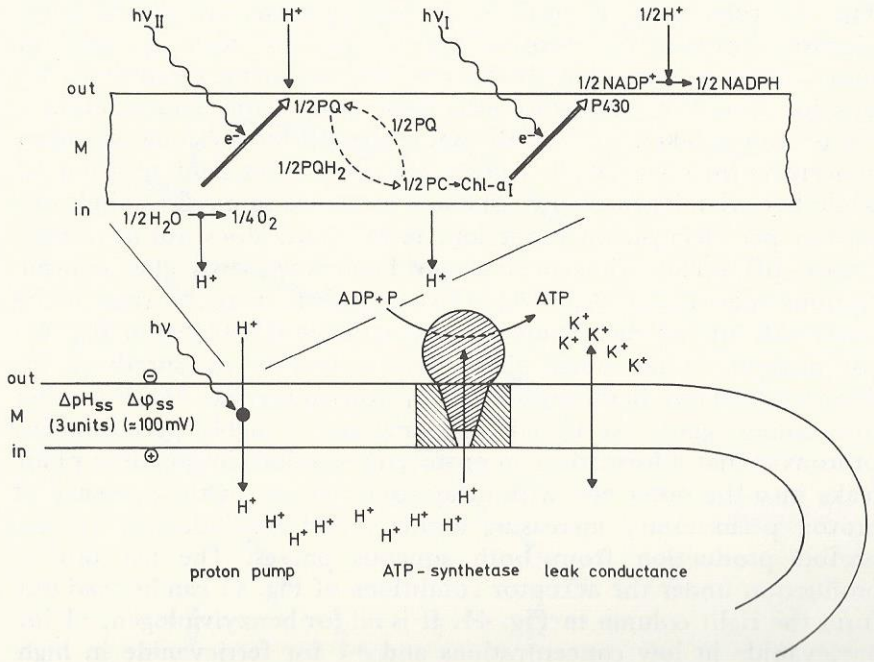

FIG. 42. Model summarizing the flash spectrophotometric results on the electrochemical potential generation and its use for photophosphorylation (for details, see text).

D PHOTOPHOSPHORYLATION

Besides reduced NADP and molecular oxygen, ATP is produced in the primary processes of photosynthesis. While it is generally accepted that in the first step light energy is transformed into the free energy of redox couples, it is still under discussion via which type of intermediate part of the redox energy may be channelled into the phosphorylation of ATP. The current discussion is governed by three hypotheses on the nature of this intermediate:

(1) a chemical high intermediate (Slater, 1953, 1958);
(2) an electrochemical potential difference of the proton (Mitchell, 1961, 1966);
(3) high energy conformational states of the membrane or an enzyme complex (Green *et al.*, 1968).

A phosphorylation mechanism, according to Mitchell's hypothesis, is characterized by two properties which are distinct from the remainder hypotheses and which are subject to experimental tests: an electrochemical potential difference of the proton is generated by a vectorial electron transport system; dissipation of the electrochemical potential difference of the proton competes with its use for ATP synthesis. The first property as experimentally tested by flash spectrophotometric methods has already been discussed above. The second property was studied by flash spectrophotometry too. The results of the respective experiments are illustrated in Figs 43–44. Figure 42 shows the time course of the electric potential difference as measured by the electrochroic absorbancy changes at 523 nm on excitation of a chloroplast suspension with a short flash group at $t = 0$ (Junge *et al.*, 1970b). Under excitation with short flash groups at a rather low repetition frequency, the contribution of the pH difference to the electrochemical potential difference of the proton is small compared with the electric component. As is obvious from Fig. 42, the time course of the decay of the electric potential difference in the dark is markedly accelerated under phosphorylation conditions. This might indicate that the synthesis of ATP opens up a special electrically conducting channel, the ion flux across which is coupled to ATP synthesis, as postulated by Mitchell (1961). However, this conclusion is convincing only if the generation of a dissipative electrically conducting channel in the membrane inhibits ATP synthesis competitively. Such a channel was introduced by adding the potassium ion carrier valinomycin at low concentrations. As is obvious from a comparison of the two traces in Fig. 44, the

decay of the electric potential difference under phosphorylating conditions is further accelerated in the presence of valinomycin. Under these conditions the ATP yield per flash group which was measured by a radioactive tracer technique (^{32}P) was decreased in the presence of valinomycin (Junge *et al.*, 1970b). This experiment was refined for another ion-transporting antibiotic, gramicidin. It was found that the minimum amount of gramicidin which competitively inhibits the synthesis of ATP is one molecule on 10^5 molecules of chlorophyll (Boeck and Witt, 1971). Therefrom it was concluded that the functional unit for photophosphorylation under flash excitation is as big as the functional unit of the electric potential difference (Junge and Witt, 1968), at least as big as one thylakoid.

A technically interesting aspect of the experiment of Boeck and Witt (1971) is that the ATP yield was measured under flash excitation optically by fluorescence changes of the pH indicating dye umbelliferone. Since the formation of one molecule of ATP causes the consumption of one proton at pH 8, the irreversible pH change in a chloroplast suspension could be attributed to ATP formation.

Since the light-induced pH difference across the thylakoid membrane relaxes within a few seconds, it did not interfere with this technique for measuring the ATP yield. The special advantage of the optical read-out of the ATP yield over the radioactive tracer technique (^{32}P) lies in the insensitivity of the optical method for

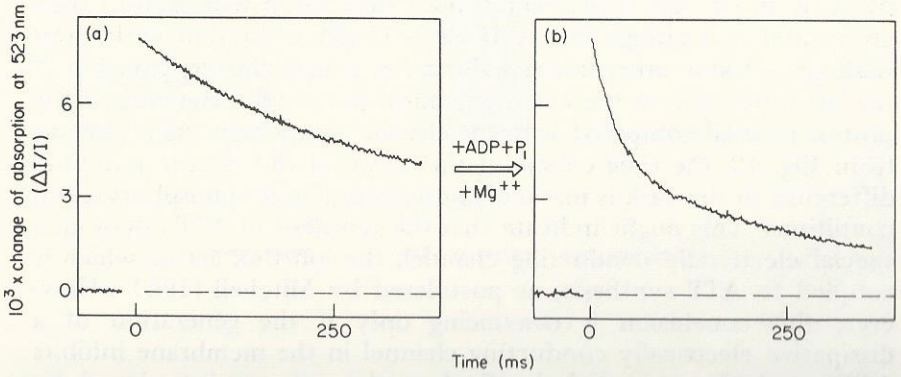

FIG. 43. The electrochroic absorbancy changes at 523 nm on excitation with a group of four short flashes depending on the presence of phosphorylating substrates (Junge *et al.*, 1970b).

P_i-exchange reactions and in the proper sensitivity for ATP hydrolysis.

The studies of the interrelationship between the electric potential difference and the ATP yield were quantitatively refined (Witt, 1971). Moreover, it was demonstrated that extraction of the coupling factor for photophosphorylation (CF_1) resulted in an increase of the electric conductivity of the membrane for protons, while recondensation of the coupling factor reduced the conductivity again (Schmid and Junge, 1974). This clearly demonstrates the existence of a Mitchellian ATPase having access to the inner phase of the thylakoid from the outer side through the membrane.

The flash spectroscopic results on the electrochemical potential generation and on the mechanism of photophosphorylation are summarized in Fig. 42. The electrochemical potential difference is generated by a vectorial electron transport as shown in the upper part of the figure. The light-driven proton pump generates a pH difference across the thylakoid membrane plus an electric potential difference which is positive inside. This electric potential difference

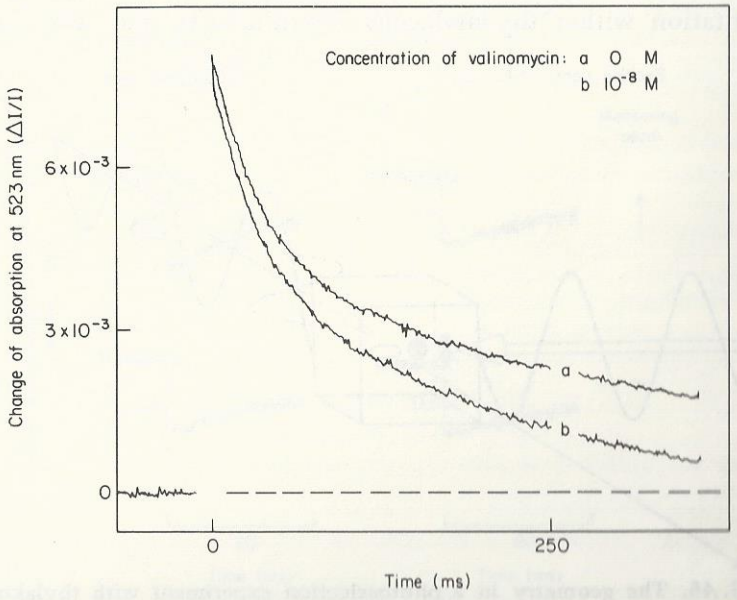

FIG. 44. The time course of the electrochroic absorbancy changes at 523 nm under phosphorylating conditions in the presence of a potassium-transporting antibiotic, valinomycin (Junge *et al.*, 1970b).

drives other cations outwards and sucks anions into the inner phase. This motion of other ions and protons in the steady state compensates for most of the electric charge of the protons in the inner phase. Thus the electric potential difference in the steady state corresponds to a small fraction of protons, those which are not electrically compensated by other ions. The electrochemical energy can be used by an ATP synthetase which couples the outflux of protons which are driven by the pH difference and by the electric potential difference to the synthesis of ATP. The energy is in part dissipated by the leak conductivity of the membrane for protons (under steady illumination) and by the leak conductivity for any other ion (under flash light conditions). These results agree with Mitchell's original hypothesis.

E PIGMENT ORIENTATION IN THE MEMBRANE

The probability that a molecule absorbs a light quantum according to equation (5) depends on the relative orientation of the E-vector of the light to the transition moment of the molecule. As discussed in Section IIB5 (see Fig. 8) the transition moment has a given orientation within the molecular coordinate system. The selective

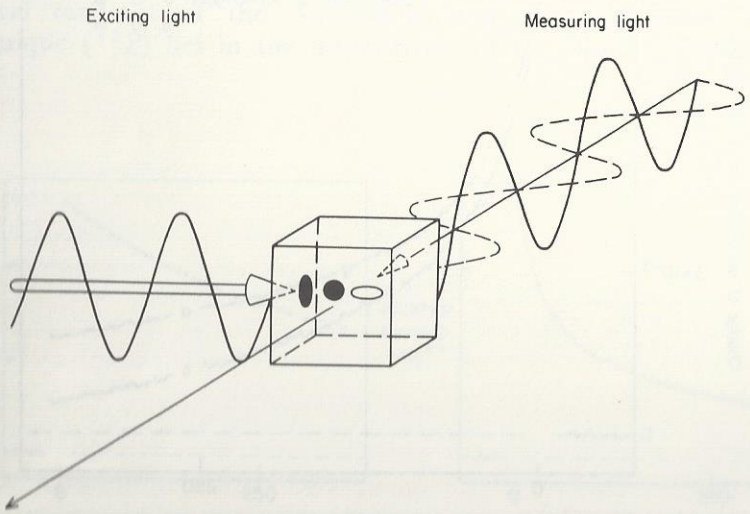

FIG. 45. The geometry in a photoselection experiment with thylakoids. The waves indicate the E-vector polarization of the exciting light and of the interrogating light. The membrane orientations, represented by full circles, are excited preferentially (Junge and Eckhof, 1973).

absorption for linearly polarized light (linear dichroism) can be used to study the orientation of reactive pigments in the thylakoid membrane. Linear dichroism studies on magnetically orientated chloroplasts (Geacintov *et al.*, 1971) and on chloroplasts orientated on dried films (Breton and Roux, 1971; Breton *et al.*, 1973) revealed that the transition moments of the antennae chlorophylls which absorb above 680 nm lie almost flat in the plane of the membrane. This information on the orientation of some of the antennae pigments is important since it makes flash photometric studies on the orientation of the chemically reactive pigments feasible. By photoselection it is possible to select a preferentially orientated subset of membranes from an isotropic chloroplast suspension. When exciting such a suspension, which in Fig. 45 is illustrated by three possible membrane orientations (circles) with a linearly polarized flash of light at non-saturating intensities the wavelength of which is tuned for the in-plane orientated antennae (above 680 nm), one preferentially excites those membrane orientations which are represented

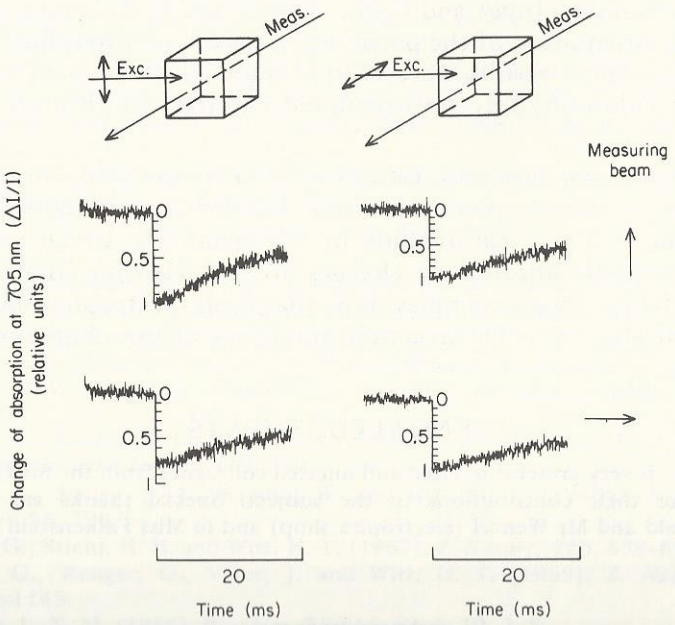

FIG. 46. The linear dichroism of the absorbancy changes of chlorophyll a_1 as induced by excitation with a linearly polarized flash in the set-up which is illustrated in Fig. 45 (Junge and Eckhof, 1974).

as full circles. The membrane orientation which is parallel to the bottom of the absorption cell is not excited because it does not contain transition moments with components parallel to the E-vector of the exciting flash. In consequence of this photoselection one expects that the absorbancy changes, say of chlorophyll a_1, which are induced by the flash result from the same subset of membranes, which was photoselected. Under the condition that chlorophyll a_1 has a preferential orientation within the membrane one expects that the extent of these absorbancy changes will differ depending on whether they are observed with linearly polarized light, the E-vector of which is parallel to the flash or perpendicular to the flash, respectively, as illustrated in Fig. 45. This, in fact, was observed as illustrated in Fig. 46 (Junge and Eckhof, 1973, 1974). Dichroic ratios ($\Delta A_{\parallel}/\Delta A_{\perp}$) greater than 1·15 were observed for both major bands of chlorophyll a_1 at 700 and 430 nm, respectively. These could be interpreted under certain assumptions on the symmetry properties of the antennae system and on the structure of the chlorophyll a_1 dimer. It was concluded that both major transition moments of chlorophyll a_1 are inclined at less than 25° to the plane of the membrane (Junge and Eckhof, 1973, 1974). This pointed to a rather flat orientation of the porphyrin rings of chlorophyll a_1 to the membrane. These results were corroborated by flash spectrophotometry of chlorophyll a_1 on orientated chloroplasts (Breton *et al.*, 1975).

Similar studies, however, carried out on magnetically orientated chloroplasts without photoselection, revealed a preferentially flat orientation of those carotenoids in the membrane which produce the electrochroic absorbancy changes around 515 nm (Breton and Mathis, 1974). These examples show that flash spectrophotometry is even applicable to tackle structural questions of the photosynthetic apparatus.

ACKNOWLEDGEMENTS

The author is very grateful to cited and uncited colleagues from the Max-Volmer Institut for their contributions to the subject. Special thanks are due to Dr Buchwald and Mr Wenzel (electronics shop) and to Miss Falkenstein (for the drawings).

REFERENCES

Amesz, J. (1964). *Biochim. biophys. Acta* 87, 257–265.
Amesz, J., Duysens, L. N. M. and Brandt, D. (1961). *J. theor. Biol.* 1, 59–74.

Ausländer, W. and Junge, W. (1974). *Biochim. biophys. Acta* 357, 285–298.
Beinert, H. and Kok, B. (1964). *Biochim. biophys. Acta* 88, 278–284.
Berzborn, R. J., Menke, W., Trebst, A. and Pistorius, E. (1966). *Z. Naturf.* 21b, 1057–1059.
Bhaumik, M. L. (1967). *Am. J. Phys.* 35, 330–338.
Bishop, E. (1972). "Indicators". Pergamon Press, Oxford.
Bishop, N. I. (1959). *J. Biochemistry, Tokyo* 45, 1696.
Boag, J. W. (1968). *Photochem. Photobiol.* 8, 565–577.
Boeck, M. and Witt, H. T. (1972). *Proc. 2nd Int. Congr. Photosyn. Res.* 903–911.
Borisov, A. Yu. and Ilina, M. D. (1973). *Biochim. Biophys. Acta* 305, 368–371.
Breton, J. and Mathis, P. (1970). *C. r. hebd. Séanc. Acad. Sci., Paris* 271, 104–1096.
Breton, J. and Mathis, P. (1974). *Biochem. biophys. Res. Commun.* 58, 1071–1077.
Breton, J. and Roux, E. (1971). *Biochem. biophys. Res. Commun.* 45, 557–563.
Breton, J., Michel-Villaz, M. and Paillotin, G. (1973). *Biochim. biophys. Acta* 314, 42–56.
Breton, J., Roux, E. and Whitmarsh, J. (1975). *Biochem. biophys. Res. Commun.* 64, 1274–1277.
Bryant, F. D., Latimer, P. and Seiber, B. A. (1969). *Archs Biochem. Biophys.* 135, 109–117.
Buchwald, H. E. (1972). *Z. Anal. Chem.* 261, 286–290.
Buchwald, H. E. and Rüppel, H. (1971). *J. scient. Instrum.* 4, 105–110.
Butler, W. L. (1972). *Meth. Enzym.* 24, 3–25.
Chance, B. and Mela, L. (1966). *J. biol. Chem.* 241, 4588–5496.
Chance, B. and DeVault, D. (1964). *Z. Elektrochem.* 68, 722–726.
Chessin, M., Livingston, R. and Truscott, T. G. (1966). *Trans. Faraday Soc.* 62, 1519–1524.
Chibisov, A. K., Karyakin, A. V. and Zubrilina, M. E. (1965). *Russ. J. Phys. Chem.* (Eng. Trans.) 39, 1224–1227.
Clayton, R. K. (1970). "Light and Living Matter", vol. 1. McGraw-Hill, New York.
Cost, K. and Frenkel, A. W. (1967). *Biochemistry, N.Y.* 6, 663–667.
Crofts, A. R., Prince, R. C., Holmes, N. G. and Crowther, D. (1974). *Proc. 3rd Int. Congr. Photosyn. Res.* 1131–1146.
Czerlinsky, G. and Eigen, M. (1959). *Z. Elektrochem.* 63, 652–661.
Deamer, D. W., Crofts, A. R. and Packer L. (1967). *Biochim. biophys. Acta* 131, 81–96.
Döring, G. Bailey, J. L., Kreutz, W., Weikard, J. and Witt, H. T. (1968a). *Naturwissenschaften* 55, 219–220.
Döring, G., Bailey, J. L., Kreutz, W. and Witt, H. T. (1968b). *Naturwissenshaften* 55, 220.
Döring, G., Stiehl, H. H. and Witt, H. T. (1967). *Z. Naturf.* 22b, 639–644.
Döring, G., Renger, G., Vater, J. and Witt, H. T. (1969). *Z. Naturf.* 24b, 1139–1143.
Duysens, L. N. M. (1956). *Biochim. biophys. Acta* 19, 1–8.
Duysens, L. N. M., Amesz, J. and Kamp, B. M. (1961). *Nature, Lond.* 190, 510.
Emerson, R. (1958). *A. Rev. Pl. Physiol.* 9, 1–10.
Emrich, H. M., Junge, W. and Witt, H. T. (1969). *Z. Naturf.* 29b, 1144–1146.

Förster, Th. (1946). *Naturwissenschaften* **33**, 166–175.
Förster, Th. (1947). *Z. Naturf.* 2b, 147–182.
Förster, Th. (1959). *Trans. Faraday Soc.* **27**, 7.
Fowler, Ch. F. and Kok, B. (1974a). *Biochim. biophys. Acta* **357**, 299–307.
Fowler, Ch. F. and Kok, B. (1974b). *Biochim. biophys. Acta* **357**, 308–317.
Geacintov, N., Van Nostrand, F., Pope, M. and Tinkel, J. B. (1971). *Biochim. biophys. Acta* **226**, 486–491.
Gläser, M., Wolff, Chr., Buchwald, H. E. and Witt, H. T. (1974). *FEBS Lett.* **42**, 81–85.
Govindjee (1975). "Bioenergetics of Photosynthesis". Academic Press, New York and London.
Green, D. E. J., Asai, J., Harris, R. A. and Penniston, J. T. (1968). *Archs Biochem. Biophys.* **125**, 684–705.
Grünhagen, H. H. and Witt, H. T. (1970). *Z. Naturf.* **25b**, 373–386.
Gürs, K. (1969). *In* "Laser" (W. Kleen and Muller, eds), pp. 119–218. Springer-Verlag, Berlin.
Haehnel, W. (1973). *Biochim. biophys. Acta* **305**, 618–631.
Haehnel, W. (1974). *Proc. 3rd Int. Congr. Photosyn. Res.* 557–568.
Haehnel, W. and Witt, H. T. (1971). *Proc. 2nd Int. Congr. Photosyn. Res.* 469–476.
Hanna, M. W. (1969). "Quantum Mechanics in Chemistry". W. A. Benjamin, New York and Amsterdam.
Hauska, G. A., McCarty, R. E., Berzborn, R. J. and Racker, E. (1971). *J. biol. Chem.* **246**, 3524–3531.
Henninger, M. D. and Crane, F. D. (1964). *Pl. Physiol., Lancaster* **39**, 598–605.
Henninger, M. D., Barr, R. and Crane, F. L. (1966). *Pl. Physiol., Lancaster* **41**, 696–700.
Hill, R. and Bendall, F. (1960). *Nature, Lond.* **186**, 136–137.
Hiyama, T. and Ke, B. (1972). *Biochim. biophys. Acta* **267**, 160–171.
Hochstrasser, R. M. and Kasha, M. (1964). *Photochem. Photobiol.* **3**, 317–331.
Holbrook, J. G. (1966). "Laplace Transforms for Electronic Engineers". Pergamon Press, Oxford.
Izawa, S., Itoh, M. and Shibata, K. (1963). *Biochim. biophys. Acta* **75**, 349–354.
Jackson, J. B. and Crofts, A. R. (1969). *FEBS Lett.* **4**, 185–188.
Joliot, P. (1965). *Biochim. biophys. Acta* **120**, 116–134.
Joliot, P., Joliot, A. and Kok, B. (1968). *Biochim. biophys. Acta* **153**, 635–652.
Joliot, P., Joliot, A., Bouges, B. and Barbieri, G. (1971). *Photochem. Photobiol.* **14**, 287–305.
Junge, W. (1968). Thesis, Technische Universität Berlin.
Junge, W. and Ausländer, W. (1972). *Proc. 6th Int. Congr. Photobiol.*
Junge, W. and Ausländer, W. (1974). *Biochim. biophys. Acta* **333**, 59–70.
Junge, W. and Eckhof, A. (1973). *FEBS Lett.* **36**, 207–212.
Junge, W. and Eckhof, A. (1974). *Biochim. biophys. Acta* **357**, 103
Junge, W. and Schmid, R. (1971). *J. memb. Biol.* **4**, 179–192.
Junge, W. and Witt, H. T. (1968). *Z. Naturf.* 23b, 244–254.
Junge, W., Emrich, H. M. and Witt, H. T. (1970a). *In* "Physical Principles of Biological Membranes" (F. Snell, J. Wolken, G. Iverson and J. Lam, eds), pp. 383–394. Gordon and Breach, New York.

Junge, W., Rumberg, B. and Schröder, H. (1970b). *Eur. J. Biochem.* **14**, 575–581.
Kasha, M. (1963). *Radiat. Res.* **20**, 55–71.
Katoh, S. and Takamiya, A. (1963). *Pl. Cell Physiol.* **4**, 335–347.
Katoh, S., Shiratori, I. and Takamiya, A. (1971). *Physiologia Pl.* **25**, 135–140.
Ke, B. (1973). *Biochim. biophys. Acta* **301**, 1–33.
Ke, B., Ogawa, T. Hiyama, T. and Vernon, L. P. (1971). *Biochim. biophys. Acta* **226**, 53–62.
Kleuser, D. and Bücher, H. (1969). *Z. Naturf.* **24b**, 1371–1374.
Kok, B. (1956). *Biochim. biophys. Acta* **22**, 399–404.
Kok, B. (1957). *Acta bot. neerl.* **6**, 316–319.
Kok, B. (1961). *Biochim. biophys. Acta* **48**, 527–535.
Kok, B. (1972). *Proc. 6th Int. Congr. Photobiol.*
Kok, B. and Hoch, G. (1961). *In* "Light and Life" (G. McElroy, ed.), pp. 397–416. Johns Hopkins Press, Baltimore.
Kok, Malkin, S., Owens, O. and Forbush, B. (1967). *Brookhaven Symp. Biol.* **19**, 446–459.
Kreutz, W. (1970). *Adv. Bot. Res.* **3**, 53–169.
Labhart, H. (1961). *Helv. chim. Acta* **44**, 447–456.
Labhart, H. (1967). *Adv. chem. Phys.* **13**, 179–204.
Land, P. L. (1971). *Rev. scient Instrum.* **42**, 420–425.
Landon, V. P. (1941). *Proc. IRE* **29**, 50–54.
Latimer, P., Moore, D. M. and Bryant, F. O. (1968). *J. theor. Biol.* **21**, 348–367.
Liptay, W. (1969). *Angew. Chem.* **81**, 195–231.
Malley, M., Feher, G. and Mauzerall, D. (1968). *J. molec. Spectr.* **25**, 544–547.
Malkin, S. and Kok, B. (1966). *Biochim. biophys. Acta* **126**, 413–432.
Marsho, T. V. and Kok, B. (1970). *Biochim. biophys. Acta* **223**, 240–250.
Mathis, P. (1969). *Photochem. Photobiol.* **9**, 55–63.
Mathis, P. and Vermeglio, A. (1972). *Photochem. Photobiol.* **15**, 157–164.
McRae, E. G. and Kasha, M. (1964). *In* "Phys. Proc. in Rad. Biol.", pp. 23–42. Academic Press, New York and London.
Mitchell, P. (1961). *Nature, Lond.* **191**, 144–148.
Mitchell, P. (1966). 41, 445–502.
Mitchell, P., Moyle, J. and Smith, L. (1968). *Eur. J. Biochem.* **4**, 9–19.
Mitsui, A. and Arnon, D. I. (1971). *Physiologia Pl.* **25**, 135–140.
Mühlethaler, K. (1972). *Chem. Phys. Lipids* **8**, 259–264.
Murrell, J. N. (1963). "The Theory of the Electronic Spectra of Organic Molecules". Methuen, London.
Netzel, T. L., Rentzepis, P. and Leigh, J. (1973). *Science, N.Y.* **132**, 238–241.
Norris, J. R., Uphaus, R. A., Crespi, H. L. and Katz, J. J. (1971). *Proc. natn. Acad. Sci. U.S.A.* **68**, 625–628.
Norrish, R. G. and Porter, G. (1949). *Nature, Lond.* **164**, 658–661.
Packer, L. (1963). *Biochim. biophys. Acta* **75**, 12–22.
Phillipson, K. D., Sato, V. L. and Sauer, K. (1972). *Biochemistry, N.Y.* **11**, 4591–4595.
Racker, E., Hauska, G. A., Lien, S., Berzborn, R. J. and Nelson, N. (1971). *Proc. 2nd Int. Congr. Photosyn. Res.* 1097–1113.
Reinwald, E., Stiehl, H. H. and Rumberg, B. (1968). *Z. Naturf.* 23b, 1616–1617.
Renger, G. (1971). *Z. Naturf.* 26b, 149–153.

Rentzepis, P. M. (1968). *Photochem. Photobiol.* **8**, 579–587.
Rüppel, H. and Witt, H. T. (1969) *Meth. Enzym.* **16**, 316–379.
Rumberg, B. and Witt, H. T. (1964). *Z. Naturf.* **19b**, 693–707.
Rumberg, B., Schmidt-Mende, P., Weikard, J. and Witt, H. T. (1963). *Publs natn. Res. Coun., Wash.* **1145**, 18..
Schliephake, W., Junge, W. and Witt, H. T. (1968). *Z. Naturf.* **23b**, 1571–1578.
Schmid, R. and Junge, W. (1975). *Biochim. biophys. Acta* **394**, 76–92.
Schmidt, S. and Reich, R. (1972). *Ber. Bunsenges. Phys. Chem.* **76**, 1202–1208.
Schmidt, S., Reich, R. and Witt, H. T. (1971a). *Naturwissenschaften* **8**, 414–415.
Schmidt, S., Reich, R. and Witt, H. T. (1972). *Proc. 2nd Int. Congr. Photosyn. Res.* 1087–1095.
Schmidt-Mende, P. and Witt, H. T. (1968). *Z. Naturf.* **23b**, 223–235.
Schröder, H., Muhle, H. and Rumberg, B. (1972). *Proc. 2nd Int. Congr. Photosynth. Res.* 919–930.
Schwarz, M. (1959). "Information Transmission, Modulation and Noise". McGraw-Hill, New York.
Seifert, K. and Witt, H. T. (1968). *Naturwissenschaften* **55**, 222–223.
Siggel, U., Renger, G., Stiehl, H. H. and Rumberg, B. (1972). *Biochim. biophys. Acta* **256**, 328–335.
Singh, J. and Wasserman, A. R. (1971). *J. biol. Chem.* **246**, 3532–3541.
Slater, E. C. (1953). *Nature, Lond.* **172**, 975–978.
Slater, E. C. (1958). *Rev. pure appl. Chem.* **8**, 221.
Stiehl, H. H. and Witt, H. T. (1968). *Z. Naturf.* **23b**, 220–224.
Stiehl, H. H. and Witt, H. T. (1969). *Z. Naturf.* **24b**, 1588–1598.
Trebst, A. (1974). *A. Rev. Pl. Physiol.* **25**, 423–458.
Van Gorkom, H. J., Tamminga, J. J., Havemann, J. and Van der Linden, I. (1974). *Biochim. biophys. Acta* **347**, 417–438.
Van Holde, K. E. (1971). "Physical Biochemistry". Prentice-Hall, Englewood Cliffs, New Jersey.
Vetter, W., Englert, G., Rigassi, N. and Schwieter, U. (1971). *In* "Carotenoids" (O. Isler, ed.), pp. 189–266. Birkhäuser, Basle.
Vredenberg, W. J. and Tonk, W. J. M. (1975). *Biochim. biophys. Acta* **387**, 580–587.
Weiss, C., Kobayashi, H. and Gouterman, M. (1965). *J. molec. Spectros.* **16**, 415–450.
Witt, H. T. (1955). *Naturwissenshaften* **42** 72–73.
Witt, H. T. (1967). *In* "Vth Nobel Symp." (S. Claesson, ed.), pp. 81–97. Almquist and Wiksell, Stockholm–Interscience, New York.
Witt, H. T. (1971). *Q. Rev. Biophys.* **44**, 365–477.
Witt, H. T. and Zickler, A. (1973). *FEBS Lett.* **37**, 307–310.
Witt, H. T. and Zickler, A. (1974). *FEBS Lett.* **39**, 205–208.
Witt, H. T., Müller, A. and Rumberg, B. (1961). *Nature, Lond.* **192**, 967–969.
Witt, K. and Wolff, Chr. (1970). *Z. Naturf.* **25b**, 387–388.
Wolff, Chr. and Witt, H. T. (1969). *Z. Naturf.* **24b**, 1031–1037.

Wolff, Chr., Buchwald, H. E., Rüppel, H., Witt, K. and Witt, H. T. (1969). *Z. Naturf.* **23b**, 1038–1041.
Yamashita, K., Itoh, M. and Shibata, (1968). *Biochim. biophys. Acta* **162**, 610–613.
Zieger, G., Müller, A. and Witt, H. T. (1961). *Z. phys. Chem.* **29**, 13–24.